ERDC/GSL TR-19-10

Geotechnical and Structures Laboratory

US Army Corps of Engineers®
Engineer Research and Development Center

ERDC
ENGINEER RESEARCH & DEVELOPMENT CENTER

Development of a Lightweight Airfield Anchor Test Kit

Andrew B. Groeneveld, M. Wesley Trim,
Mariely Mejías-Santiago, and Craig A. Rutland

March 2019

Approved for public release; distribution is unlimited.

The U.S. Army Engineer Research and Development Center (ERDC) solves the nation's toughest engineering and environmental challenges. ERDC develops innovative solutions in civil and military engineering, geospatial sciences, water resources, and environmental sciences for the Army, the Department of Defense, civilian agencies, and our nation's public good. Find out more at www.erdc.usace.army.mil.

To search for other technical reports published by ERDC, visit the ERDC online library at http://acwc.sdp.sirsi.net/client/default.

ERDC/GSL TR-19-10
March 2019

Development of a Lightweight Airfield Anchor Test Kit

Andrew B. Groeneveld, M. Wesley Trim, and Mariely Mejías-Santiago

Geotechnical and Structures Laboratory
U.S. Army Engineer Research and Development Center
3909 Halls Ferry Road
Vicksburg, MS 39180-6199

Craig A. Rutland

Civil Engineering Branch, Engineering Division
Air Force Civil Engineer Center
Tyndall Air Force Base, FL 32403-5319

Final report

Approved for public release; distribution is unlimited.

Prepared for U.S. Army Corps of Engineers
Washington, DC 20314-1000

Under Project 462312

Abstract

The Air Force Civil Engineer Center (AFCEC) tasked the U.S. Army Engineer Research and Development Center (ERDC) with developing a lightweight kit for proof load testing anchors used in airfield operations. The design was required to be rapidly deployable, lightweight (i.e., no heavy equipment), and leave no permanent damage to the airfield. For the purposes of the project, airfield anchors were divided into three main types: studs/threaded anchors, aircraft trim pad anchors, and aircraft tie-downs/mooring points.

Stud or threaded anchor testing can be performed expediently using a commercial testing device. Operability of the commercial device was tested at ERDC by pulling poly panel threaded rods to failure.

A prototype anchor loading apparatus for trim pad anchors, the Lightweight Anchor Inspection Kit (LAIK), was designed, built, and successfully tested to demonstrate operability. Trim pad anchors at Eglin AFB were proof loaded to 100 kips using the LAIK. The LAIK user's manual, list of components, and design drawings are included as an appendix to the report.

A tie-down anchor testing device was also designed and built. This testing device is intended to proof load aircraft tie-downs/mooring points up to 70 kips. The tie-down tester makes use of the same hydraulic equipment included in the LAIK.

DISCLAIMER: The contents of this report are not to be used for advertising, publication, or promotional purposes. Citation of trade names does not constitute an official endorsement or approval of the use of such commercial products. All product names and trademarks cited are the property of their respective owners. The findings of this report are not to be construed as an official Department of the Army position unless so designated by other authorized documents.

DESTROY THIS REPORT WHEN NO LONGER NEEDED. DO NOT RETURN IT TO THE ORIGINATOR.

Contents

Abstract ii

Figures and Tables v

Preface ix

Unit Conversion Factors x

1 Introduction 1
1.1 Background 1
1.2 Objective 1
1.3 Report outline 2

2 Site Visits 3
2.1 Dannelly Field 3
2.2 Eglin AFB 5

3 Stud and Threaded Anchor Test Device 7
3.1 Background 7
3.2 Evaluation of Stud and Threaded Anchor Test Device 8

4 Aircraft Tie-Down Test Rig 11

5 Combined Shear-Tensile Loading for Testing Trim Pad Anchors 15
5.1 Interaction equations 15
5.2 Combined loading tests 17
5.3 Finite element analysis 18
5.3.1 Bidirectional high-capacity thrust anchor 19
5.3.2 Omnidirectional thrust anchor 29
5.3.3 Summary 38

6 Lightweight Anchor Inspection Kit (LAIK) Design Evolution 40
6.1 Sling concept 40
6.1.1 Center jack variant 40
6.1.2 Inline jack variant 41
6.1.3 Expedient deadman anchor 41
6.2 In-joint anchor concept 44
6.3 Lever concepts 47
6.4 Angled core concept and variants 49
6.5 Deadman anchor concepts 52
6.6 Small-scale proof-of-concept tests 57
6.6.1 Test overview 57
6.6.2 Design and fabrication 58
6.6.3 Test setup 61

6.6.4 Instrumentation *65*
6.6.5 Loading *67*
6.6.6 Results *67*
6.6.7 Lessons learned through proof-of-concept testing *70*
6.7 Final LAIK design 71
6.7.1 LAIK design overview *71*
6.7.2 LAIK design analysis *75*

7 Lightweight Anchor Inspection Kit (LAIK) Field Evaluation 82
7.1 Test site and overview 82
7.2 Test procedure 83
7.2.1 Instrumentation *85*
7.2.2 Loading *87*
7.3 Results 88
7.4 Summary 91

8 Conclusions and Future Work 92

References 94

Appendix A: Lightweight Anchor Inspection Kit (LAIK) User Manual 96

Report Documentation Page

Figures and Tables

Figures

Figure 1. (a) Overview of Dannelly Field hush house and (b) primary anchor points for reacting thrust loads. 4
Figure 2. Dannelly Field hush house floor slab with embedments. 5
Figure 3. Various anchor types inspected during the Eglin AFB site visit. 6
Figure 4. QualiAnchor 2005 (QualiTest n.d.). 7
Figure 5. Poly panel threaded stud prepared for test. 8
Figure 6. Threaded coupler attached to stud. 9
Figure 7. COTS test device supported on two steel plates to distribute reactions and avoid poly panel damage. 9
Figure 8. Load readout during operation. The displayed load is in kN and corresponds to approximately 32.3 kips. 10
Figure 9. Tie-down tester overview drawing. 11
Figure 10. Load cell and readout (Transducer Techniques 2015). 12
Figure 11. Tie-down tester actuator base plate. 13
Figure 12. Tie-down tester load spreader beam. 13
Figure 13. Comparison of some interaction equations for embedded concrete anchors. 17
Figure 14. Plot of test results reported by Grau and Cooksey (1992). 18
Figure 15. BHCTA drawing (Department of the Air Force 2001). 19
Figure 16. Isometric view of BHCTA model with transparency applied to concrete. 20
Figure 17. Isometric view of finite element mesh for BHCTA model. 20
Figure 18. Illustration of BHCTA model boundary conditions: (a) Z-symmetry boundary condition and (b) pinned boundary condition. 22
Figure 19. Loads and constraints applied to BHCTA model: (a) 90-deg load case and (b) 20-deg load case. 23
Figure 20. Isometric view of displacements, 90-deg load case for BHCTA model. 24
Figure 21. Isometric view of displacements, 20-deg load case for BHCTA model. 24
Figure 22. Comparison of BHCTA concrete surface displacements along Path *Z*. 25
Figure 23. Comparison of BHCTA concrete surface displacements along Path *X*. 25
Figure 24. Comparison of stresses in BHCTA for 90-deg and 20-deg load cases. 26
Figure 25. Front view of concrete maximum principal stress, 90-deg load case for BHCTA model. 27
Figure 26. Front view of concrete maximum principal stress, 20-deg load case for BHCTA model. 27
Figure 27. Comparison of BHTCA maximum principal stress at concrete surface along Path *Z*. 28
Figure 28. Comparison of BHTCA maximum principal stress at concrete surface along Path *X*. 28

Figure 29. Comparison of cracking observed around trim pad anchor at Eglin AFB with analysis results (BHCTA, 20-deg load case).....29
Figure 30. Dannelly Field OTA drawing (Capt A. W. Sanders, pers. comm., 15 March 2017).....29
Figure 31. Isometric view of OTA model with transparency applied to concrete.....30
Figure 32. Isometric view of finite element mesh for OTA model.....31
Figure 33. Illustration of OTA model boundary conditions: (a) Z-symmetry boundary condition and (b) pinned boundary condition.....32
Figure 34. Loads and constraints applied to OTA model: (a) 90-deg load case and (b) 20-deg load case.....33
Figure 35. Isometric view of displacements, 90-deg load case for OTA model.....34
Figure 36. Isometric view of displacements, 20-deg load case for OTA model.....34
Figure 37. Comparison of OTA concrete surface displacements along Path *Z*.....35
Figure 38. Comparison of OTA concrete surface displacements along Path *X*.....35
Figure 39. Comparison of stresses in OTA for 90-deg and 20-deg load cases.....36
Figure 40. Front view of concrete maximum principal stress, 90-deg load case for OTA model.....37
Figure 41. Front view of concrete maximum principal stress, 20-deg load case for OTA model.....37
Figure 42. Comparison of OTA maximum principal stress at concrete surface along Path *X*.....38
Figure 43. Comparison of OTA maximum principal stress at concrete surface along Path *Z*.....38
Figure 44. Current test method shown with forklift configuration (Department of the Air Force 2000).....40
Figure 45. Sling concept with center jack.....41
Figure 46. Sling concept with inline jack.....41
Figure 47. Universal PCC anchor for 6-in. core.....43
Figure 48. Tri-Talon schematic.....44
Figure 49. Diagram of in-joint anchor.....45
Figure 50. L-shaped load frame using in-joint anchor for horizontal resistance only.....45
Figure 51. Load bridge using in-joint anchor for horizontal resistance only.....46
Figure 52. 3-D view of load bridge concept.....46
Figure 53. Effect of load bridge aspect ratio on reactions.....47
Figure 54. Lever concepts with sling attached near (a) the end and (b) the pivot point.....48
Figure 55. Geometry of the lever problem. The initial, unstressed position of the sling is shown in green; the final position when stressed to the proof load is shown in red.....49
Figure 56. Angled core concept.....50
Figure 57. Commercial soil anchor load locker (A-Aerial Service Company n.d.).....51

Figure 58. Designs for proof-of-concept test. 52
Figure 59. An array of six slings equally spaced over a 90-deg arc. 53
Figure 60. Plot of six-anchor optimized layout. Plot uses r_3 = 48 in. for proportions. The direction of displacement is shown by the blue arrow. 55
Figure 61. Reaction force distribution from Abaqus/Standard simulation. Reaction forces shown in lbf. 56
Figure 62. Proof-of-concept test site schematic. 57
Figure 63. Modified Manta Ray COTS load locker. 59
Figure 64. Footing plate for MR device to anchor in angled core holes. 60
Figure 65. Roller device for center jack. 60
Figure 66. Layout for proof-of-concept Test #1. 61
Figure 67. Positioning core drill on portable jig. 62
Figure 68. Core drilling. 63
Figure 69. Cored holes after core removal and cleaning. 63
Figure 70. Footing plate in cored holes. 64
Figure 71. MR mounted to footing plate. 64
Figure 72. Drilling holes for drop-in anchors. 65
Figure 73. Instrumentation for proof-of-concept Test #1. 66
Figure 74. Instrumentation for proof-of-concept Test #2. 66
Figure 75. Proof-of-concept Test #1 (center jack) load and displacement time-histories. 68
Figure 76. Proof-of-concept Test #2 (MR and angled core) load and displacement time-histories for stability check #1. 69
Figure 77. Proof-of-concept Test #2 (MR and angled core) load and displacement time-histories for stability check #2. 69
Figure 78. Proof-of-concept Test #2 (MR and angled core) load history for tensioning up to 3,500 lbf. 70
Figure 79. Schematic overview of final LAIK design. 72
Figure 80. Setup geometry. The initial (untensioned) geometry is shown in black. The loaded (tensioned) geometry is shown in red. 73
Figure 81. Wej-It PS2-34 POWER-Sert adhesive insert anchor (adapted from Wej-It 2015). 74
Figure 82. Free-body diagram showing magnitude and direction of the forces acting on LAIK components. 75
Figure 83. Deadman anchor finite element model (a) overview and (b) bolt connector properties. 76
Figure 84. Deadman anchor FEA contours: (a) displacement, (b) equivalent strain, and (c) von Mises stress. 77
Figure 85. Load bridge finite element model (a) overview and (b) rotated view showing boundary condition representing actuator. 78
Figure 86. Load bridge FEA contours: (a) displacement, (b) equivalent strain, and (c) von Mises stress. 79

Figure 87. Actuator base finite element model overview. 80
Figure 88. Actuator base FEA contours: (a) displacement, (b) equivalent strain, and (c) von Mises stress. 81
Figure 89. Map of Eglin AFB showing the test location. 82
Figure 90. Hardstand 10 looking toward blast deflector. 83
Figure 91. Permanently attached link on Anchor A. 84
Figure 92. Rebar encountered during hammer drilling. 84
Figure 93. Inserting a plastic cap into a hole that broke through the slab. 85
Figure 94. Instrumentation setup for LAIK Test #1. 86
Figure 95. Instrumentation setup for LAIK Tests #2 and #3. 87
Figure 96. Load vs. time for anchor proof load tests using the LAIK prototype. 88
Figure 97. Sling tension vs. actuator displacement for proof load tests using the LAIK prototype. 89
Figure 98. Load vs. angle of application. Angle is relative to the horizontal and was measured with a digital angle indicator mounted on the load cell. 90
Figure 99. Load vs. dial indicator displacement reading. The non-zero displacement after unloading is attributed to suspected drift of the positioner holder, not permanent deformation of the anchors. 91

Tables

Table 1. Minimum and objective testing capacities for kit. 2
Table 2. Summary of QualiAnchor capability demonstration tests on poly panel studs. 10
Table 3. Tie-down tester hardware. 14
Table 4. Element type and material properties for BHCTA model. 21
Table 5. Element type and material properties for OTA model. 31
Table 6. Expedient anchors, current and under development. Current anchor test results from unpublished draft report. 42
Table 7. Hoist ring capacities. 55
Table 8. Force distribution for six-anchor optimized layout. 56
Table 9. Curing and working times for HIT-HY 200-A epoxy (Hilti n.d.). 74
Table 10. Proof load test matrix for Eglin AFB trim pad anchors. 83
Table 11. Loading schedule with approximate hydraulic pressures. 87

Preface

This study was conducted for the Air Force Civil Engineer Center (AFCEC) under Project 462312.

The work was performed by the Structural Engineering Branch (StEB) of the Geosciences and Structures Division (GSD) and the Airfields and Pavements Branch (APB) of the Engineering Systems and Materials Division (ESMD), U.S. Army Engineer Research and Development Center, Geotechnical and Structures Laboratory (ERDC-GSL).

Support provided by the machine shop and welding shop of the ERDC Department of Public Works (DPW) was instrumental in the production of the prototype developed in this project.

At the time of publication, Dr. Jay Shannon was Acting Chief, StEB; Dr. Timothy W. Rushing was Chief, APB; Mr. James L. Davis was Chief, GSD; and Mr. Nicholas Boone was the Technical Director for Force Projection. The Deputy Director of ERDC-GSL was Mr. Charles W. Ertle, and the Director was Mr. Bartley P. Durst.

COL Ivan P. Beckman was the Commander of ERDC, and Dr. David W. Pittman was the Director.

Unit Conversion Factors

Multiply	By	To Obtain
degrees (angle)	0.0174533	radians
degrees Fahrenheit	(°F-32)/1.8	degrees Celsius
feet	0.304800	meters
inches	0.0254000	meters
kips (force)	4,448.22	newtons
pounds (force)	4.44822	newtons
pounds (force) per square inch	6,894.76	pascals
tons (force)	8,896.44	newtons

1 Introduction

1.1 Background

The Air Force Civil Engineer Center (AFCEC) frequently receives requests for methods to test the integrity of various types of airfield anchors. The anchors that require testing range from conventional concrete anchor bolts to tie-downs and mooring points for aircraft. Testing needs to be completed as quickly as possible to minimize impact on airfield operations. Therefore, a testing kit is needed that is shippable and expedient to use. AFCEC reached out to the U.S. Army Engineer Research and Development Center (ERDC) to develop a prototype testing kit to meet these needs.

1.2 Objective

The objective of this project was to develop an anchor testing kit, capable of being fielded quickly and at little cost, to verify the load carrying capacity of the following airfield anchors:

- Studs or threaded anchors for
  - engine stands
  - fairlead beams used in aircraft arresting systems
  - poly panels used in aircraft arresting systems
  - aircraft arresting system in the vault (BAK 12)
- Aircraft tie-downs and mooring points
- Aircraft trim pad anchors

For the trim pad anchors, it is important that the proof load can be applied at angle of roughly 20 deg relative to the pavement surface to simulate actual in-service conditions. Design criteria for the anchor testing kit comprise:

- Lightweight (easy to ship and at minimal cost)
- Capable of proof load testing several different anchor types
- Capable of testing at several different load levels
- Capable of applying loads in multiple directions

Finally, AFCEC gave threshold and objective capacities for testing each of the anchor types. These are summarized in Table 1.

Table 1. Minimum and objective testing capacities for kit.

Anchor type	Testing capacity (kip)	
	Threshold	Objective
Studs or threaded anchors	30	35
Aircraft tie-downs and mooring points	35	70
Aircraft trim pad anchors	70	100

ERDC's deliverables under this project are:

- A prototype anchor testing kit
- Testing kit documentation (user's manual, design specifications, and components list)
- ERDC technical report documenting the design process and testing results

1.3 Report outline

This report is organized as follows. Chapter 2 documents observations from site visits conducted to survey typical airfield anchor installations. Chapter 3 summarizes the approach to testing studs/threaded anchors using a commercial off-the-shelf (COTS) testing device and documents operability testing on poly panel studs at ERDC. Chapter 4 presents the design for a tie-down/mooring point testing device. Chapter 5 describes a preliminary study into the use of correlations between vertical and angled loading. Chapter 6 provides an overview of the design process: the concepts that were considered, the calculations and small-scale testing used to evaluate the concepts leading to the final prototype design. Chapter 7 documents testing performed on trim pad anchors at Eglin AFB using the prototype kit. Chapter 8 presents conclusions from the current work and identifies possible areas for future work. Finally, Appendix A contains the user's manual, data sheets for testing and inspection, a components list, and design drawings for the anchor testing kit. Appendix A is a stand-alone document that can be used separately from this report.

2 Site Visits

In order to gain a better understanding of typical airfield anchor installations, two site visits were conducted at nearby airfields. On March 8, 2017, ERDC personnel visited the jet engine testing facility (hush house) at Dannelly Field in Montgomery, AL. On March 31, 2017, ERDC personnel visited Eglin AFB in Okaloosa County, FL. During each site visit, measurements and photographs were taken of all anchor installations available for inspection. The findings from each site visit are summarized in Sections 2.1 and 2.2.

2.1 Dannelly Field

Captain Adam Sanders of the USAF 187th FW facilitated a brief site visit for ERDC personnel to view the jet engine testing facility (hush house) at Dannelly Field in Montgomery, AL. Captain Sanders also provided the construction drawings for the hush house foundation, showing the details for all of the floor slab embedments. The drawings also show construction specifications for a trim pad and blast deflector located on the opposite side of the airfield from the hush house. However, the trim pad was not available for inspection during the site visit. The Dannelly Field hush house and trim pad were constructed in the early 1990s and no issues with any of the tie-down systems at Dannelly Field have been reported. All of the existing equipment is original.

The Dannelly Field hush house was found to have accommodations for testing both installed and uninstalled jet engines. For uninstalled engines, an engine stand cradle is used to support the engine. Two embedded footings serve as the primary thrust reaction supports for the engine stand. For installed engines, the primary tie-down is an embedded deadman anchor. Since the jets typically have twin engines, the deadman must react twice as much load as the engine stand footings.

In addition to the primary thrust anchors, a wide variety of smaller embedments were observed within the hush house:

- Embedded plates with threaded holes that serve as additional tie-down points during installed engine testing.
- Embedded plates with attached rings that serve as additional tie-down points during uninstalled engine testing.

- Engine stand rails comprising steel bar angle welded to a steel plate and held in place with embedded threaded anchors. The rails allow the engine stand to be moved out of the way for installed engine tests.

Figure 1 shows the hush house layout and various anchor types.

Figure 1. (a) Overview of Dannelly Field hush house and (b) primary anchor points for reacting thrust loads.

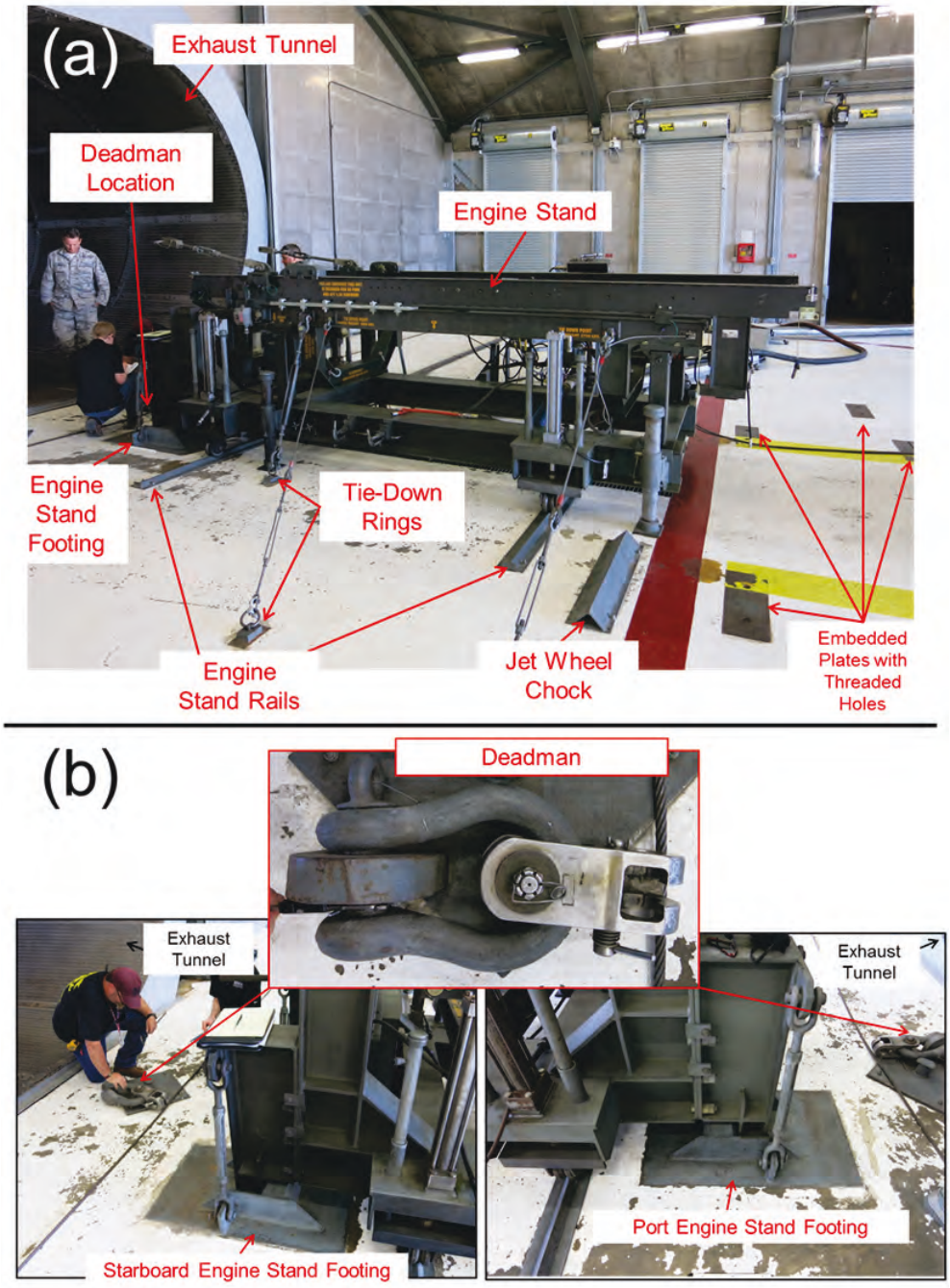

The hush house construction drawings were used to create a CAD model of the floor slab and embedments, shown in Figure 2. The CAD model would later be used to inform design decisions for the lightweight anchor kit.

Figure 2. Dannelly Field hush house floor slab with embedments.

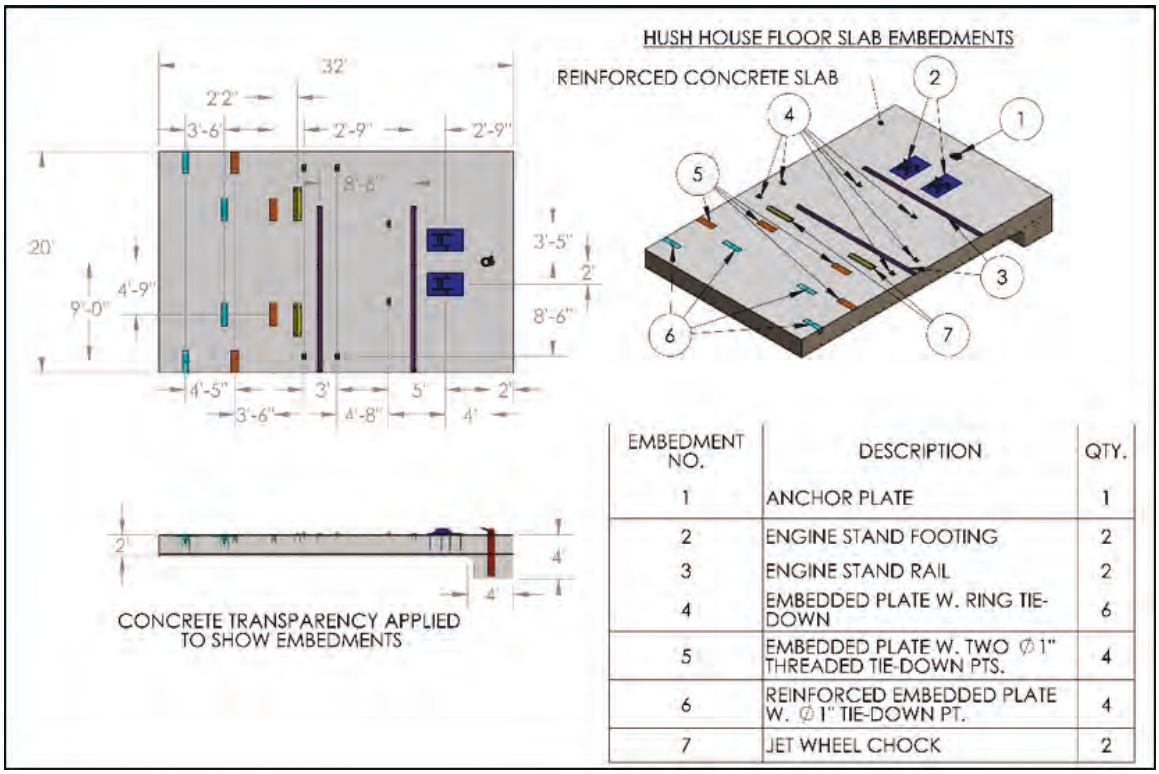

EMBEDMENT NO.	DESCRIPTION	QTY.
1	ANCHOR PLATE	1
2	ENGINE STAND FOOTING	2
3	ENGINE STAND RAIL	2
4	EMBEDDED PLATE W. RING TIE-DOWN	6
5	EMBEDDED PLATE W. TWO ∅1" THREADED TIE-DOWN PTS.	4
6	REINFORCED EMBEDDED PLATE W. ∅1" TIE-DOWN PT.	4
7	JET WHEEL CHOCK	2

2.2 Eglin AFB

On March 31, 2017, Mr. Steve Ray of the 796 Civil Engineer Squadron facilitated a site visit for ERDC personnel to inspect and photograph several anchor types installed around the Eglin airfield. During the site visit, seven areas were available for inspection: two ramps, two aprons, two trim pads, and a BAK-12 arresting system located on the south end of runway 01-19. These represent only a subset of the embedded anchors at Eglin. Many areas, including several hush houses, were not available for inspection during the site visit. The locations and anchor types inspected during the Eglin site visit are summarized in Figure 3.

Figure 3. Various anchor types inspected during the Eglin AFB site visit.

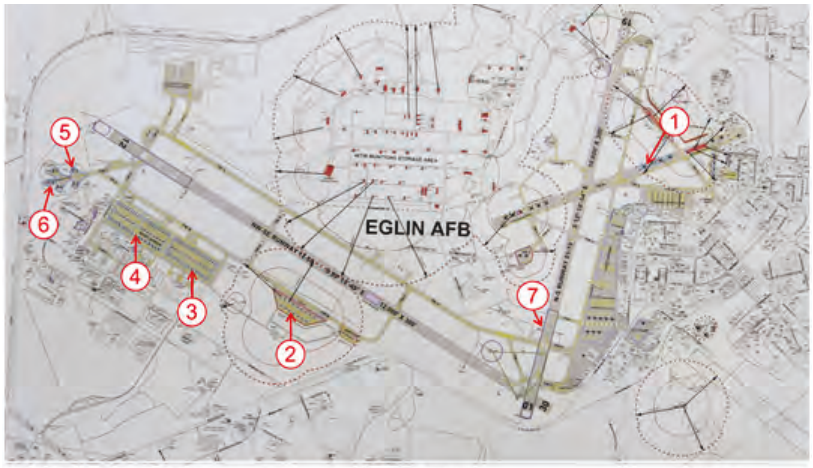

Eglin Site Location	Anchor Type	Photo*
1: M East Ramp	Hat-Type Tiedowns (11/16" bar ∅)	
2: LOLA Ramp	Hat-Type Tiedowns (1-1/4" bar ∅)	
	Static Ground Points (11/16" bar ∅)	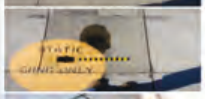
3: West Apron (new section)	Hat-Type Tiedowns (1" bar ∅)	
4: West Apron (old section)	Hat-Type Tiedowns (1/2" bar ∅)	
5: Trim Pad Z-1	2x Hat-Type Thrust Anchors (3" bar ∅)	
	Hat-Type Tiedowns (11/16" bar ∅)	
6: Trim Pad Z-3	Hat-Type Thrust Anchor (3" bar ∅)	
	Hat-Type Tiedowns (11/16" bar ∅)	
7: BAK-12 on South End of Runway 01-19	Threaded Anchors: Poly Panels (3/4" bolt ∅)	
	Embedded Eyebolts: Arresting Cable Tiedowns (3/4" bolt ∅)	
	Threaded Anchors: Fairlead Beam (1 1/8" bolt ∅)	
	Threaded Anchors: Energy Absorber (1" bolt ∅)	

* Reference stick is 18" long with 1" increments.

3 Stud and Threaded Anchor Test Device

3.1 Background

After a thorough evaluation, a commercial off-the-shelf (COTS) device was deemed the most cost-effective solution for gaining the capability to test threaded anchor studs. The selection criteria used to evaluate COTS options were:

- The minimum and objective capacity for the test device are 30 kips and 35 kips, respectively.
- The device should be portable and expedient.
- The device should be capable of testing anchors of various size.

A number of COTS testing devices for threaded anchors were found in market research. However, the majority of these devices did not have sufficient capacity; only two were found to have capacities exceeding 30 kips. These heavy-duty anchor testers, the NDT James Instruments P-C-7290 and the QualiTest QualiAnchor 2005, had rated capacities of 32,600 lbf (145 kN). Both devices were of essentially the same design, a hand-operated loading unit with a torque multiplier that applies tension through a threaded rod. A coupler is used to attach the threaded rod to the anchor to be tested. Both devices were also available with metric or imperial threaded couplers. A test device produced by QualiTest, the QualiAnchor 2005 (Figure 4), was selected as most promising for this application. At the time of purchase, the cost was approximately $9,500.

Figure 4. QualiAnchor 2005 (QualiTest n.d.).

3.2 Evaluation of Stud and Threaded Anchor Test Device

ERDC personnel acquired a QualiAnchor 2005 and conducted a test to determine its performance. Poly panel threaded studs were tested on 30 November 2017, at an ERDC airfield test section in Vicksburg, MS.

Three threaded studs were identified for testing to failure. The sealant around the top of the stud was removed, and a chemical cleaner was applied to the stud and nut. The nut was removed with a socket and breaker bar. However, one of the nuts was seized and the stud began to extract instead of removing the nut. The other two nuts were easily removed and the studs were tested. Figure 5 shows a stud ready for testing.

Figure 5. Poly panel threaded stud prepared for test.

Figure 6 shows a close-up of the QualiAnchor 2005 device attached to the stud via a threaded coupler. Note that two of the feet rest on the poly panel. After the test, indentations were observed under these feet. Therefore, steel plates were used to distribute the reaction for a second test to avoid damaging the panels (Figure 7). The steel plates could add some confinement, as discussed later.

Figure 6. Threaded coupler attached to stud.

Figure 7. COTS test device supported on two steel plates to distribute reactions and avoid poly panel damage.

Figure 8 shows the load display during operation. Note that the device displays the load in kN only. Conversion to customary units can be readily performed.

Figure 8. Load readout during operation. The displayed load is in kN and corresponds to approximately 32.3 kips.

The QualiAnchor 2005 has a peak value display mode, in which the display shows the maximum load attained since activated. Because the objective of the ERDC test was to pull the anchors to failure, it was decided to use the standard load readout mode. It was important to be able to see the load change in real-time during the test, as the load would decrease rapidly once failure occurred. Had the peak value display mode been activated, the post-peak load decrease would not be reflected in the displayed value.

The results of testing are shown in Table 2. For reference, the proof load for a stud with the poly panel in place is 19 kips [*]. Stud 2 had a significantly higher peak load than Stud 1; this could be due to installation quality, confinement, or a combination of the two. Further testing would be required to provide more insight into the effect of testing procedure on poly panel stud proof load results.

Table 2. Summary of QualiAnchor capability demonstration tests on poly panel studs.

Test	Peak load (kN)	Peak load (kip)
Stud 1	125	28.1
Stud 2	160	36.0

[*] C. Rutland, n.d. UHMW PE Anchor Extraction Protocol. Air Force Civil Engineer Center, Tyndall Air Force Base, FL 32403-5319.

4 Aircraft Tie-Down Test Rig

Tie-downs and mooring points have some characteristics in common with both threaded anchors and trim pad anchors. Small tie-downs or mooring points (with proof loads ≤ 35 kips) could be tested using the COTS anchor tester with a clevis attachment. Larger tie-downs could be tested using the trim pad anchor testing apparatus described in Section 6.7. The trim pad anchor tester is appropriate, if higher load or angled loading are needed. However, if a large number of tie-downs or mooring points need to be tested, the trim pad testing apparatus could be cumbersome. To provide a solution for expedient testing of tie-downs and mooring points with a vertical load, a load beam device was designed (Figure 9).

Figure 9. Tie-down tester overview drawing.

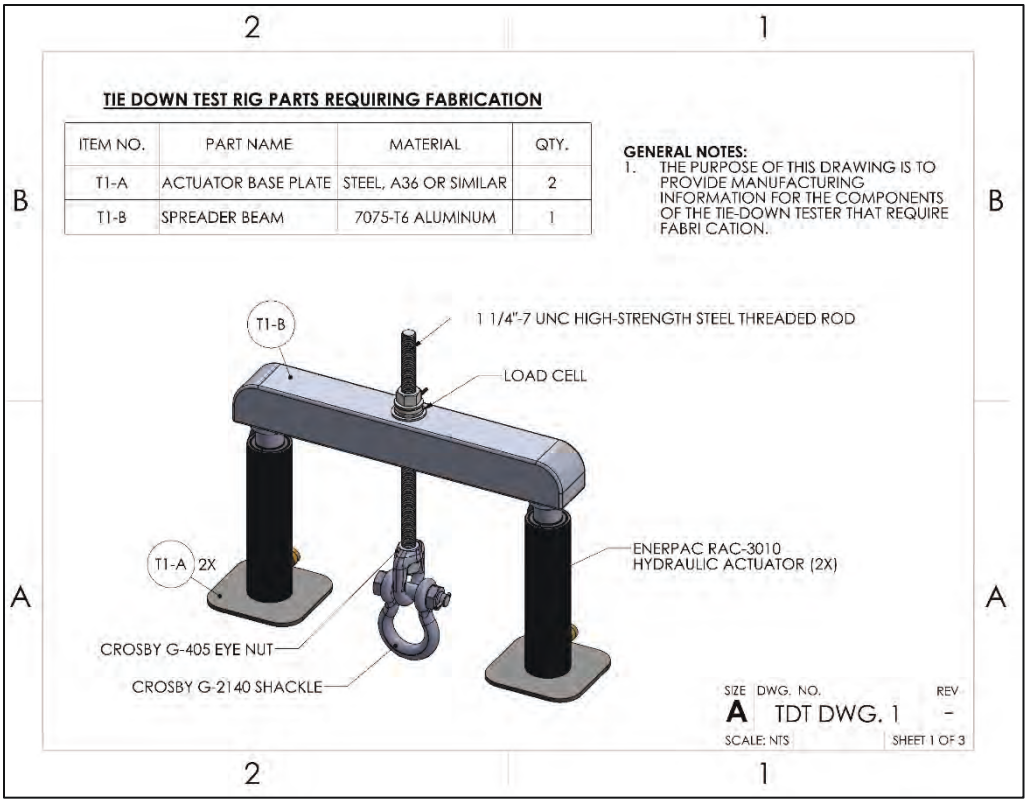

A through-hole load cell is used to read the force applied to the tie-down. A 50-kip load cell (model THD-50K-Z with optional “plug-and-play” connector) and handheld readout (model SSI) were sourced from Transducer Techniques (see Figure 10). The handheld readout provides excitation for the load cell and converts the output voltage to a force. The load cell capacity (50 kips) was the highest that could be obtained in a

through-hole load cell with reasonable accuracy. A load washer with a 125-kip capacity was also considered, but it was determined to be overly sensitive to even slight deviations from plumb loading. Research indicated that an accuracy of 3–4 percent full range (an error of ±5 kips) could be expected from the load washer in normal usage. This was deemed unacceptable for proof load testing.

Figure 10. Load cell and readout (Transducer Techniques 2015).

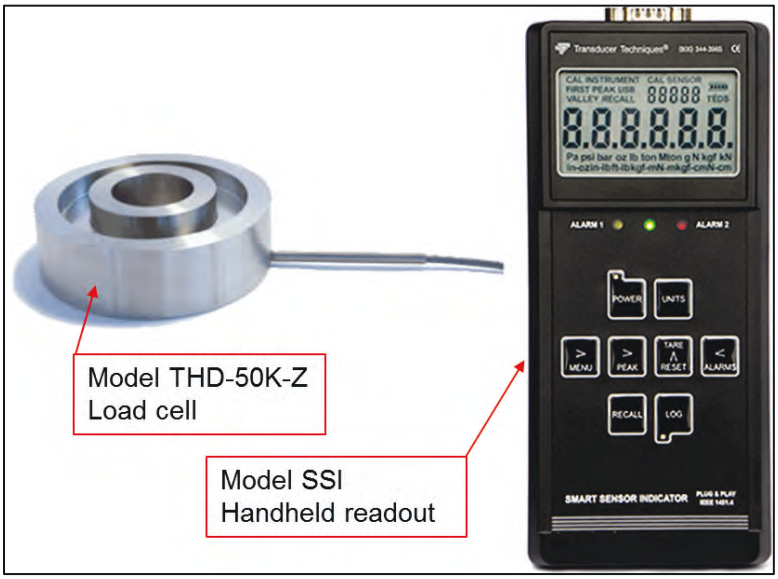

The tie-down tester requires two actuator base plates (Figure 11) and one load spreader beam (Figure 12) to be fabricated. These items are designed to fit the same Enerpac RAC-3010 aluminum hydraulic actuators used in the trim pad testing apparatus. The other components required are commercially available and are listed in Table 3. Note that the tie-down tester is a prototype, and different components may be required for some applications.

Figure 11. Tie-down tester actuator base plate.

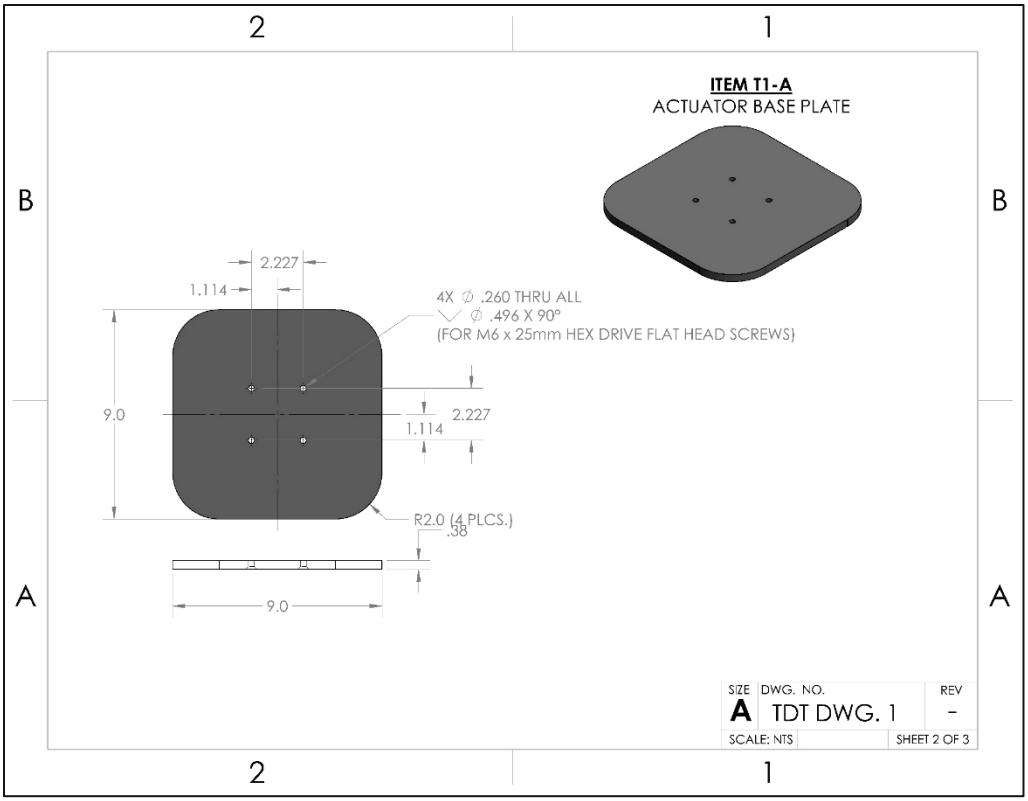

Figure 12. Tie-down tester load spreader beam.

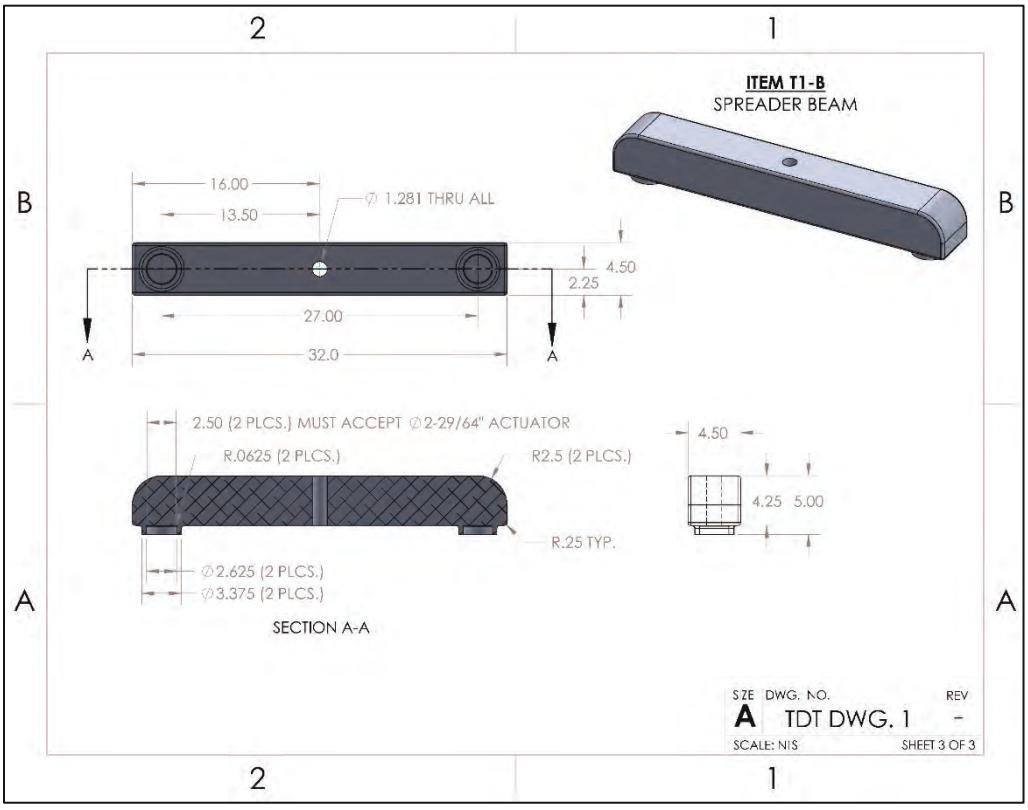

Table 3. Tie-down tester hardware.

Item	Quantity
High-strength steel threaded rod, 1-1/4"-7 thread, length as required by application	1
High-strength steel hex nut, grade 8, zinc yellow-chromate plated, 1-1/4"-7 thread	1
washer, structural, 1.375" ID, 2.5" OD *OR* cadmium-plated steel mil. spec. washer, 3" OD (MS-27183-30)	At least 2
Hex drive flat head screw, M6 × 25mm	8
Crosby G-405 eye nut, size 8 (Stock # 1090633)	1
Crosby G-2140 shackle, 1-1/4" (Stock # 1021083)	1

5 Combined Shear-Tensile Loading for Testing Trim Pad Anchors

Trim pad anchors must be proof loaded at an angle of about 20 deg relative to the pavement surface to simulate in-service conditions. Coupled with the high loads required (70–100 kips), a robust reaction structure for the proof test is needed. It was recognized that an airfield anchor testing device designed to apply only tensile loading would be more economical and less cumbersome compared to a shear-loading device. However, it raises the question of what load should be used for a vertical proof load test. This chapter gives some background on combined shear-tensile loading of concrete anchors and presents results of a preliminary finite element analysis of load angle effect on trim pad anchors.

5.1 Interaction equations

A literature review was conducted to determine the state-of-knowledge on combined shear and tensile loading applied to anchors embedded in concrete. With the assistance of the ERDC Library, more than 100 research articles were examined to find relevant work. To date, however, comparatively little research has dealt with both combined loading and embedded anchors. This is particularly true for airfield anchors.

In general, a power-law interaction equation can be used for anchor bolts or headed studs embedded in concrete (Lotze et al. 2001):

$$\left(\frac{V}{V_{ult}}\right)^{p} + \left(\frac{P}{P_{ult}}\right)^{p} = 1 \tag{1}$$

where:

V = shear load
V_{ult} = shear capacity
P = tensile load
P_{ult} = tensile capacity
p = exponent, determined experimentally.

For failure by steel rupture, p is typically 1.67–1.80, and for failure by concrete fracture, p = 1.6.

Oluokun and Burdette (1993) studied channel anchors in thin concrete slabs. Channel anchors consist of multiple legs welded to a C-channel section. The outer face of the channel is typically flush with the slab surface. Channel anchors were included, since they are more complex embedments than the bolts or studs that are often studied. Some types of airfield anchors, notably trim pad anchors, also consist of large, embedded structures. Oluokun and Burdette suggested a modification to Equation 1, as shown in Equation 2.

$$\left(\frac{V}{V_{ult}}\right)^{5/3} + \left(\frac{P}{0.87P_{ult}}\right)^{5/3} = 1 \quad (2)$$

This equation was developed based on tests where failure occurred in the concrete. Shear loading reduced the pullout capacity, which was attributed to weakening of concrete at the end of the anchorage (Oluokun and Burdette 1993). Note that the shear load was applied and held, and then the pullout load was applied. When failure occurred in the steel, the unmodified interaction equation (Equation 1) with $p = 5/3$ was conservative.

The various criteria can be described by a single equation with different exponents, plotted in Figure 13. A reduction on tensile pullout capacity, r, was added for channel anchors subject to combined loading (Oluokun and Burdette 1993). General applicability of the reduction is not known.

Figure 13. Comparison of some interaction equations for embedded concrete anchors.

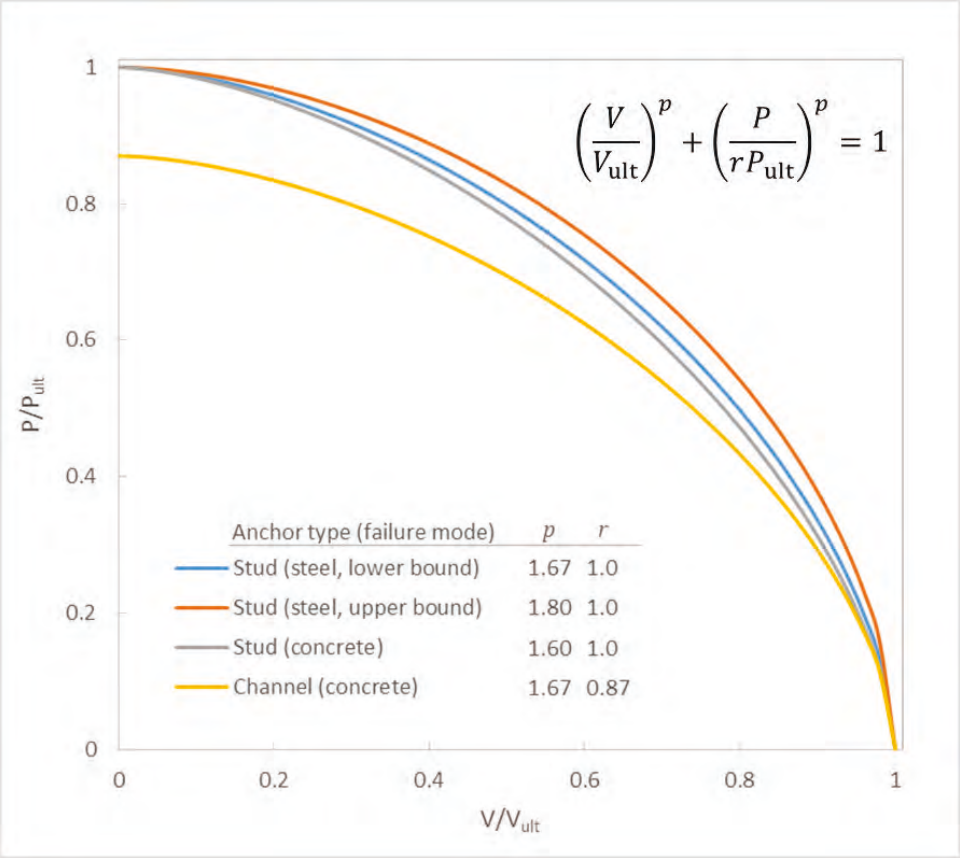

5.2 Combined loading tests

The literature search uncovered two test series for tie-downs or mooring points tested at multiple angles of loading. These test series are briefly described in the following paragraphs.

The U.S. Army Engineer Waterways Experiment Station, one of ERDC's precursor organizations, conducted tests on shepherd's hook mooring points at Ft. Polk, LA (Grau and Cooksey 1992). A total of eight tests were performed (summarized in Figure 14), but the data are of limited use for the current work. The Ft. Polk tests were performed to verify that the mooring points met the requirements at the time (15 kips at ~20 deg), so not all anchors were pulled to failure.

Figure 14. Plot of test results reported by Grau and Cooksey (1992).

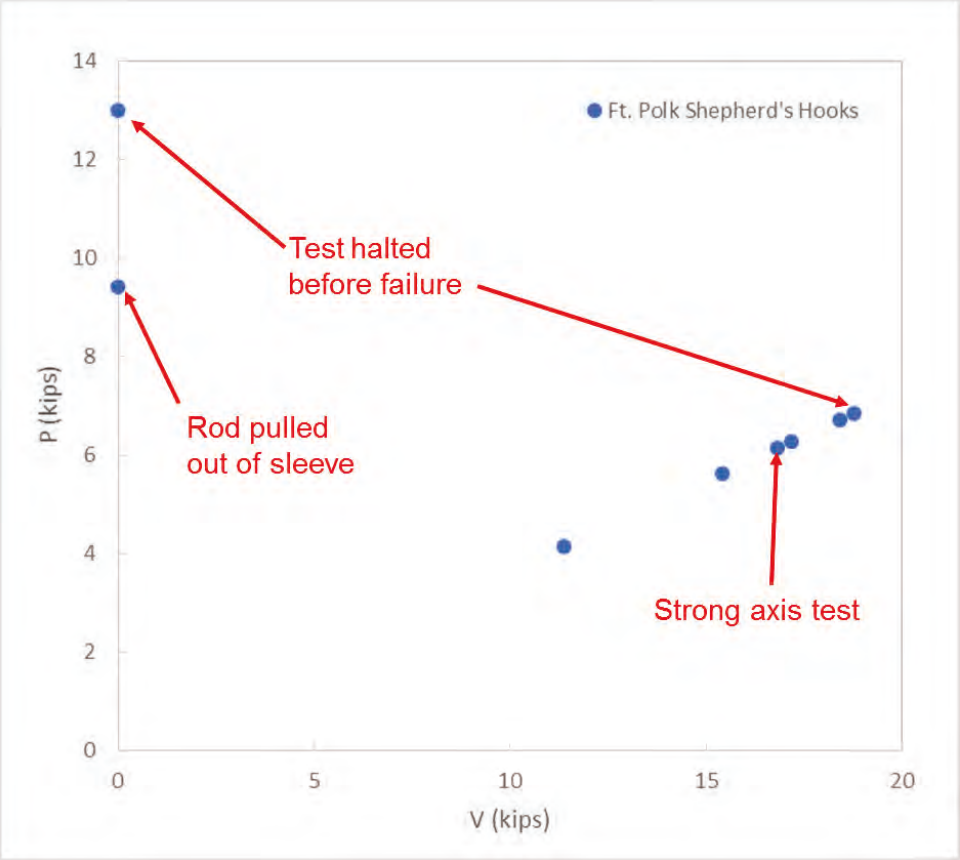

The U.S. Naval Civil Engineering Laboratory conducted tests on hat-type tie-downs (Smith and Schroeder 1958). These tests varied the compass direction the tie-downs were loaded in, but the angle with respect to the pavement was kept constant. The results of this study provide insight into the effect of shear loading in the plane of the eye vs. out of the plane of the eye. However, the effect of varying combinations of tensile and shear loading was not investigated.

5.3 Finite element analysis

As mentioned before, an airfield anchor testing device designed to apply only tensile loading would be more economical and less cumbersome compared to a shear-loading device. However, in order to maintain conservatism during proof testing, correlation between the tensile and shear strengths of the anchors is needed. Finite Element Analysis (FEA) was performed on two types of thrust anchor designs. For each design, two load cases were investigated: 90 deg (vertical) and 20 deg, which is the recommended load angle given in ETL 00-2 (Department of the Air Force

2000) and UFC 3-260-01 (Department of Defense 2008). The FEA methodology and results are presented in the following subsections.

5.3.1 Bidirectional high-capacity thrust anchor

An FEA model of a bidirectional high-capacity thrust anchor (BHCTA) was constructed using drawings in ETL 01-10 Appendix A (Department of the Air Force 2001). The design drawing is shown in Figure 15.

Figure 15. BHCTA drawing (Department of the Air Force 2001).

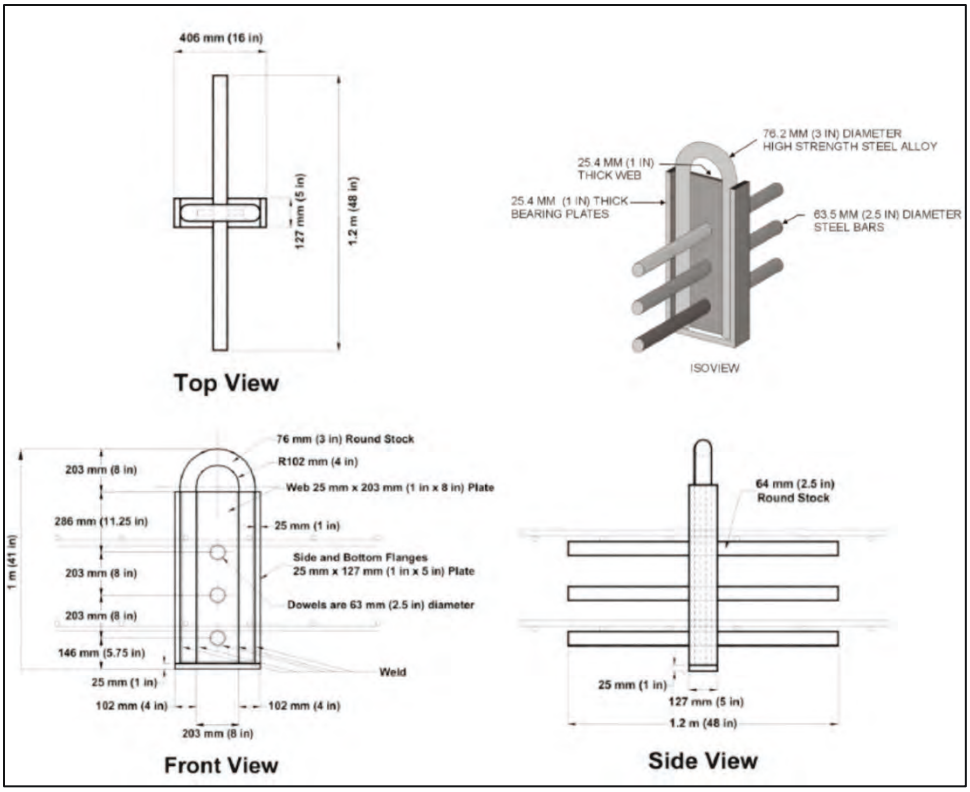

The model was constructed in Abaqus/CAE using half symmetry in *Z*. An isometric view of the model with transparency applied to the concrete is shown in Figure 16, and the finite element mesh is shown in Figure 17.

Figure 16. Isometric view of BHCTA model with transparency applied to concrete.

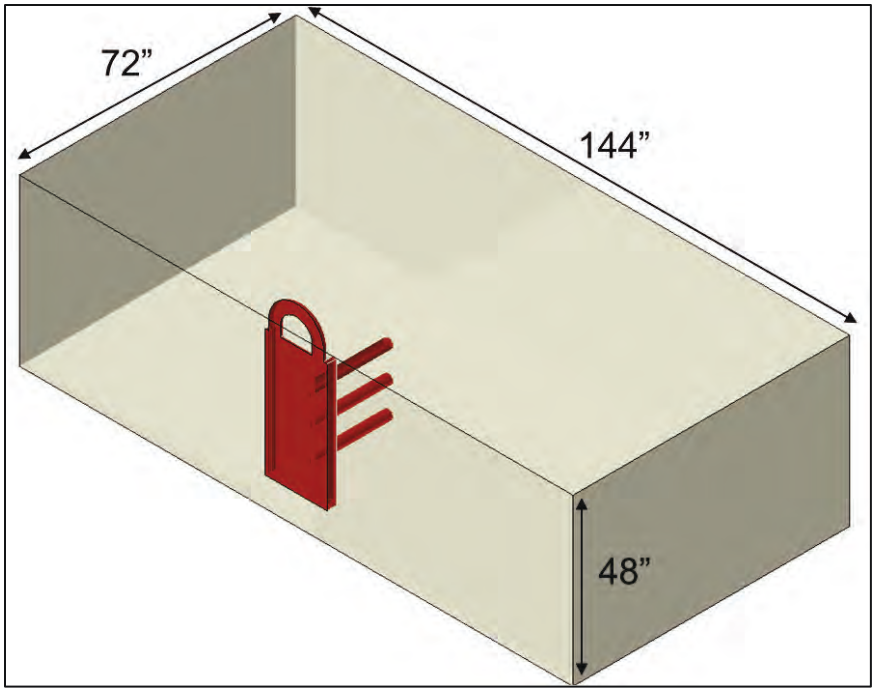

Figure 17. Isometric view of finite element mesh for BHCTA model.

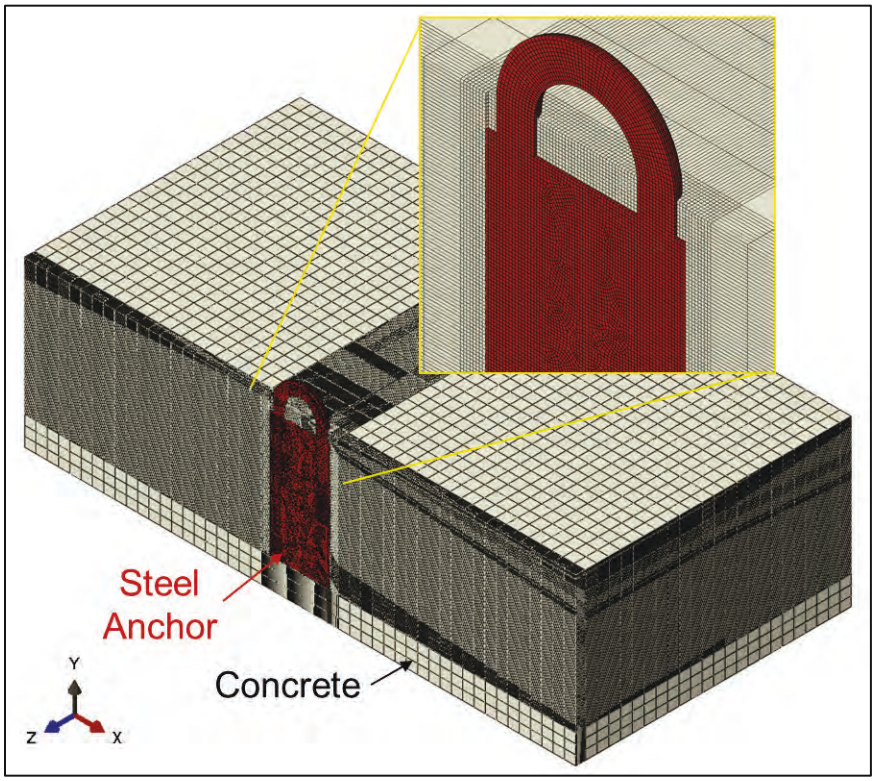

The Abaqus V6R2016 implicit (direct sparse) solver was used. Linear elastic, small-displacement theory was assumed. The mesh comprises solid (continuum), three-dimensional (3-D), 8-noded linear brick (hexahedral), reduced integration elements with hourglass control (type C3D8R). Typical mechanical properties for concrete and steel were used (see Table 4). The model contained a total of 674,704 elements and 721,433 nodes.

Table 4. Element type and material properties for BHCTA model.

Material	Number of elements	Elastic modulus (psi)	Poisson's ratio
Concrete	588,555	3.6×10^6	0.15
Steel	86,149	29×10^6	0.3

Boundary conditions for the BHCTA model are shown in Figure 18. *Z*-symmetry boundary conditions were applied to all nodes lying on the symmetry plane. All nodes on the $\pm x$ face and the $-z$ face were pinned, i.e., fixed.

The loads and constraints applied to the model are shown in Figure 19. A 50-kip load (equivalent to a 100-kip load without symmetry) was statically applied to an independent node, i.e., reference point (RP), located in the middle of the bent rod. A rigid spider element, i.e., multi-point constraint (MPC), was used to constrain the reference point to the bent rod. The embedded element technique was used to constrain the anchor to the concrete.

Contour plots of displacement are given in Figure 20 for the 90-deg load case and Figure 21 for the 20-deg load case. The maximum displacement for the 90-deg load is 0.0038 in., compared to 0.0065 in. for the 20-deg load case. However, the 90-deg load engages more of the slab, as shown by the larger extent of the displaced region.

Figure 18. Illustration of BHCTA model boundary conditions: (a) Z-symmetry boundary condition and (b) pinned boundary condition.

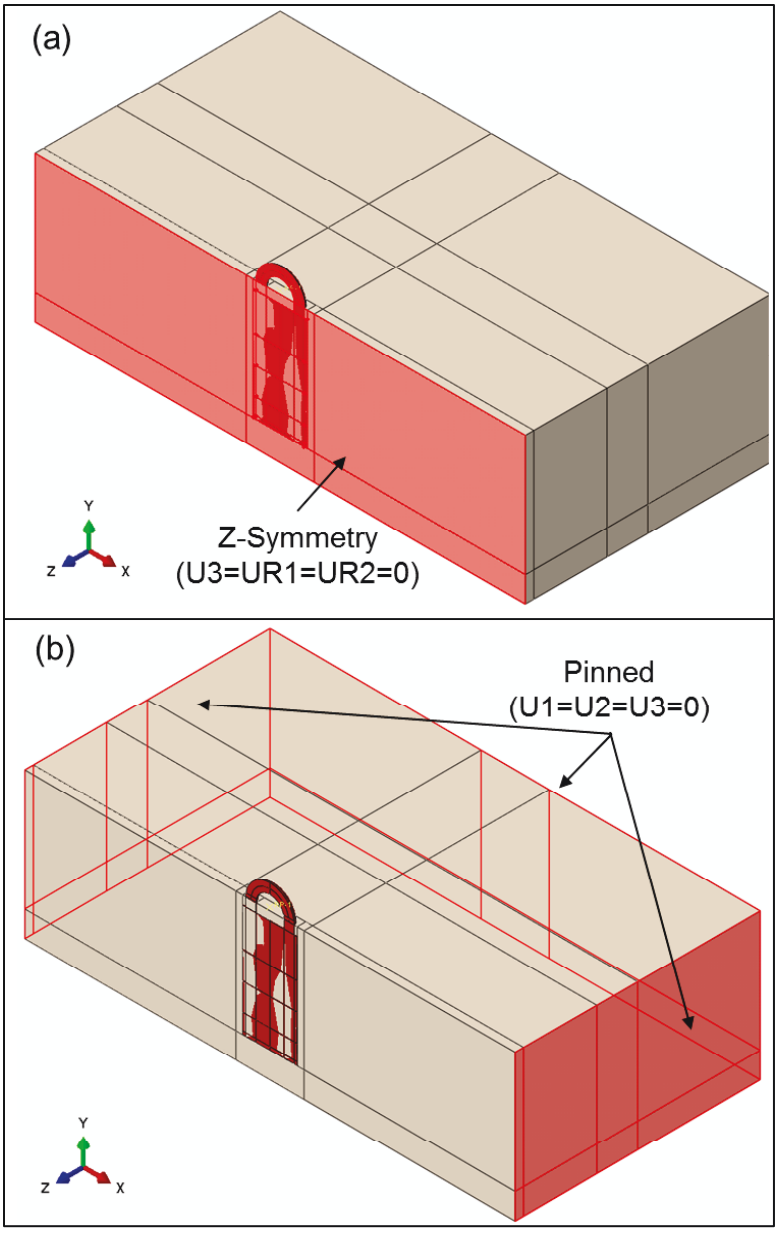

Figure 19. Loads and constraints applied to BHCTA model:
(a) 90-deg load case and (b) 20-deg load case.

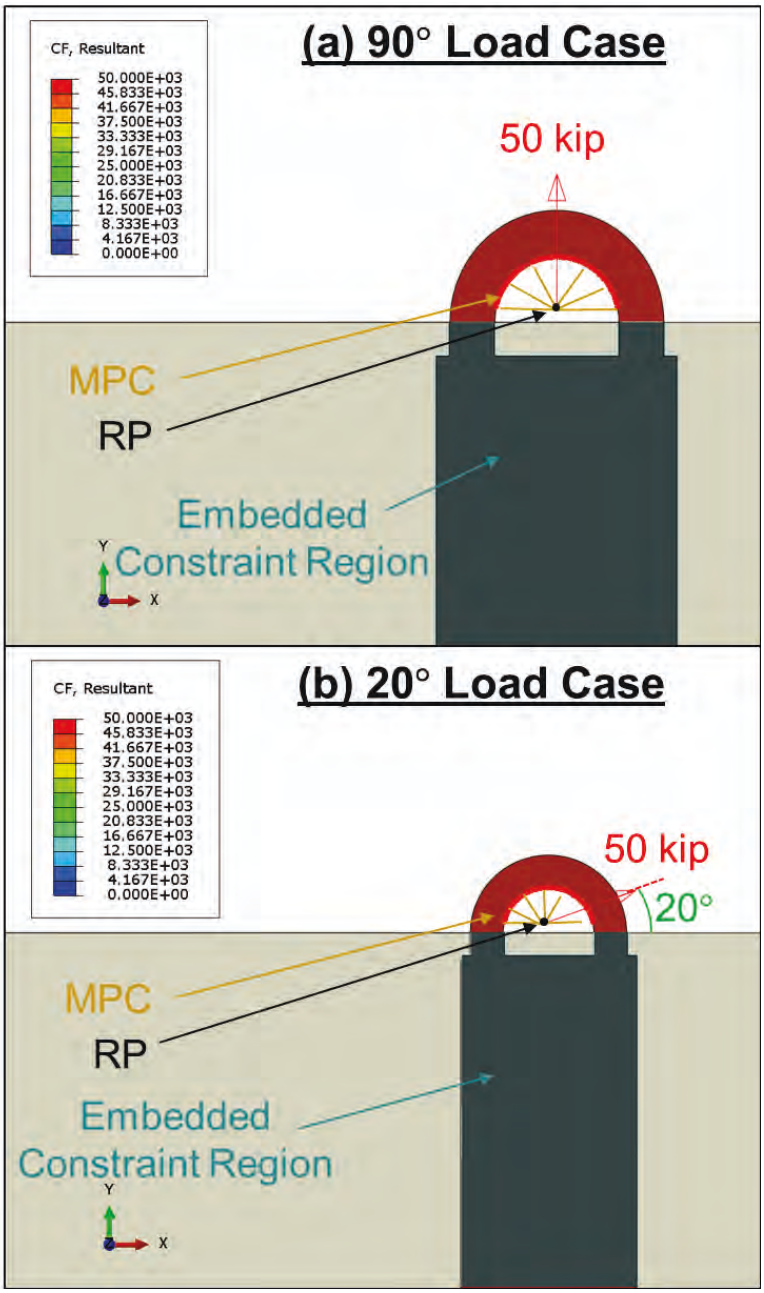

Figure 20. Isometric view of displacements, 90-deg load case for BHCTA model.

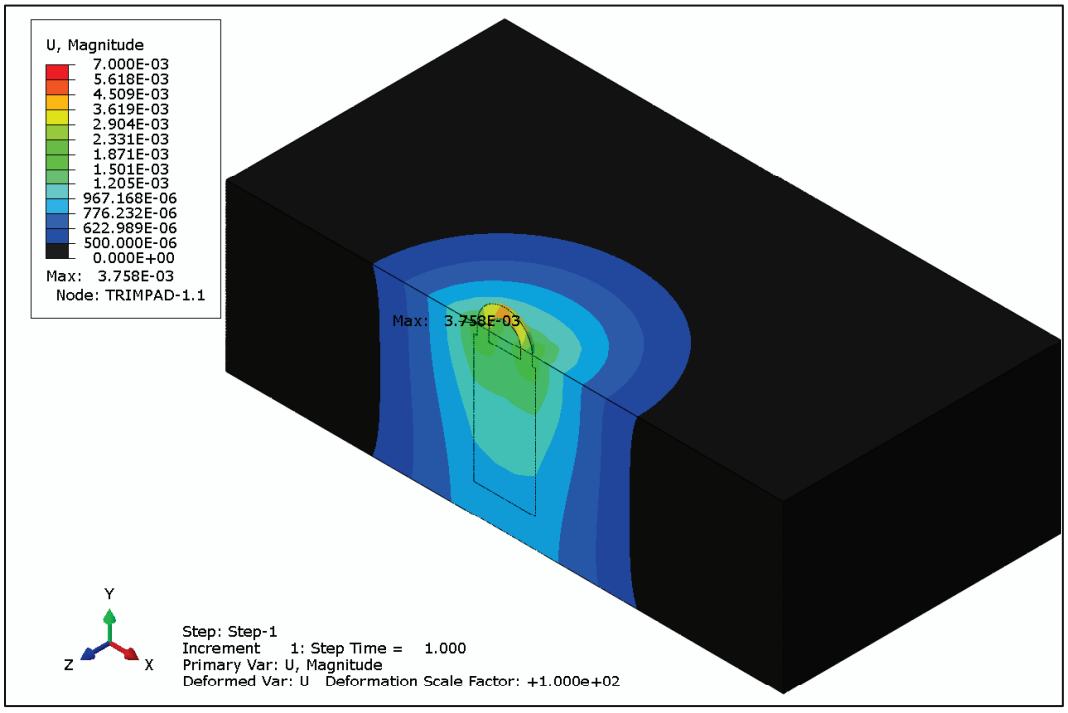

Figure 21. Isometric view of displacements, 20-deg load case for BHCTA model.

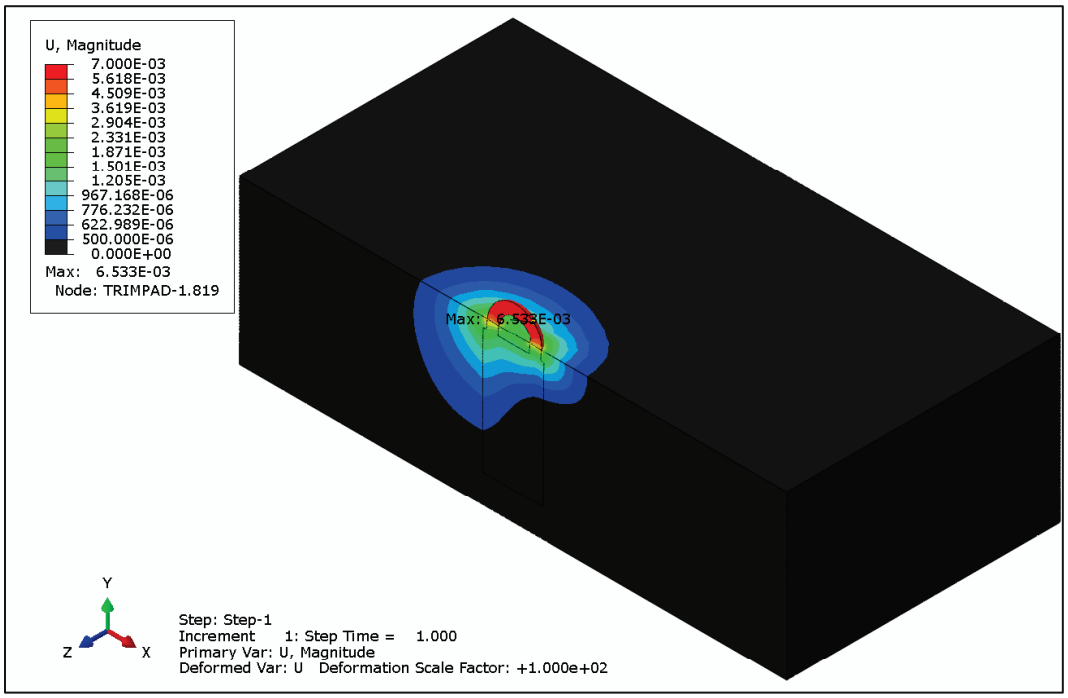

Figure 22 shows the displacement at the pavement surface along a line normal to the symmetry plane, while Figure 23 shows the displacement at the pavement surface along the line of symmetry. As noted before, the 20-deg load creates higher displacements near the anchor, but the 90-deg load results in higher displacements far from the anchor.

Figure 22. Comparison of BHCTA concrete surface displacements along Path *Z*.

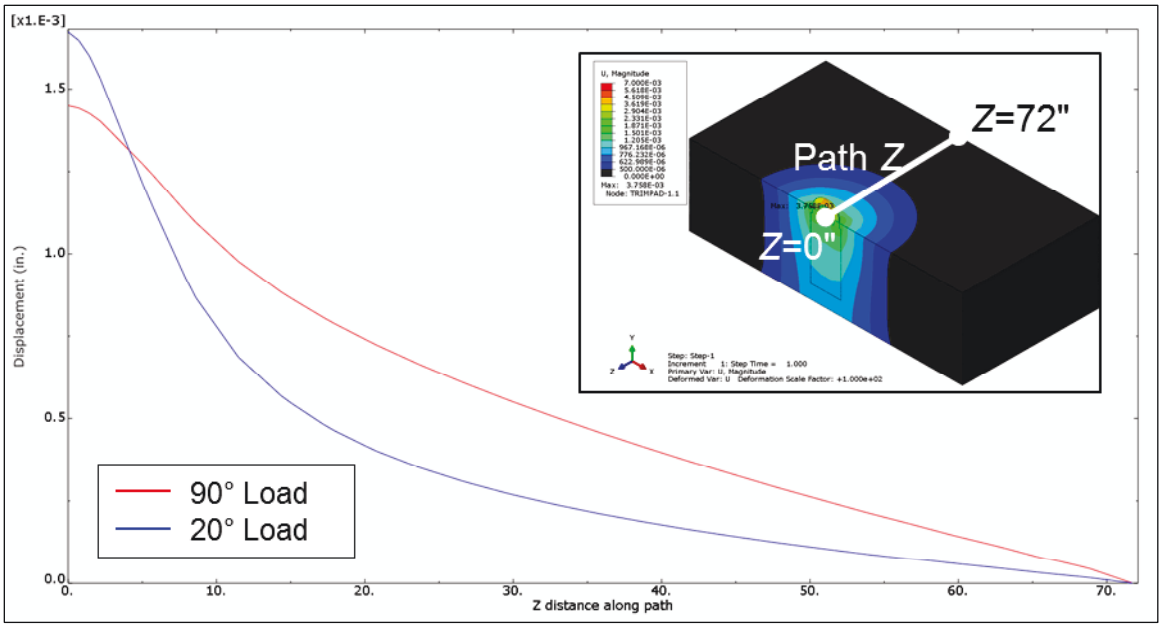

Figure 23. Comparison of BHCTA concrete surface displacements along Path *X*.

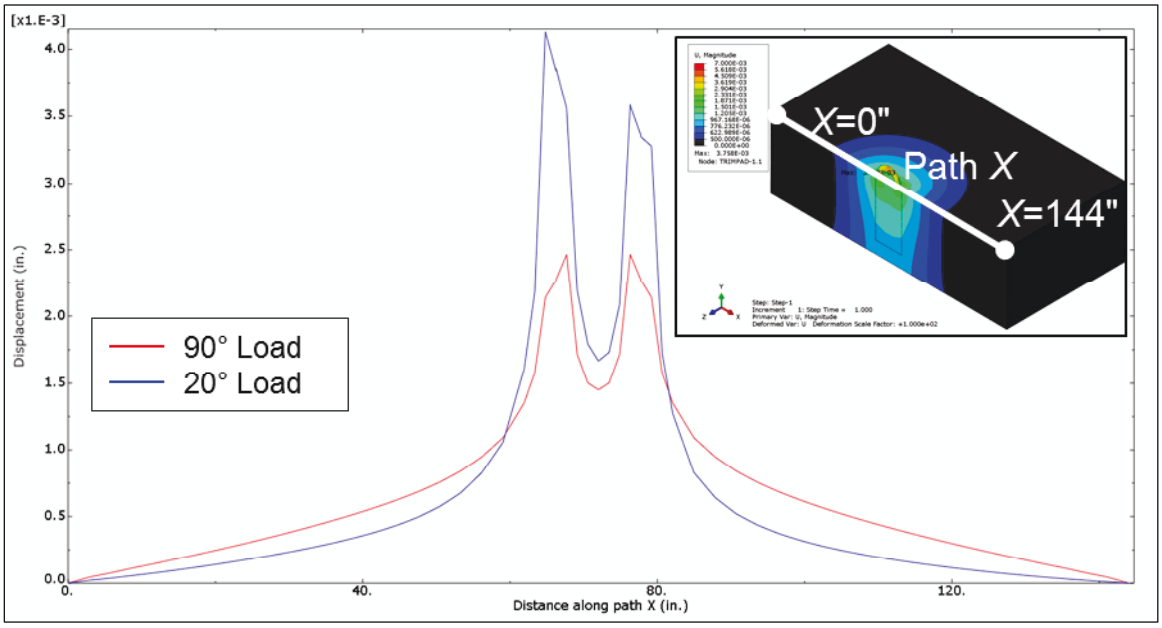

Figure 24 compares the von Mises stress in the steel anchor for the two load cases. The 20-deg load produces higher stresses compared to the 90-deg load. For both the 20-deg and 90-deg load cases, the most likely failure location is in the above-grade section of the 3-in. diameter bent rod.

Figure 24. Comparison of stresses in BHCTA for 90-deg and 20-deg load cases.

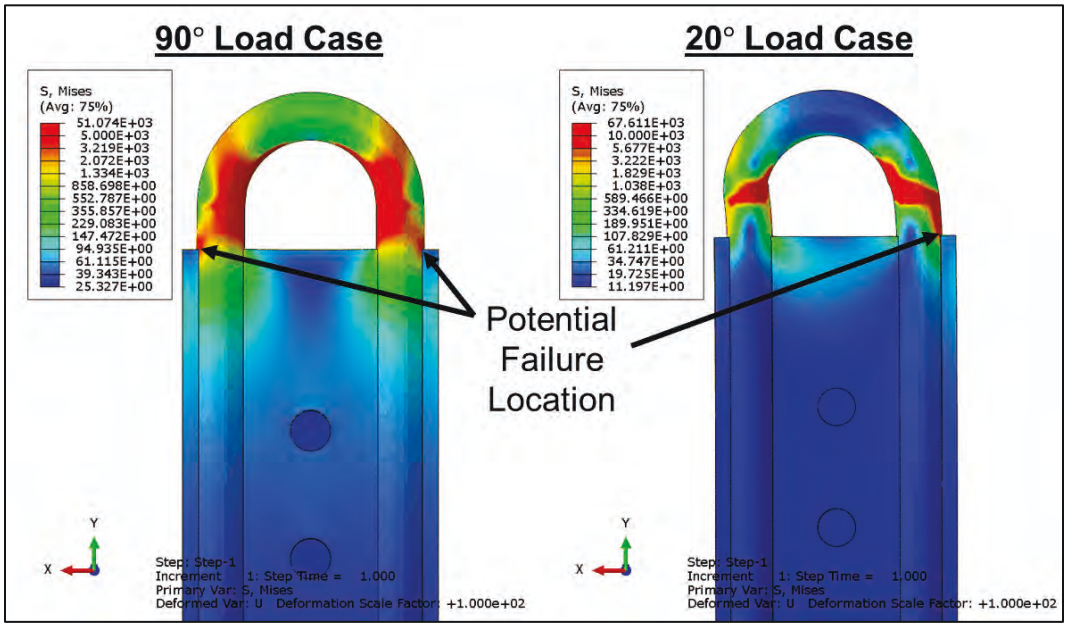

Contour plots of the maximum principal stress in the concrete are given in Figure 25 for the 90-deg load case and Figure 26 for the 20-deg load case. The 90-deg load case produces an uplift response with a symmetric distribution of principal stress in the concrete. The 20-deg load case has a large shear component, causing high stresses adjacent to the bent rod. To better compare the magnitude and extent of the stresses, plots of principal stress along the pavement surface are given. Figure 27 shows the maximum principal stress at the pavement surface along a line normal to the symmetry plane. The peak stresses for the two cases in this plot are comparable, but the 20-deg case produces higher stresses within a larger area. Figure 28 shows the maximum principal stress at the pavement surface along the line of symmetry. The 20-deg load produces the highest stresses on the left side of each rod (i.e., the side away from the direction of pull), with a high stress by the rear leg of the bent rod. In comparison, the 90-deg load results in equal stresses on each side of the rods.

Figure 25. Front view of concrete maximum principal stress, 90-deg load case for BHCTA model.

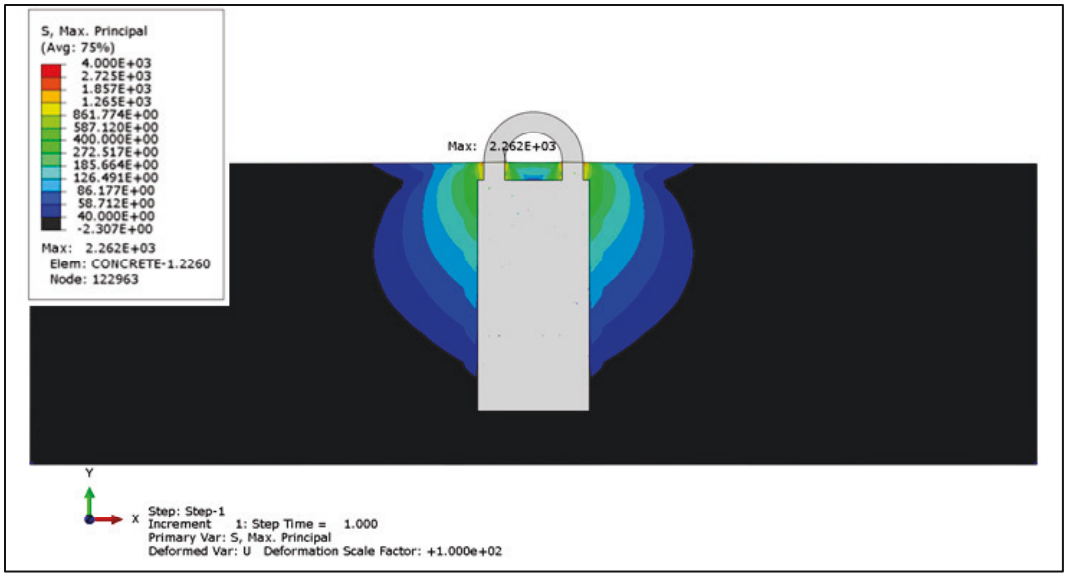

Figure 26. Front view of concrete maximum principal stress, 20-deg load case for BHCTA model.

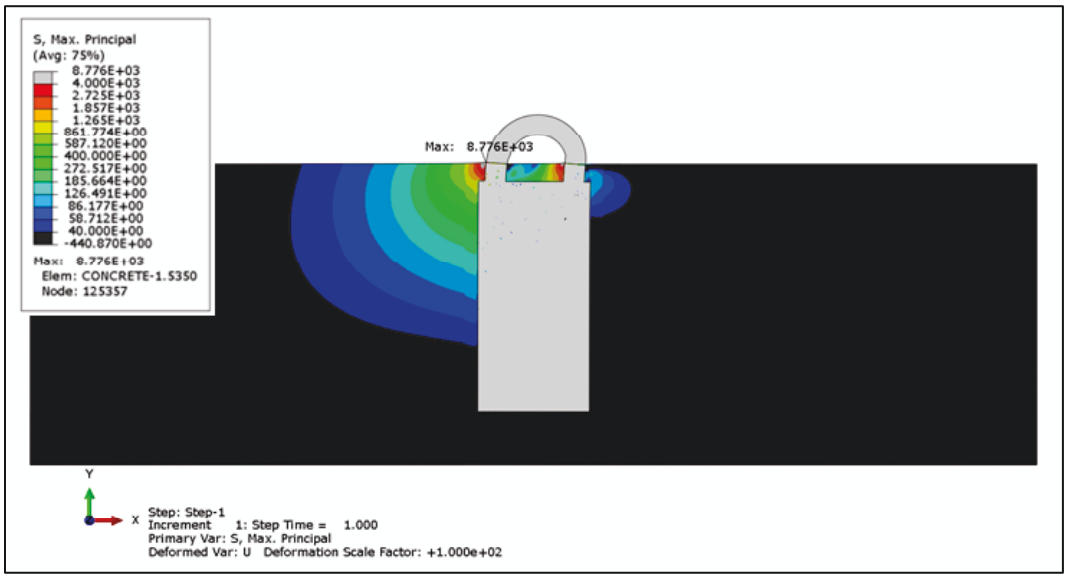

Figure 27. Comparison of BHTCA maximum principal stress at concrete surface along Path *Z*.

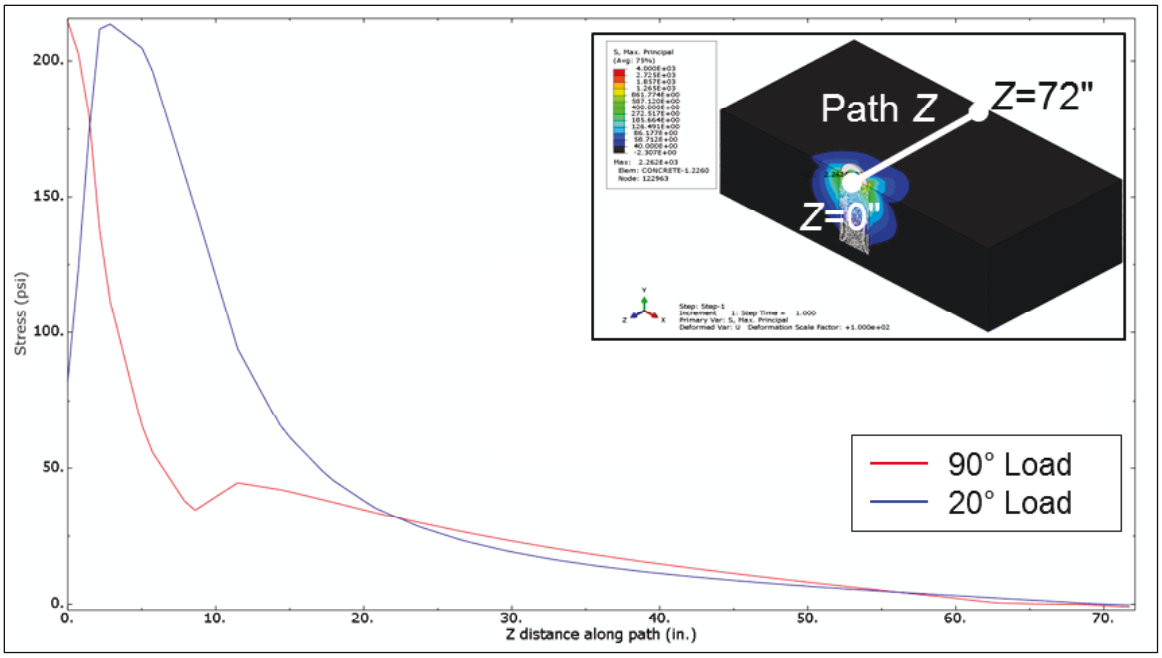

Figure 28. Comparison of BHTCA maximum principal stress at concrete surface along Path *X*.

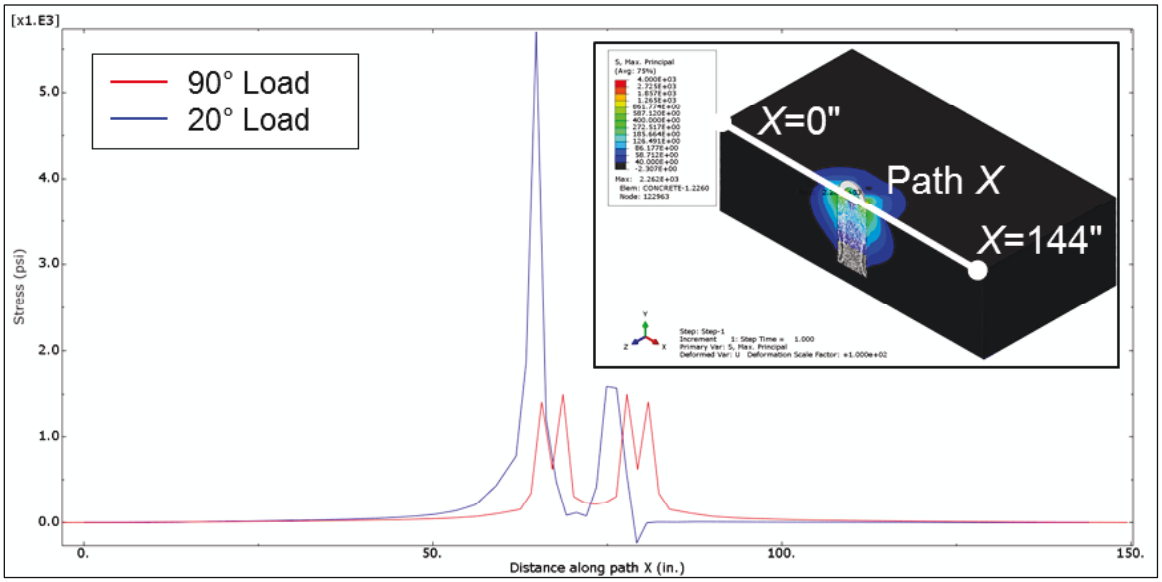

The 20-deg load case produces tensile stresses in the concrete of sufficient magnitude to create surface cracks in the concrete. These stresses are localized such that anchor pull-out is extremely unlikely. Surface cracking was observed around the trim pad anchor at Eglin AFB in the same area predicted by FEA (see Figure 29).

Figure 29. Comparison of cracking observed around trim pad anchor at Eglin AFB with analysis results (BHCTA, 20-deg load case).

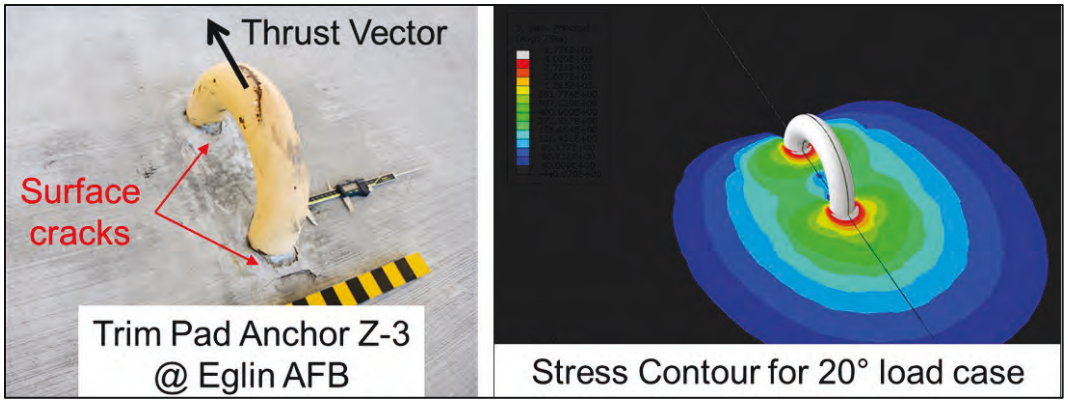

The 20-deg load produces higher stresses and larger displacements compared to the 90-deg load. However, for both load cases, the most likely failure location is in the above-grade section of the 3-in. diameter bent rod.

5.3.2 Omnidirectional thrust anchor

An FEA model of an omnidirectional thrust anchor (OTA) was constructed using Dannelly Field trim pad construction drawings (Capt A. W. Sanders, pers. comm., 15 March 2017), shown in Figure 30.

Figure 30. Dannelly Field OTA drawing (Capt A. W. Sanders, pers. comm., 15 March 2017).

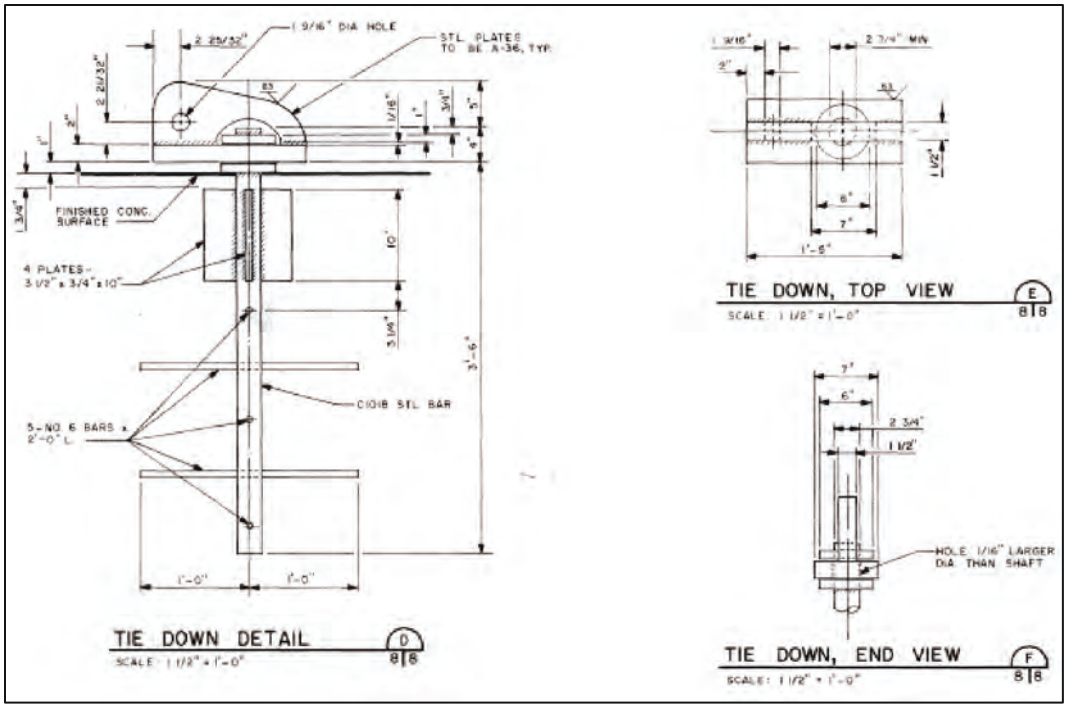

The model was constructed in Abaqus/CAE using half symmetry in *Z*. An isometric view of the model with transparency applied to the concrete is shown in Figure 31, and the finite element mesh is shown in Figure 32.

Figure 31. Isometric view of OTA model with transparency applied to concrete.

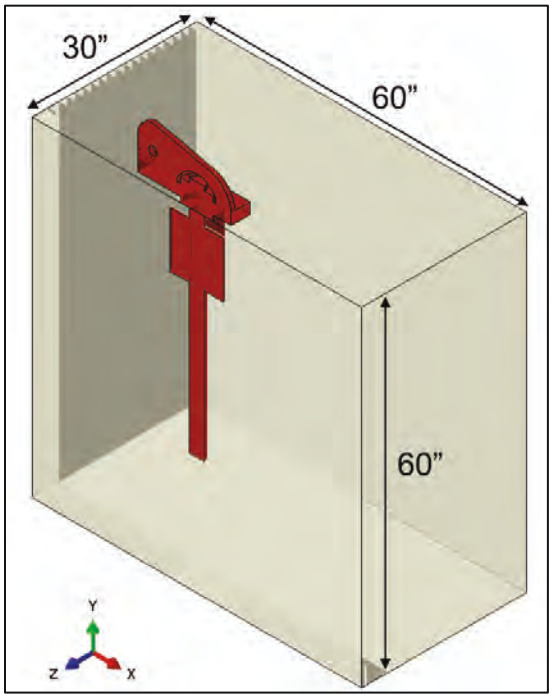

Figure 32. Isometric view of finite element mesh for OTA model.

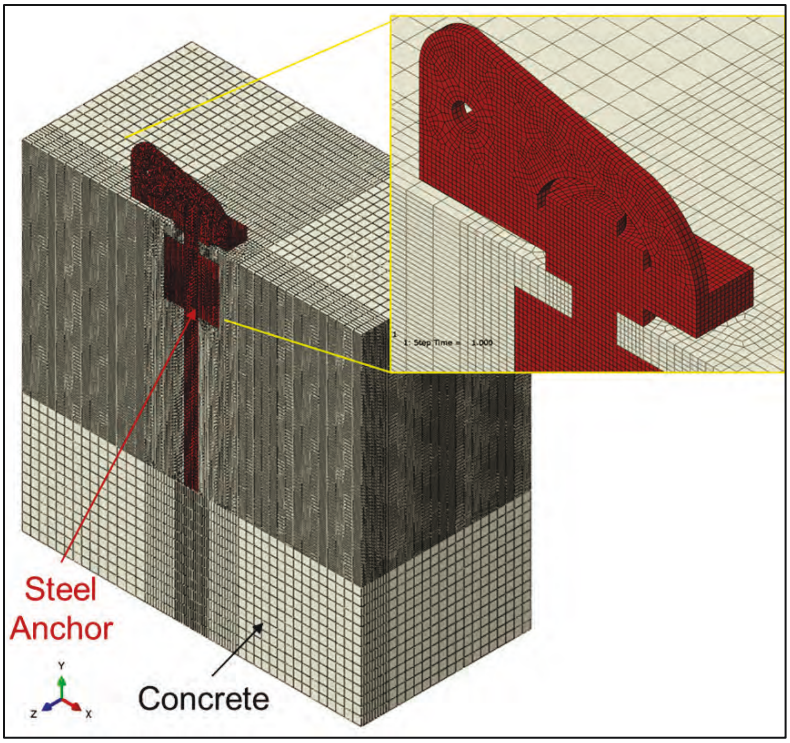

The Abaqus V6R2016 implicit (direct sparse) solver was used. Linear elastic, small-displacement theory was assumed. The mesh comprises solid (continuum), 3-D, 8-noded linear brick (hexahedral), reduced integration elements with hourglass control (type C3D8R). Typical mechanical properties for concrete and steel were used (see Table 5). The model contained a total of 404,610 elements and 432,112 nodes.

Table 5. Element type and material properties for OTA model.

Material	Number of elements	Elastic modulus (psi)	Poisson's ratio
Concrete	374,166	3.6×10^6	0.15
Steel	30,444	29×10^6	0.3

Boundary conditions for the OTA model are shown in Figure 33. *Z*-symmetry boundary conditions were applied to all nodes lying on the symmetry plane. All nodes on the $\pm x$ face and the $-z$ face were pinned, i.e., fixed.

Figure 33. Illustration of OTA model boundary conditions: (a) Z-symmetry boundary condition and (b) pinned boundary condition.

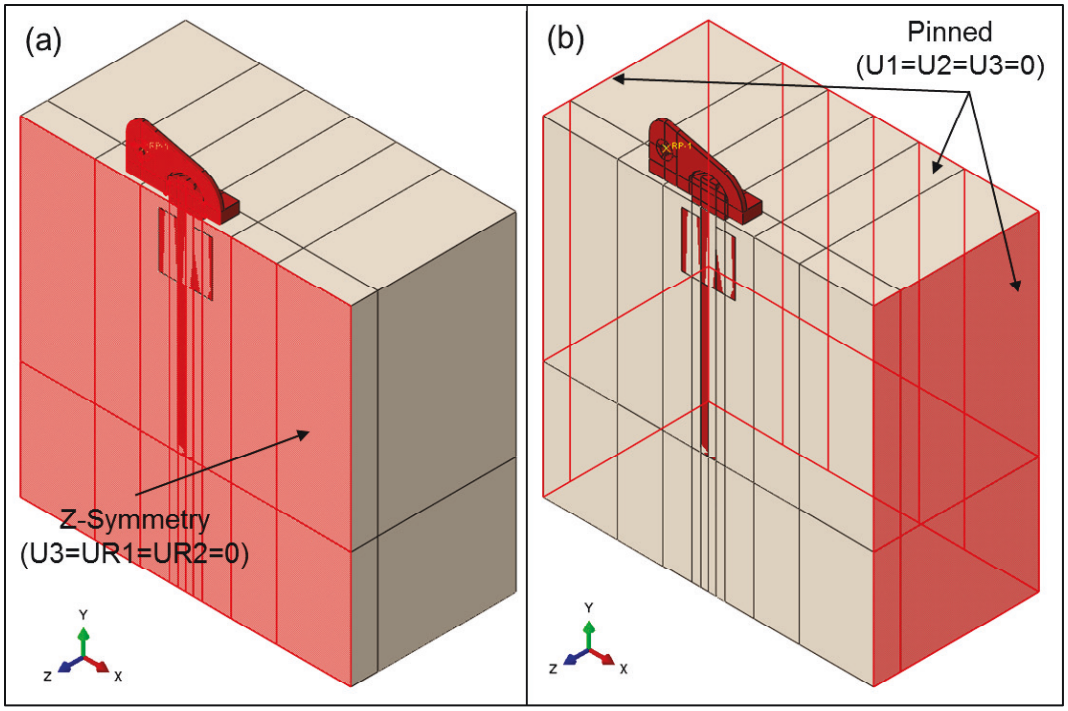

The loads and constraints applied to the model are shown in Figure 34. A 50-kip load (equivalent to a 100-kip load without symmetry) was statically applied to an independent node (RP) located in the middle of the load eye. A rigid spider element (MPC) was used to constrain the reference point to the load eye. The embedded element technique was used to constrain the anchor to the concrete.

Contour plots of displacement are given in Figure 35 for the 90-deg load case and Figure 36 for the 20-deg load case. Notice that the attachment plate with the load eye rotates in opposite directions for the two load cases. The maximum displacement for the 90-deg load is 0.025 in., compared to 0.030 in. for the 20-deg load case. The 90-deg load engages slightly more of the slab, though the overall extent of displacement is fairly similar.

Figure 34. Loads and constraints applied to OTA model:
(a) 90-deg load case and (b) 20-deg load case.

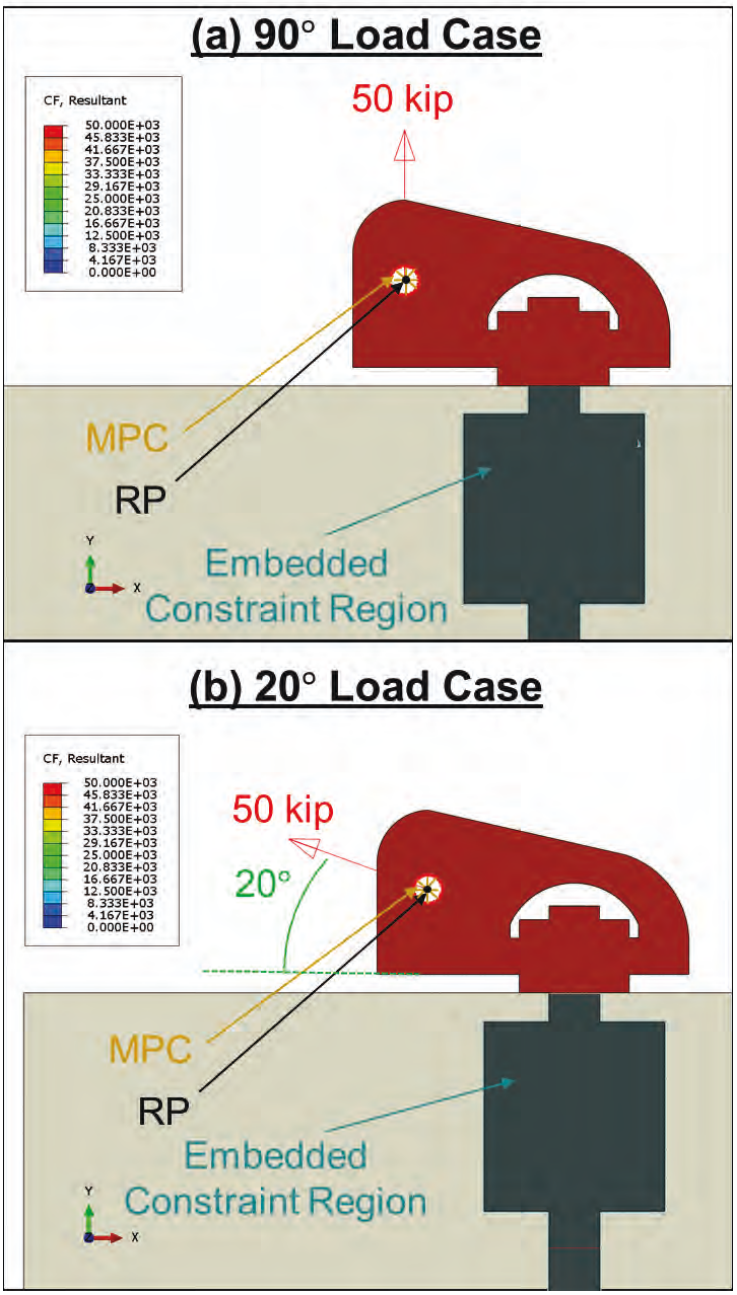

Figure 35. Isometric view of displacements, 90-deg load case for OTA model.

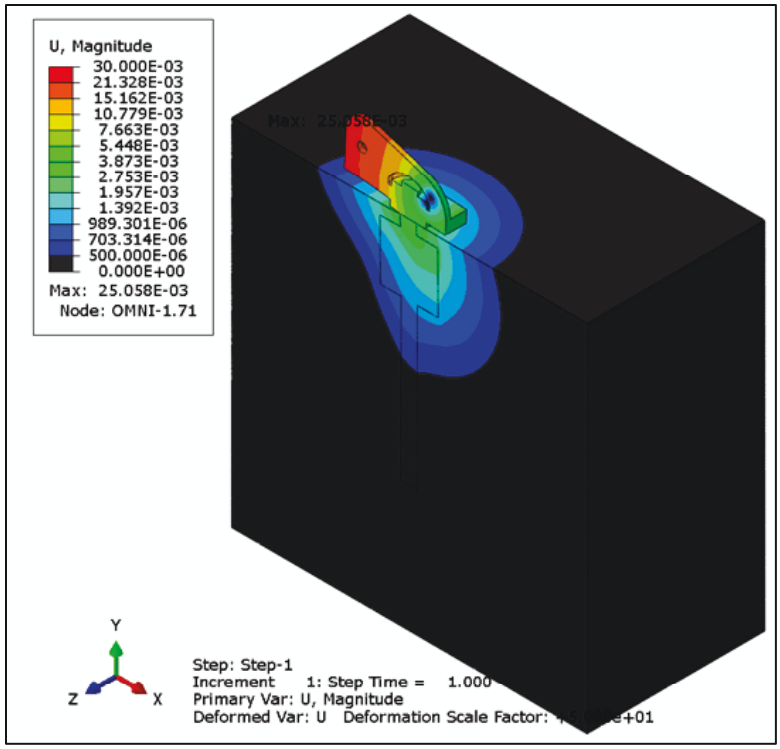

Figure 36. Isometric view of displacements, 20-deg load case for OTA model.

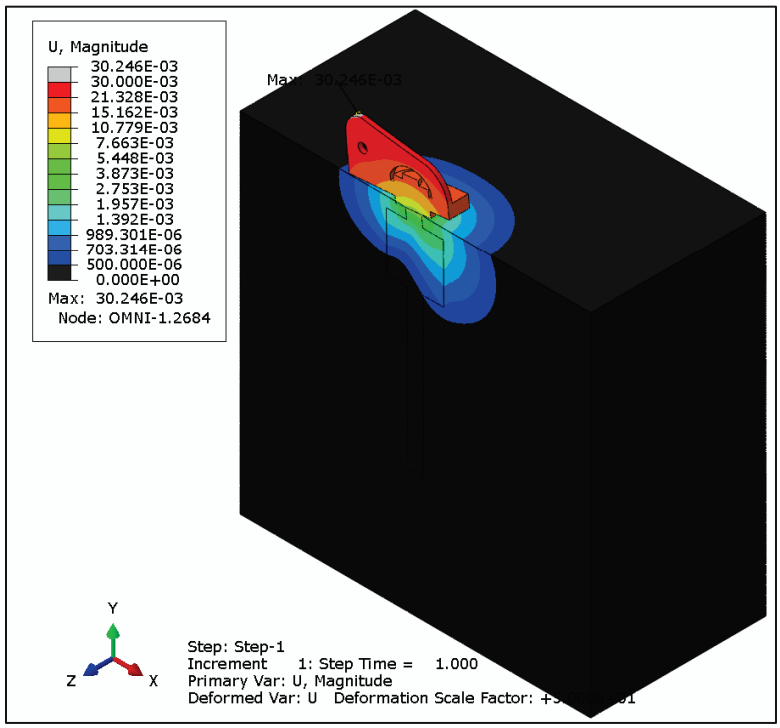

Figure 37 shows the displacement at the pavement surface along a line normal to the symmetry plane. Figure 38 shows the displacement at the pavement surface along the line of symmetry. The 20-deg load creates slightly higher displacements near the anchor, but the displacements are comparable farther from the anchor. The Path *X* plot (Figure 38) shows differences in displacement on either side of the rod that are caused by bending in the rod.

Figure 37. Comparison of OTA concrete surface displacements along Path *Z*.

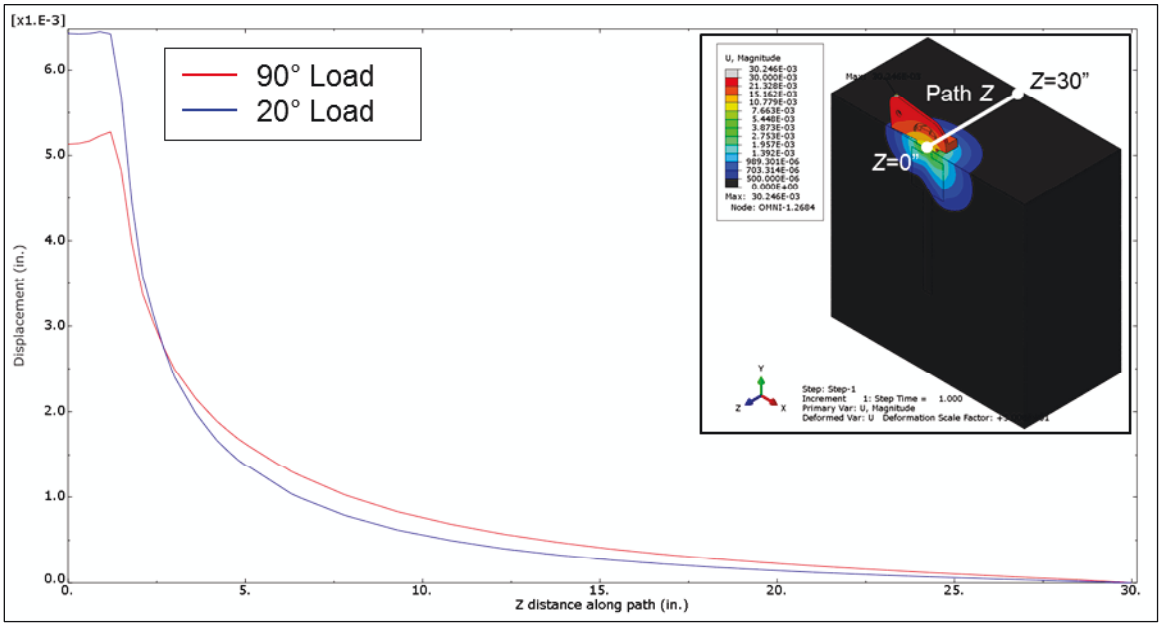

Figure 38. Comparison of OTA concrete surface displacements along Path *X*.

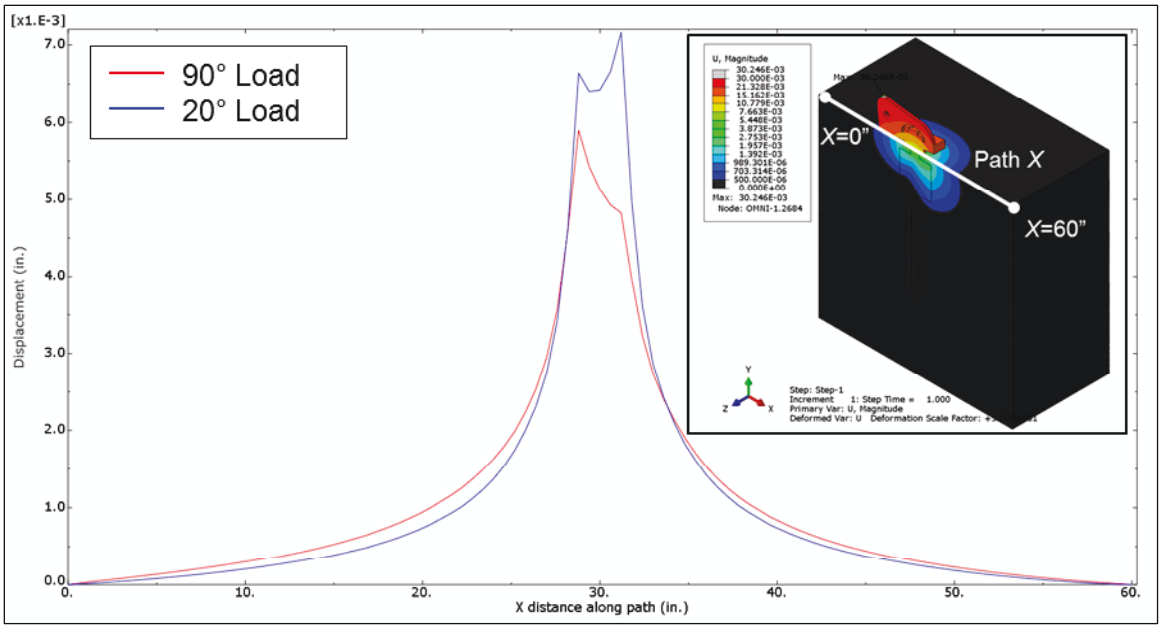

Figure 39 compares the von Mises stresses in the anchor for the two load cases. Note that the method used to apply the load creates artificially high stresses around the loading eye, since the inner surface of the loading eye is constrained to remain circular. The 20-deg load produces marginally higher stresses compared to the 90-deg load. For both cases, the most likely failure location is in the 2.75-in. diameter rod.

Figure 39. Comparison of stresses in OTA for 90-deg and 20-deg load cases.

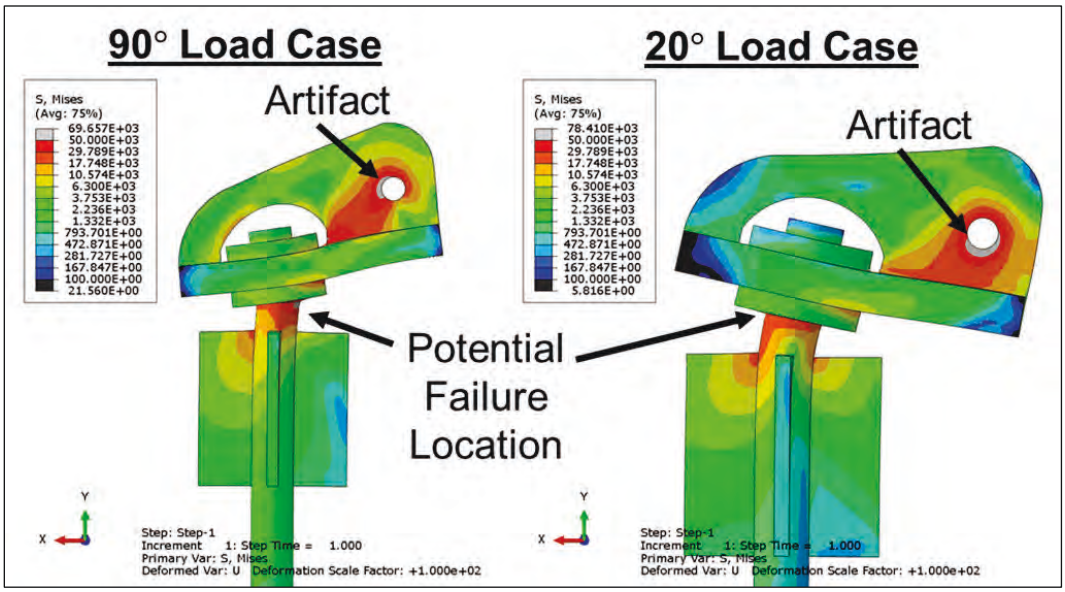

Contour plots of the maximum principal stress in the concrete are given in Figure 40 for the 90-deg load case and Figure 41 for the 20-deg load case. To better compare the magnitude and extent of the stresses, plots of principal stress along the pavement surface are given. Figure 42 shows the maximum principal stress at the pavement surface along a line normal to the symmetry plane. The curves for the two cases are fairly similar, though the 20-deg load case produces a slightly higher peak stress. Figure 43 shows the maximum principal stress at the pavement surface along the line of symmetry. The highest concrete stresses occur in the same location for both cases.

Figure 40. Front view of concrete maximum principal stress, 90-deg load case for OTA model.

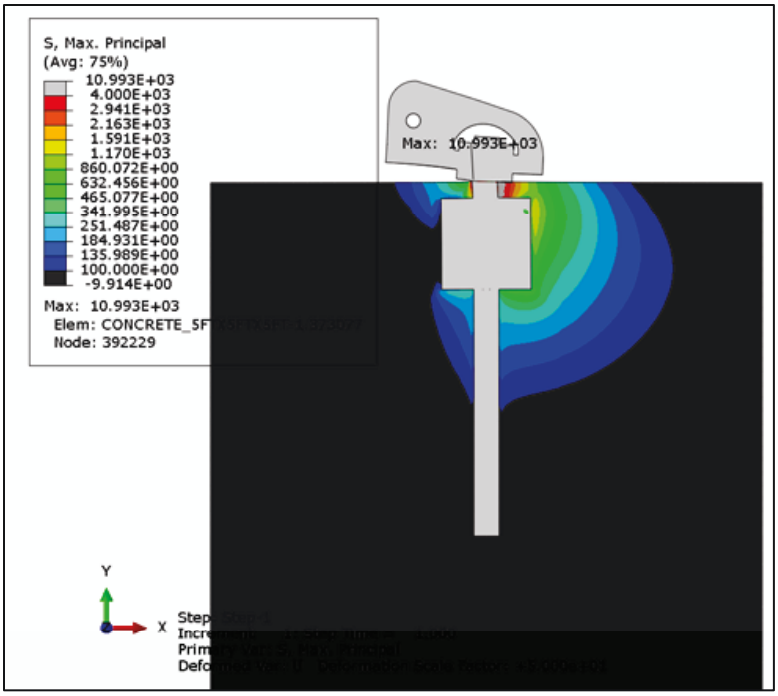

Figure 41. Front view of concrete maximum principal stress, 20-deg load case for OTA model.

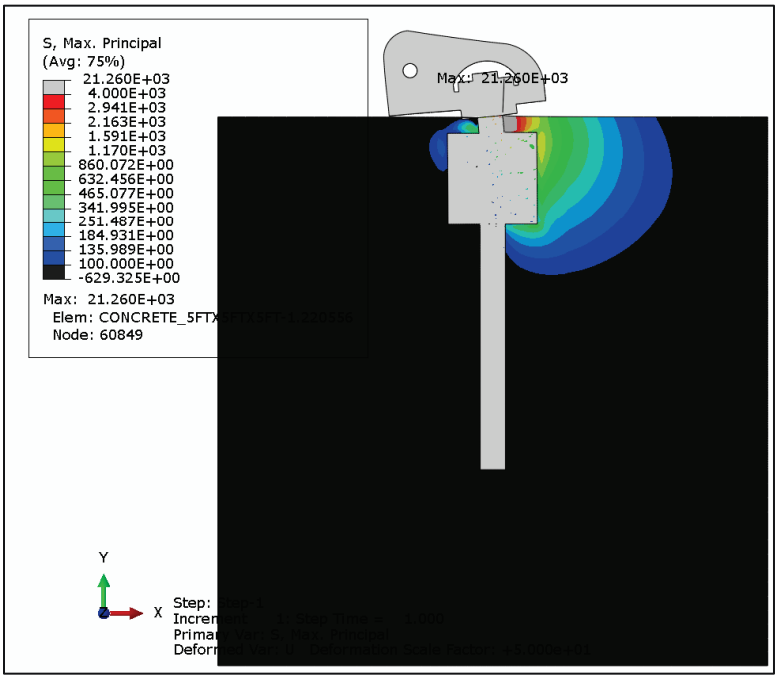

Figure 42. Comparison of OTA maximum principal stress at concrete surface along Path *X*.

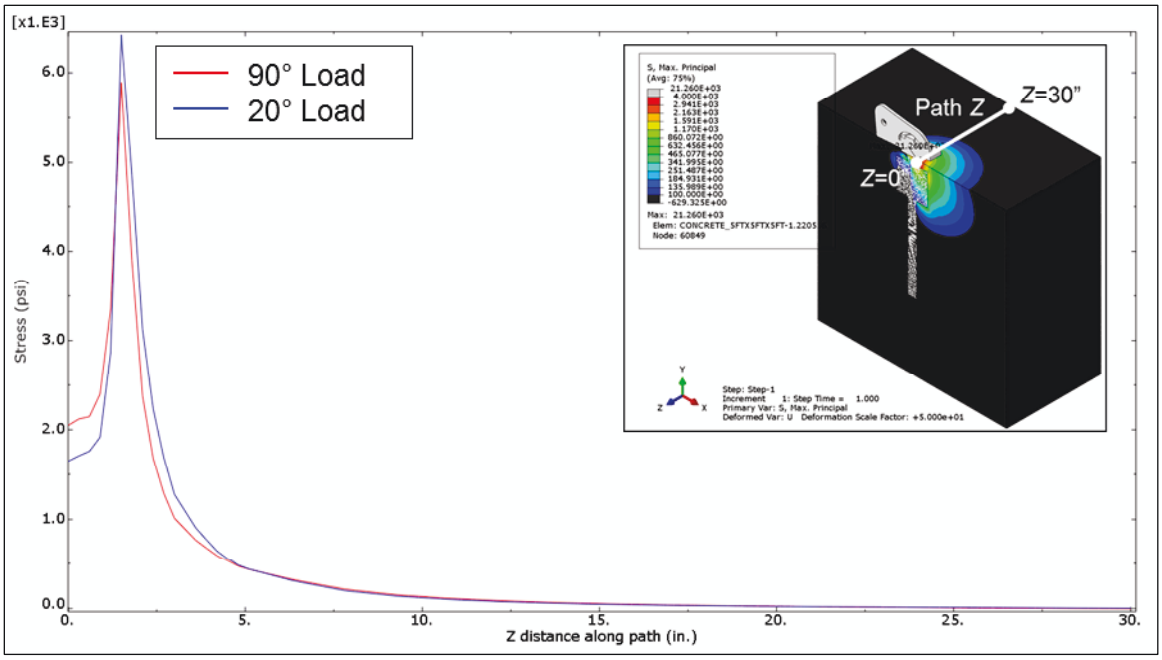

Figure 43. Comparison of OTA maximum principal stress at concrete surface along Path *Z*.

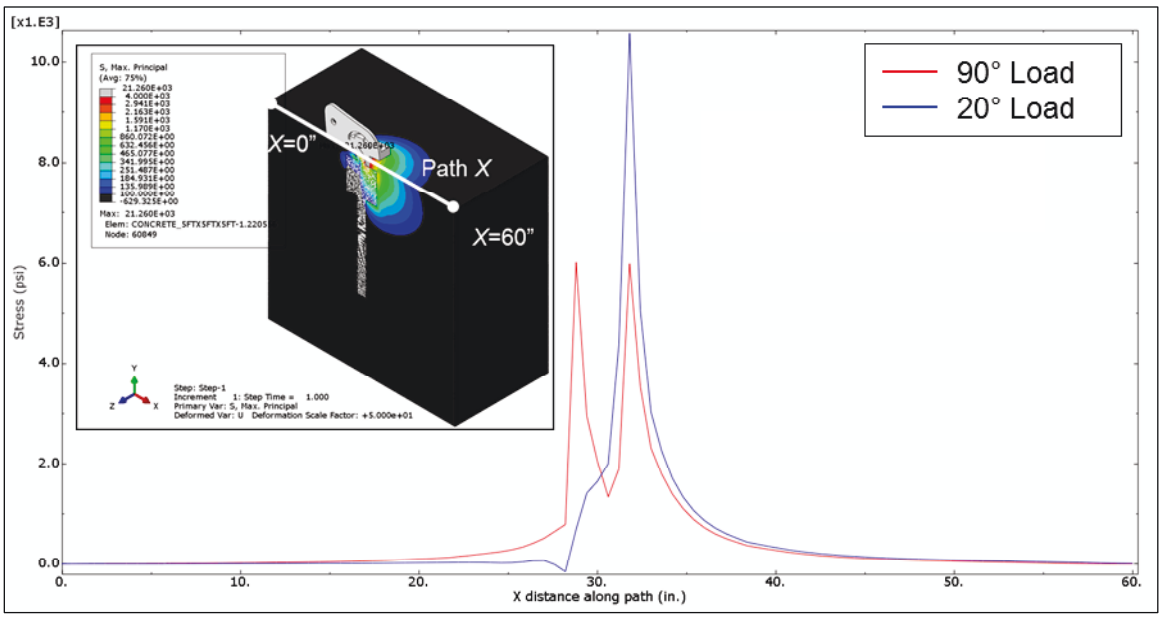

5.3.3 Summary

A preliminary finite element analysis was conducted to compare the effects of 90-deg and 20-deg angles of loading on two trim pad anchor designs. The preliminary results suggest the following:

- Loading thrust anchors at 90 deg produces similar results compared to loading at 20 deg.
- Failure is expected to occur via the same mode and at the same location for both load angles.
- Loading applied at 20 deg generates higher stresses than the same load applied at 90 deg.

If a 90-deg load angle is to be used for proof testing, the load magnitude will need to be increased by some (yet to be determined) factor such that equivalent stresses from a 20-deg load are produced. Prior to making a decision regarding the load angle to be used for proof testing, a more detailed nonlinear analysis should be performed, which includes the pin connection and contact. Other types of anchors could also be included as desired.

6 Lightweight Anchor Inspection Kit (LAIK) Design Evolution

A number of concepts were considered during the design phase of this project. This chapter provides an overview of the ideas considered and the design constraints and decisions that led to the final design.

6.1 Sling concept

A number of the concepts draw inspiration from the current test method described in ETL 00-2 (Department of the Air Force 2000). This setup uses either a forklift or crane to lift on a sling assembly which runs between the anchor to be tested and a deadman anchor. The current test requires heavy equipment, and uses a heavy (32 in. by 52 in. by 1 in. thick) steel plate for the deadman anchorage. Therefore, the design process began by attempting to optimize the load application and deadman anchor (reaction) portions of the current system.

Figure 44. Current test method shown with forklift configuration (Department of the Air Force 2000).

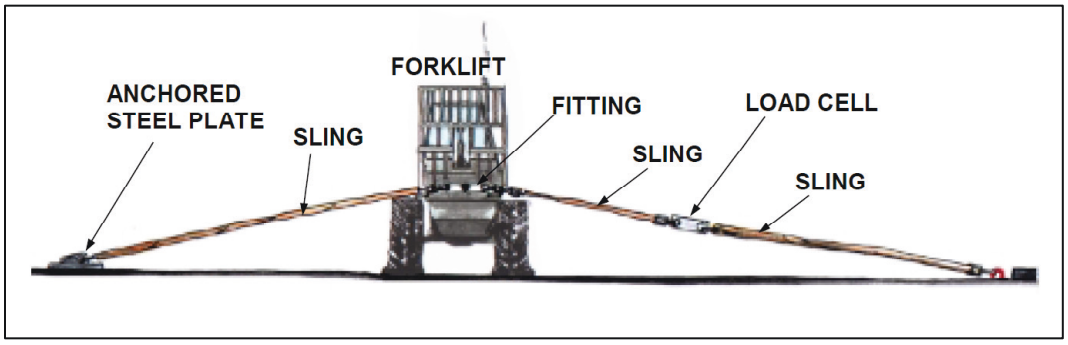

6.1.1 Center jack variant

The load could be applied with a jack or hydraulic cylinder (Figure 45), replacing the heavy equipment. The test rig is conceptually a king post truss, and the use of compression/tension members allows for efficient, lightweight elements. A jack with a capacity of at least 35 tons would be required to achieve a sling tension of 100 kips at β = 20 deg. The available stroke is also critical to ensure that the slack can be taken up and the sling tensioned to the desired load. Finally, the angle of loading changes as the load is increased.

The reaction would require installing an anchor to resist uplift and horizontal forces. The setup, as shown in Figure 45, requires distances L_1 and L_2 be equal, or there will be unbalanced lateral forces and an overturning moment acting on the jack.

Figure 45. Sling concept with center jack.

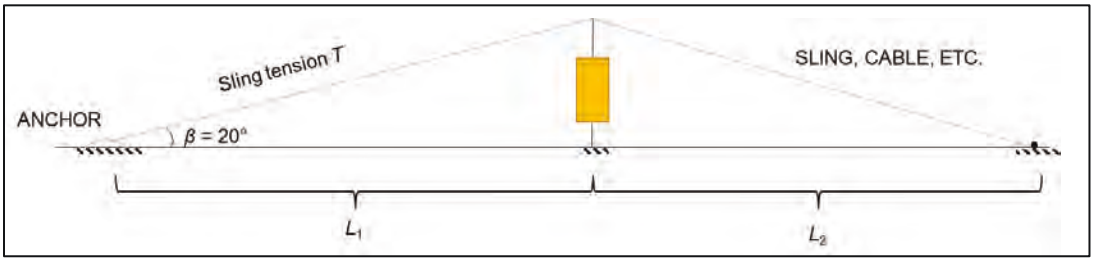

6.1.2 Inline jack variant

If the jack is placed in line with the sling (Figure 46), the jack stroke is directly applied to the sling. Also, the sling will maintain a constant angle throughout the loading process. However, the required jack capacity is now equal to the desired sling tension, 100 kips.

This variant also requires an anchor for reacting uplift and horizontal forces. The same overturning concern also apples: if $L_1 \neq L_2$, lateral forces are unbalanced and an overturning moment acts on the vertical support.

Figure 46. Sling concept with inline jack.

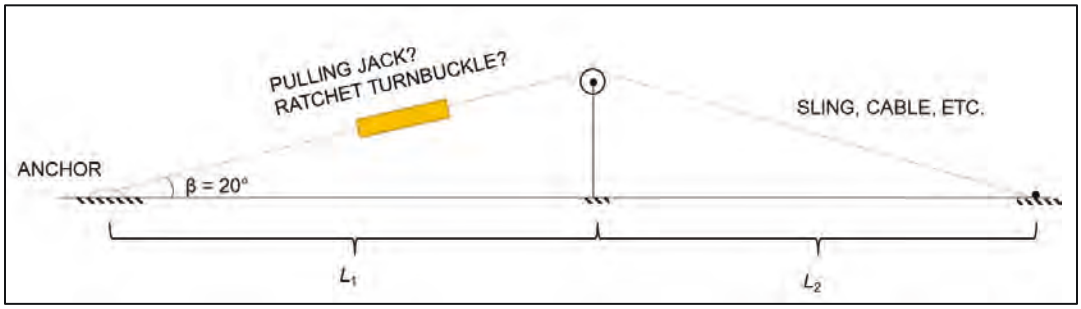

6.1.3 Expedient deadman anchor

Both of the concepts from Sections 6.1.1 and 6.1.2 require the installation of a deadman anchor. The use of an existing expedient airfield anchor design was considered. Information and capacities for several of these anchors, as well as an anchor design currently in development (C-130 Talon), are given in Table 6.

Table 6. Expedient anchors, current and under development. Current anchor test results from unpublished draft report.*

Anchor type	Core diameter (in.)	Cross rod diameter (in.)	Cross rod min. yield (ksi)	Average test load[1] (kip)	Observed failure mode
Universal PCC	6	1.5	60.5	69.0	No failure[2]
Universal PCC	8	1.5	60.5	70.8	No failure[2]
Modified Universal PCC	6	1	60.5	63.6	Cross rod bent, cracks in PCC
Universal Adapter w/ Tri-Talon	6	1.5	60.5	45.1	Spalling in soil plug and PCC
C-130 Talon[3]	12	0.875	55.8	No test data	N/A

[1] All tests performed at 60 deg relative to pavement surface.

[2] Tests were terminated after reaching roughly 70 kips.

[3] Currently in development.

All of these anchor designs incorporate deployable talons to increase pullout resistance. Four of the anchors are designed for the talons to bear on the bottom of a portland cement concrete (PCC) slab. These are the Universal PCC, Modified Universal PCC, and C-130 Talon anchors. An example of these box-type anchors with talons is shown in Figure 47. At the time of this writing, the C-130 Talon anchor is being developed. The Tri-Talon anchor consists of a rod with deployable talons, creating a soil plug to resist uplift (Figure 48). The Tri-Talon was tested with a Universal Adaptor attached at its top to provide a mooring connection.

Unfortunately, no test data were available for loads greater than about 70 kips, so the suitability of these anchors for the 100-kip proof load was unknown. Therefore, the design of an expedient anchorage was also undertaken.

* G. J. Norwood and C. J. Jackson, 2012. Air Force Tie-down Research – Phase II. Unpublished draft report prepared by Applied Research Associates (ARA) for ERDC. Applied Research Associates, P.O. Box 40128, Tyndall Air Force Base, FL 32403.

Figure 47. Universal PCC anchor for 6-in. core.*

* G. J. Norwood and C. J. Jackson, 2012. Air Force Tie-down Research – Phase II. Unpublished draft report prepared by Applied Research Associates (ARA) for ERDC. Applied Research Associates, P.O. Box 40128, Tyndall Air Force Base, FL 32403.

Figure 48. Tri-Talon schematic.*

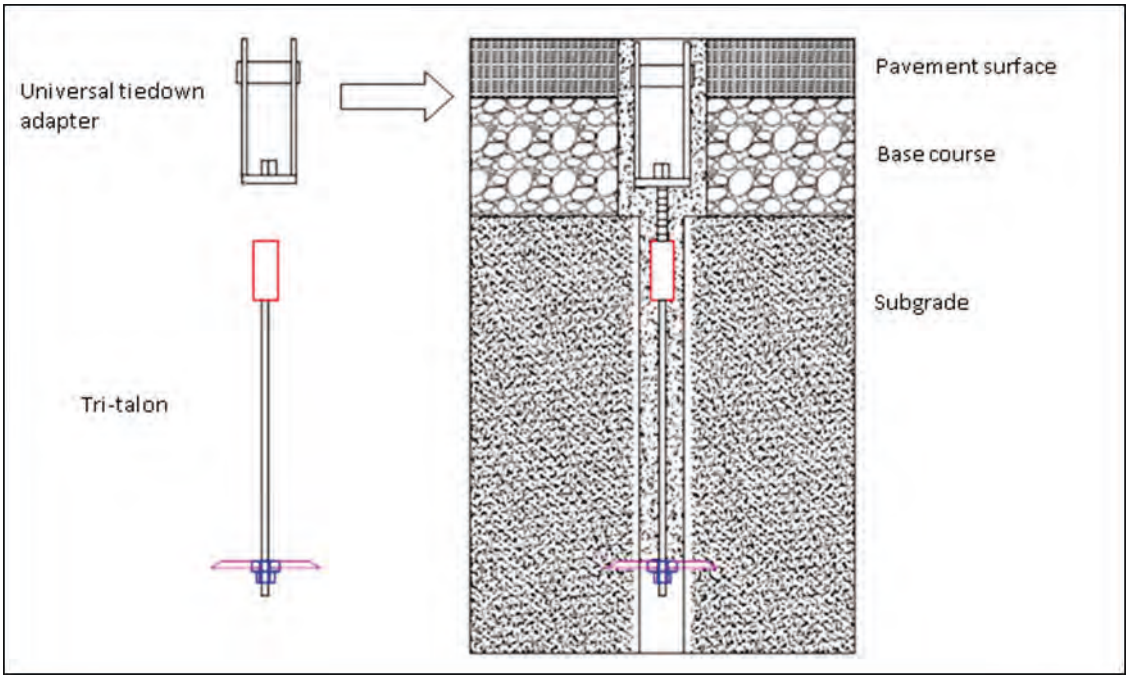

6.2 In-joint anchor concept

All of the anchors listed in Section 6.1.3 require relatively large diameter cored holes. Another concept considered using saw cuts or pavement joints for placing the anchorage. A pavement joint, in particular, has the advantage of requiring minimal damage to the pavement, apart from removal of the joint sealant. However, the design of an anchorage for a joint presents several challenges. The in-joint anchor is inherently prone to overturning and possible pullout from the joint, even under horizontal loading only. A horizontal load on such a device will always have some eccentricity (Figure 49).

* G. J. Norwood and C. J. Jackson, 2012. Air Force Tie-down Research – Phase II. Unpublished draft report prepared by Applied Research Associates (ARA) for ERDC. Applied Research Associates, P.O. Box 40128, Tyndall Air Force Base, FL 32403.

Figure 49. Diagram of in-joint anchor.

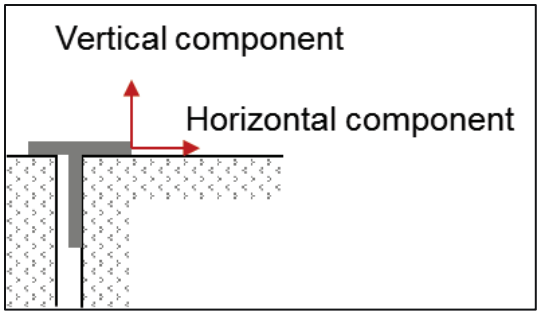

Application of a vertical load worsens the situation, since the joint anchor has no way (other than friction) to resist vertical forces unless part of the anchor is wedged underneath the slab. Also, joint width tends to vary significantly from site to site, making the design of an anchor to fit snugly in the joint impractical, since tight tolerances would be required to guarantee secure anchorage. Installing an undercut device in the joint would preclude the anchor from being installed without damaging the slab.

The design concept shown in Figure 50 consists of a large plate, or perhaps two beams, with a short vertical column to mount a tensioning device. The base must extend past the anchor to be tested in order to avoid uplift. The plate could have a cutout for the anchor or the base could be constructed with beams that pass on either side of the anchor. Regardless, the base would still provide some confinement to the anchor block.

The vertical component of the test load is reacted by bearing against the pavement. The horizontal component of the test load is carried to an in-joint anchor using a chain or cable. The eccentricity of the horizontal load should be minimized to mitigate overturning issues.

Figure 50. L-shaped load frame using in-joint anchor for horizontal resistance only.

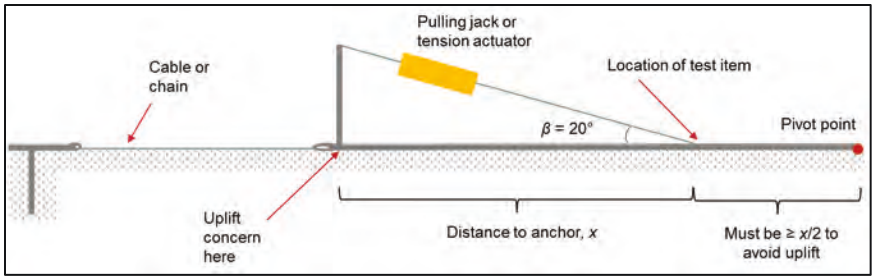

An improved version of this device is shown in Figure 51. This device keeps the low, broad profile of the L-shaped frame in order to avoid uplift at the left corner. The load bridge spreads the load out farther from the anchor block, but requires a heavier frame to carry the loads. A 3-D view of the concept is shown in Figure 52. Since the entire frame is proportioned based on the height, H, it is advantageous to have the puller jack located as close to the anchor as possible.

Figure 51. Load bridge using in-joint anchor for horizontal resistance only.

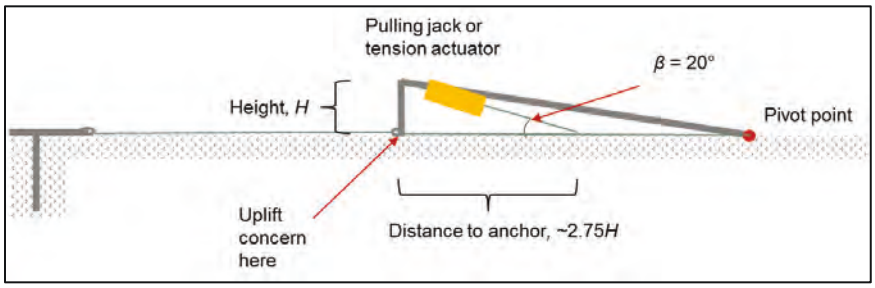

Figure 52. 3-D view of load bridge concept.

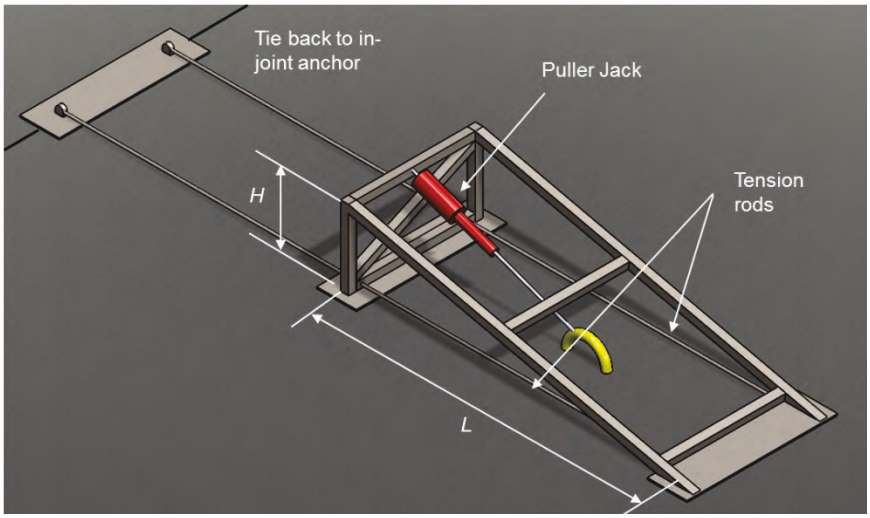

Figure 53 presents a simple static analysis of the load bridge system. To avoid uplift at the left leg (point A), the height (H) should be no more than about 0.36 times the overall length (L) of the frame. Limiting the aspect ratio (H/L) also helps to reduce the reactions and member forces. However, the horizontal force on the in-joint anchor is constant at $P = 0.940T$, where T is the test load.

Figure 53. Effect of load bridge aspect ratio on reactions.

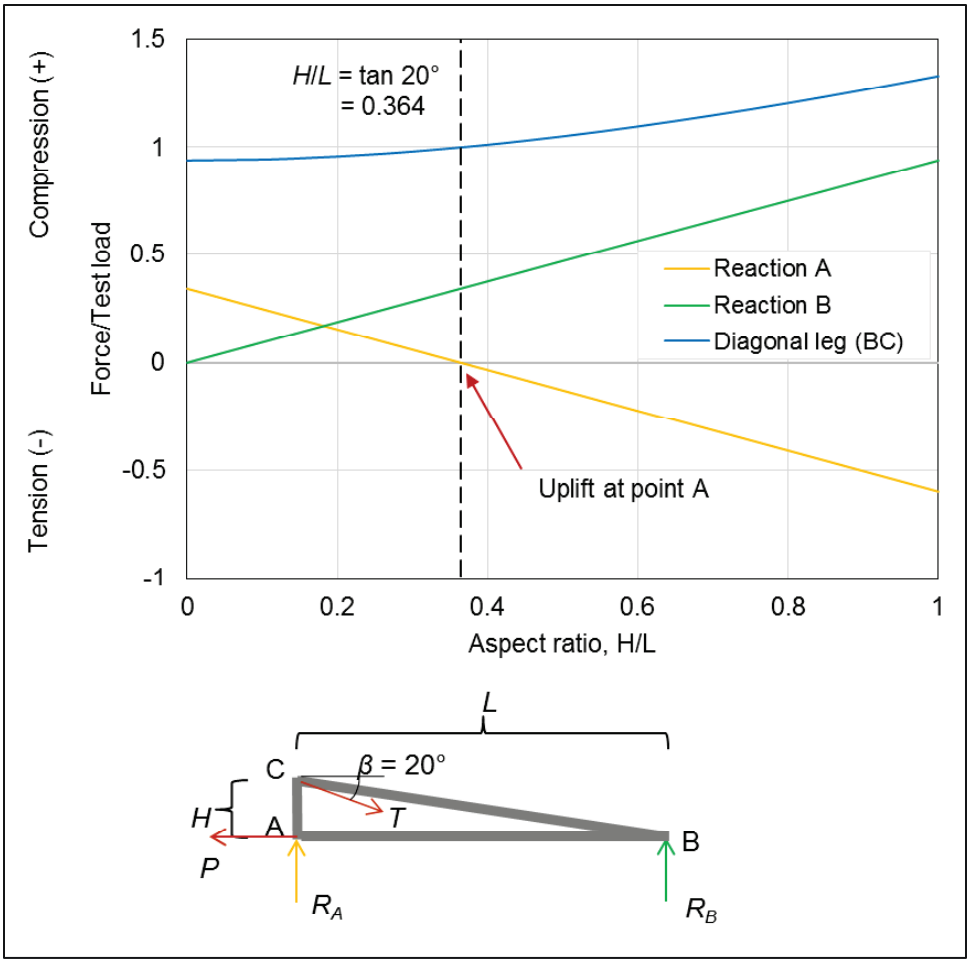

6.3 Lever concepts

Two concepts in which a sling or cable is attached to a rotating lever were also considered. These are shown in Figure 54. The concept in Figure 54(a) provides little mechanical advantage, but the change in loading angle is not too great (comparable to the center jack sling concept). Overall, the lever with end-attached sling is fairly similar to the load bridge concept. The concept in Figure 54(b) provides a mechanical advantage through the lever, but the sling angle can change significantly as the lever rotates.

Figure 54. Lever concepts with sling attached near (a) the end and (b) the pivot point.

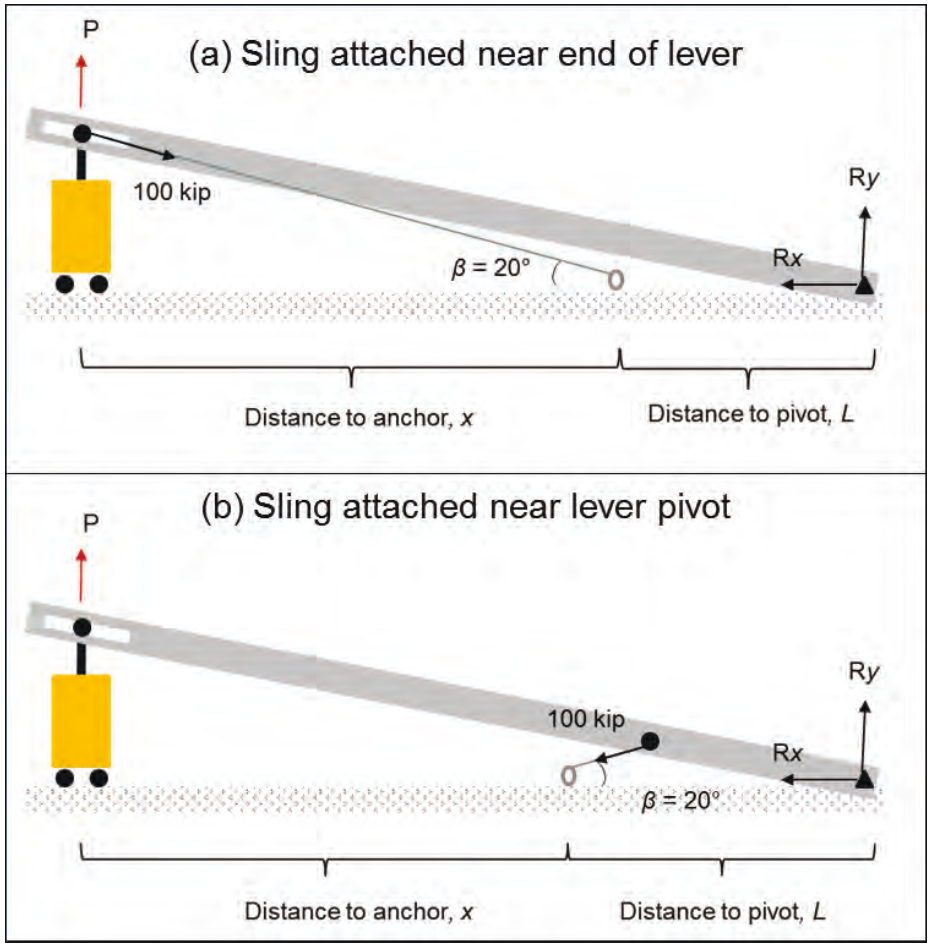

It may be difficult to ensure that the sling is actually at 20 deg when the sling is stretched sufficiently for the 100 kip load. Some preliminary calculations were performed to determine how the following parameters affect the required setup:

- Sling stretch at the proof load
- Sling angle prior to loading, θ_0

Assuming the lever is rigid, the problem reduces to simple algebra. Let the sling have initial length L_0 and initial angle θ_0 with respect to the horizontal, and final length $L_1 = \text{stretch} \cdot L_0$ and the final angle be 20 deg. Figure 55 illustrates the geometric relation between the location of the lever pivot, the anchor, and the initial and final sling positions. Solving for the circle that passes through points A and B determines where the pivot for the end of the lever should be, and at what point on the lever the sling should attach.

Figure 55. Geometry of the lever problem. The initial, unstressed position of the sling is shown in green; the final position when stressed to the proof load is shown in red.

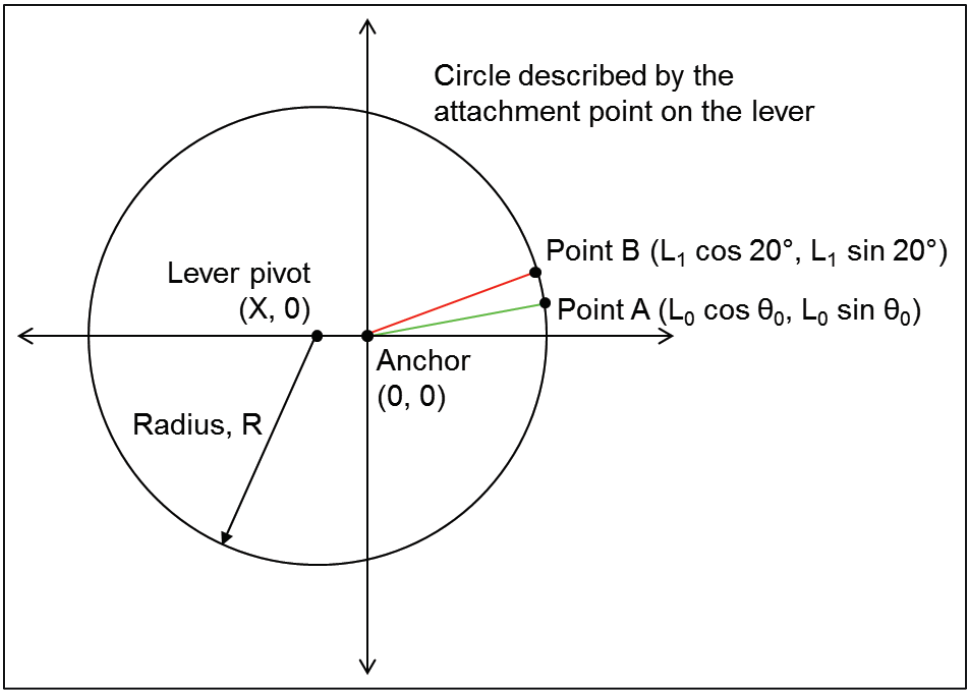

The unknowns X and R are given by

$$X = \frac{L_1^2 - L_0^2}{2\left(L_1 \cos 20^\circ - L_0 \cos\theta_0\right)}, \tag{3}$$

$$R = \left(L_0^2 - 2XL_0 \cos\theta_0 + X^2\right)^{1/2}. \tag{4}$$

Increasing either the stretch or θ_0 requires the pivot be located farther away from the anchor being tested and the attachment point be farther from the pivot. The total length of the lever is a tradeoff between mechanical advantage and weight; increasing the lever's length increases both. The lever concept was ultimately abandoned due to the large levers required.

6.4 Angled core concept and variants

A novel idea for anchorage employing angled cores was also considered. In theory, this type of anchorage could resist the applied load through bearing, and not require the installation of adhesive or permanent mechanical anchorage to the concrete. A pipe or pile could be inserted in a cored hole, and then simply removed when testing was complete. The

concept is illustrated in Figure 56, where the core is angled at α relative to the pavement surface, and the applied load has an angle of β relative to the surface. The component of the applied load, P, in the direction of the pile is $P\cos(\alpha + \beta)$, with a negative value indicating uplift. As long as $\alpha + \beta \leq 90°$, no component of the applied load acts to pull the pile out of the cored hole. The distribution of bearing stress on the front and back of the hole depends on the stiffness of the pile. For this design, failure occurring in the concrete above the pile was one of the main concerns.

Figure 56. Angled core concept.

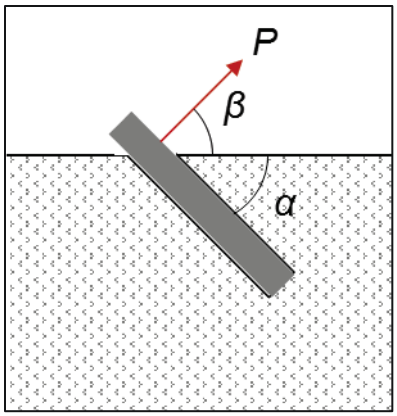

To further simplify the installation, it was decided to try combining the load application device and deadman anchor assembly. One promising candidate was a COTS soil anchor load locker, shown in Figure 57. This device, the Manta-Ray LL-2 load locker, is used to load lock and proof test soil anchors, typically used to secure guy wires. These anchors are installed at an angle, and the Manta-Ray LL-2 is capable of applying a load at an angle without the need for a second (deadman) anchor. However, there are three caveats for airfield anchor testing applications:

1. The loads applied by the Manta-Ray LL-2 cannot exceed 8,000 lbf;
2. The load locker sits directly over top the anchor that is being pulled, thereby introducing confinement; and
3. The load locker feet dig into the soil for stability, which is not possible on a paved airfield.

Figure 57. Commercial soil anchor load locker (A-Aerial Service Company n.d.).

The angled core concept with a modified Manta-Ray LL-2 load locker was selected for a small-scale proof-of-concept test (Section 6.6). This would allow the concept to be evaluated relatively inexpensively in a small-scale experiment, before devoting resources to designing and building a device capable of the full 100 kips.

A modified Manta Ray LL-2 was coupled with a center stand (Figure 58) so that the load locker could apply an angled load without confining the area directly around the anchor (concern #2 above). The angled cores addressed concern #3 in the above list. For the proof-of-concept test, a trolley jack was used for the center stand. The center jack was also tested on its own, for use when a deadman anchor was available (e.g., an adjacent tie-down anchor).

Figure 58. Designs for proof-of-concept test.

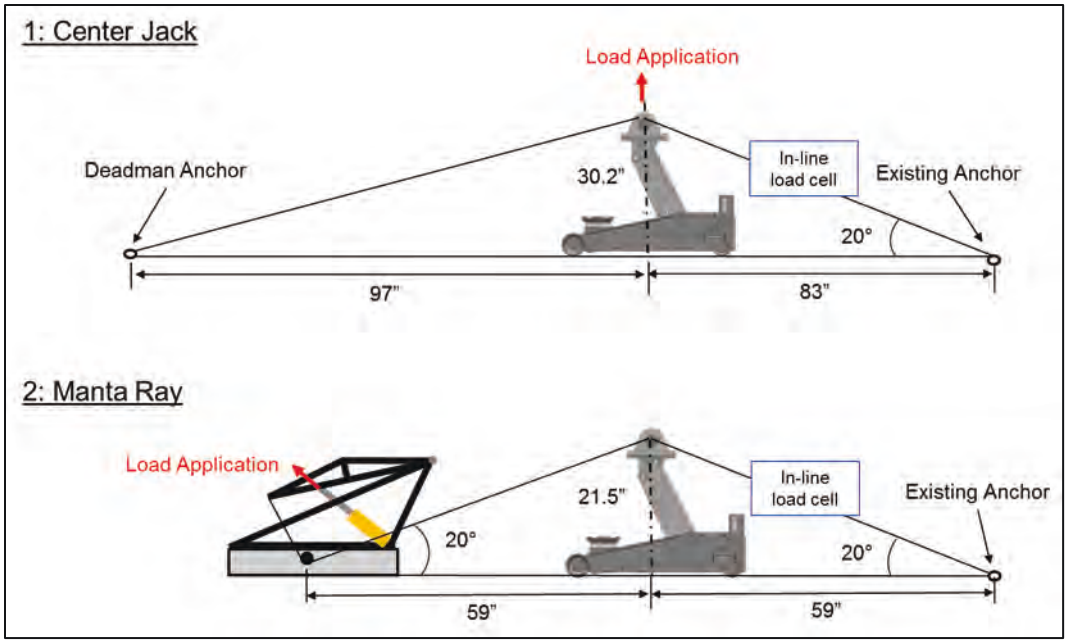

6.5 Deadman anchor concepts

Using commercially available concrete anchors, either mechanical or adhesive, to resist the 100-kip load would require at least 10–15 anchors (though this varies depending on anchor pattern and other factors). If the recommended spacing is observed, the anchorage pattern would become undesirably large (c.f. the ETL 00-2 anchor plate). To obtain the correct spacing without requiring a large plate, the use of slings or cables to distribute load was investigated.

Equal load distribution by the tensile "spider" structure is crucial to avoid a zipper-type progressive failure. If a practical number of anchors are included in a load-distributing spider arrangement, the structure is indeterminate. Thus, both the geometry and the axial stiffness of the members affect load distribution.

The most promising spider configuration was chosen for further analysis to determine if an arrangement could be determined such that the load was shared approximately equally between the anchors. This configuration consists of six slings equally spaced around a 90-deg arc, as shown in Figure 59. The geometric parameters used for the optimizations are also shown, namely, the height of the center (h) and the radial distance to each anchor (r_i). The layout is symmetric about the horizontal projection of the applied load. Note that an odd number of anchors is not practical, as the center anchor will receive a large share of the load compared to the others.

Figure 59. An array of six slings equally spaced over a 90-deg arc.

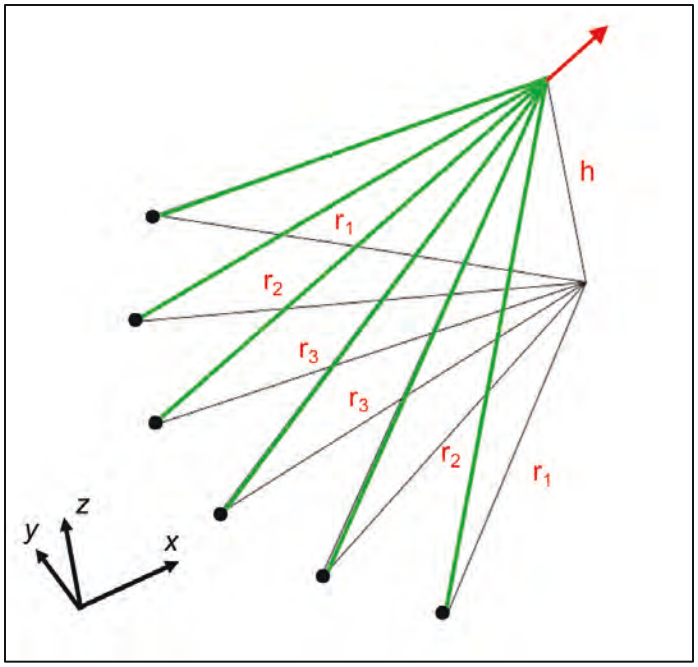

For optimization, only the proportions are relevant, so $r_3 = 1$ was chosen for convenience. Note that, for a practical design with slings, it would be useful to optimize the lengths of the slings, considering only lengths that are in increments convenient for manufacturing. Optimizing the radial anchor spacing is suitable for the purpose of assessing feasibility.

The objective is to minimize the standard deviation of reaction forces. For n anchors, the function to be minimized has ceil$(n/2)$ arguments because of symmetry.

A simple brute-force search method was implemented in GNU Octave (Eaton et al. 2017), building on code by Ferreira (2009). The method is described in pseudocode format.

1. For each combination of geometric parameters (h, r_1, r_2):
   1.1. Compute node coordinates
   1.2. Form global stiffness matrix
   1.3. Apply load (either 70 or 100 kips depending on configuration being investigated) at 20 deg
   1.4. Solve for displacements
   1.5. Compute vector of element forces, **F**

1.6. If any element is in compression, continue to next parameter combination
1.7. If any element force exceeds the anchor working load limit (Table 7), continue to next parameter combination
1.8. Otherwise, print the parameters

2. Sort results by StDev(**F**), then by displacement magnitude at the loaded node

The slings are idealized as truss elements that can only carry tensile loads. The cross-sectional area, A, and Young's modulus, E, were estimated for the analysis in the following way. The axial stiffness is defined by $k = F/\Delta$. If a 1 percent elongation is assumed at the working load limit (WLL), then $k = \text{WLL}/0.01L$, where L is the sling's length. Also, $k = AE/L$ for a truss element. Therefore, as an estimate, $AE = WLL/0.01$. Since only axial behavior is considered, A will always appear with E, so assume A = 1 in.^{2}. A sling with a 20-kip WLL was chosen, with a corresponding estimated E of 2,000 ksi.

The approach previously described results in the best solution out of the permutations of parameters that were tried, not necessarily the optimal solution. As long as the force distribution is approximately equal, this is sufficient for these purposes. It should also be noted that this method uses a small-displacement, linear analysis to assess each of combination of parameters. Because the slings are highly compliant, the structure can experience large displacements leading to nonlinear geometry. The slings also have a nonlinear force-displacement relationship, since slackening displacements cause no force. Due to the number of parameter combinations considered in step 1 (97 thousand for a six-anchor configuration and 4.6 million for an eight-anchor configuration) a more refined analysis was not practical for all cases. However, each optimal configuration from the quick analysis was analyzed in detail using Abaqus/Standard.

Working load limits for step 1.7 are given in Table 7 for Crosby HR-125 Swivel Hoist Rings (Crosby Group LLC 2017). Crosby HR-1000 Heavy Lift Swivel Hoist Rings were considered, but were 29–52 percent heavier than HR-125 hoist rings with the same working load limit. For testing components, a factor of safety of 2 on the hoist ring capacity was used. This is because the test is carried out under tightly controlled conditions, and the rings are not used in overhead or lifting applications.

Table 7. Hoist ring capacities.

Bolt size	Weight (lbf)	Crosby working load[1] (lbf)	Ultimate load (lbf)	Test kit working load[2] (lbf)
3/4-10 x 2.25	2.52	5,000	25,000	12,500
3/4-10 x 2.75	6.72	7,000	31,500	15,750

[1]Factor of safety of 5 or 4.5 (for 7,000-lb model)

[2]Factor of safety of 2

The "best" solution of the 97,366 combinations that were evaluated for a six-anchor configuration has the following proportions:

$$r_1 = 0.78$$
$$r_2 = 0.92$$
$$r_3 = 1$$
$$h = 0.28$$

For the six-anchor configuration, a load of 70 kips was applied at 20 deg relative to the horizontal. Note that eight anchors would be required to resist 100 kips. The optimized layout is illustrated in Figure 60, and the force distribution to the anchors is given by Table 8. The anchors see a load that is nearly the same, but the load on each anchor is 0.19, not 1/6, of the 70-kip force applied to the assembly. The analysis shows that six of the 3/4"-10 × 2.75" hoist rings could be used with this configuration to resist a 70,000-lbf load applied at 20 deg.

Figure 60. Plot of six-anchor optimized layout. Plot uses r_3 = 48 in. for proportions. The direction of displacement is shown by the blue arrow.

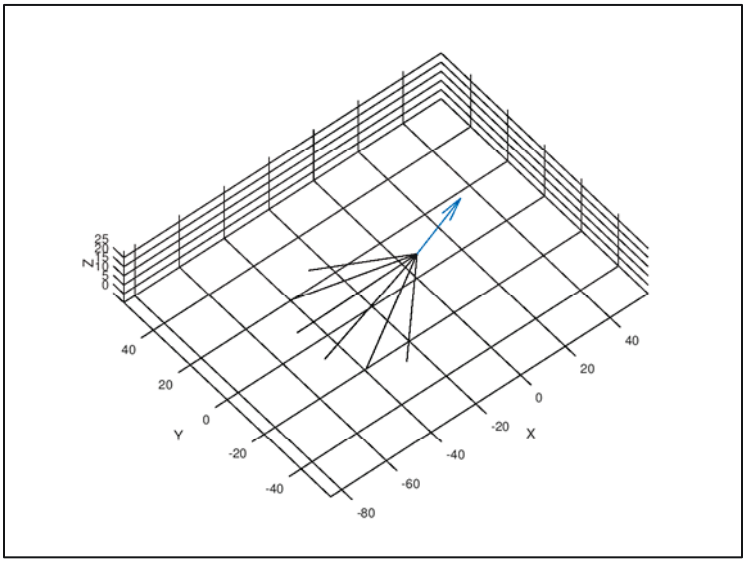

Table 8. Force distribution for six-anchor optimized layout.

Anchor	Anchor load (lbf)	Fraction of applied load
1	13,314	0.1902
2	13,349	0.1907
3	13,307	0.1901
4	13,307	0.1901
5	13,349	0.1907
6	13,314	0.1902
St Dev	21	0.0003

For comparison, and to validate the quick analysis method used to arrive at the optimized configuration, the optimized configuration was also analyzed using Abaqus/Standard (Dassault 2016). This analysis was performed using truss elements (type T3D2) with a tension-only linear elastic material for the slings and with nonlinear geometry enabled (e.g., using large displacement theory). The Abaqus V6R2016 implicit (direct sparse) solver was used. Due to the geometric and material nonlinearities, automatic viscous stabilization (via the *STATIC, STABILIZE keyword) was used to aid convergence.

Figure 61. Reaction force distribution from Abaqus/Standard simulation. Reaction forces shown in lbf.

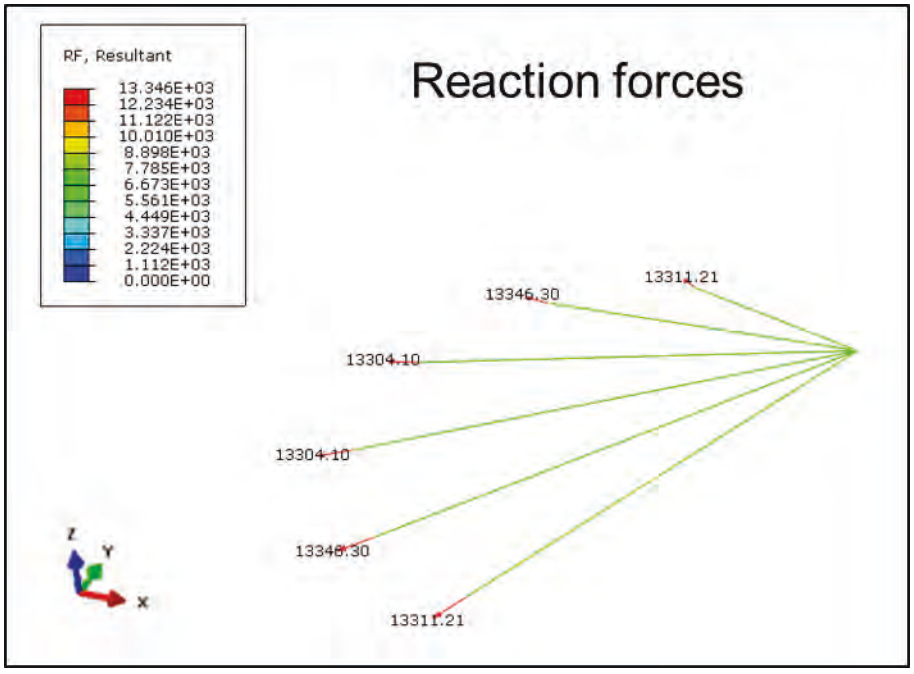

6.6 Small-scale proof-of-concept tests

Proof-of-concept (PoC) testing was performed at ERDC on 25 and 26 July 2017. The objective was to perform a scaled-down test to quickly and cost effectively evaluate the effectiveness of the most promising concepts developed.

The test series was intended to address the following questions to inform the design of the full-scale prototype:

- Is the angled core concept prone to overturning or other stability issues?
- Do the rollers help center and stabilize the center jack?
- How quickly can installation be performed?
- How destructive is the installation process?
- How much stroke is required to compensate for sling stretch?

6.6.1 Test overview

The ERDC test site was previously used for tie-down testing, yet many of the existing slabs were in good condition. A survey of the site revealed that three hat-type tie-downs were undamaged and could be used as deadman anchors for testing. In previous proof load testing, the hat-type tie-downs were found to have a minimum capacity of 60 kips. The layout of the test site is shown in Figure 62.

Figure 62. Proof-of-concept test site schematic.

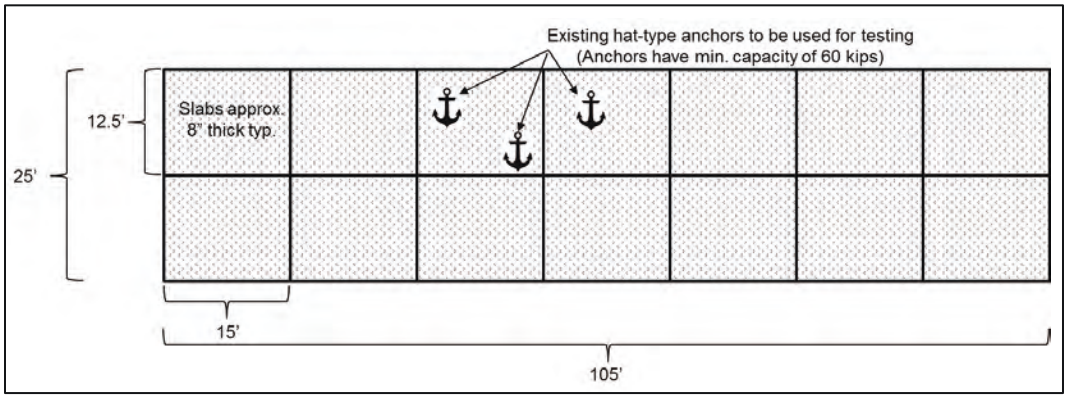

The proof-of-concept test series comprised two tests, replicating two different conditions:

1. A preexisting anchor is available for use as a deadman: Center jack with sling anchored at both ends. A trolley jack was used to prevent an overturning moment that would develop if the jack was not perfectly centered.
2. No preexisting anchor available: Manta Ray loading device. Two methods of anchoring the Manta Ray to the concrete slab were tested to compare ease of installation:

   A. Two 3-in. diameter cored holes @ 45 deg

   B. Ten drop-in threaded anchors with 3/4"-10 bolts

Load testing was performed on Configuration A only. Configuration B was not load tested, since threaded anchors are already well characterized and stability is not a concern. Only the installation process was tested for Configuration B.

6.6.2 Design and fabrication

A COTS Manta Ray (MR) load locker was acquired and modified such that it could be bolted to a footing plate with two steel pipes welded on at 45 deg (Configuration A) or directly anchored using threaded drop-in anchors and bolts (Configuration B). The MR was modified by adding an angle iron base with 10 through holes for attachment to the footing plate or to the drop-in anchors (see Figure 63). Rollers were also added to allow the sling to run back through the base of the MR as shown in the concept drawing, Figure 58.

Figure 63. Modified Manta Ray COTS load locker.

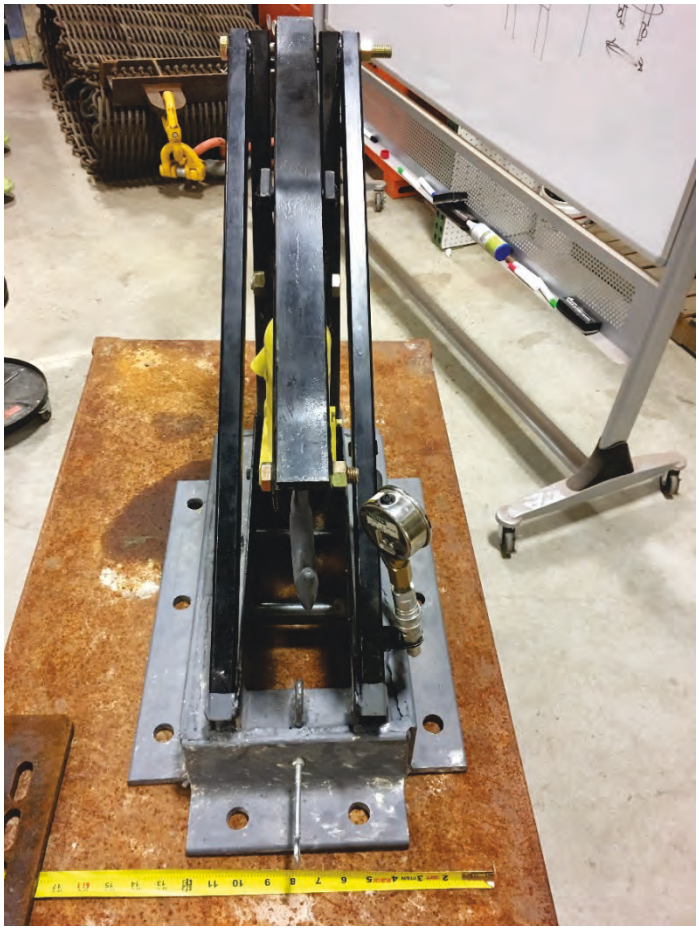

The 3/8-in. footing plate (Figure 64) was fabricated by the ERDC Department of Public Works (DPW) shops. The footing plate has two 2.5-in.-nominal Schedule 80 pipes angled at 45 deg and ten 3/4"-10 Grade 8 threaded studs for attachment to the MR.

Figure 64. Footing plate for MR device to anchor in angled core holes.

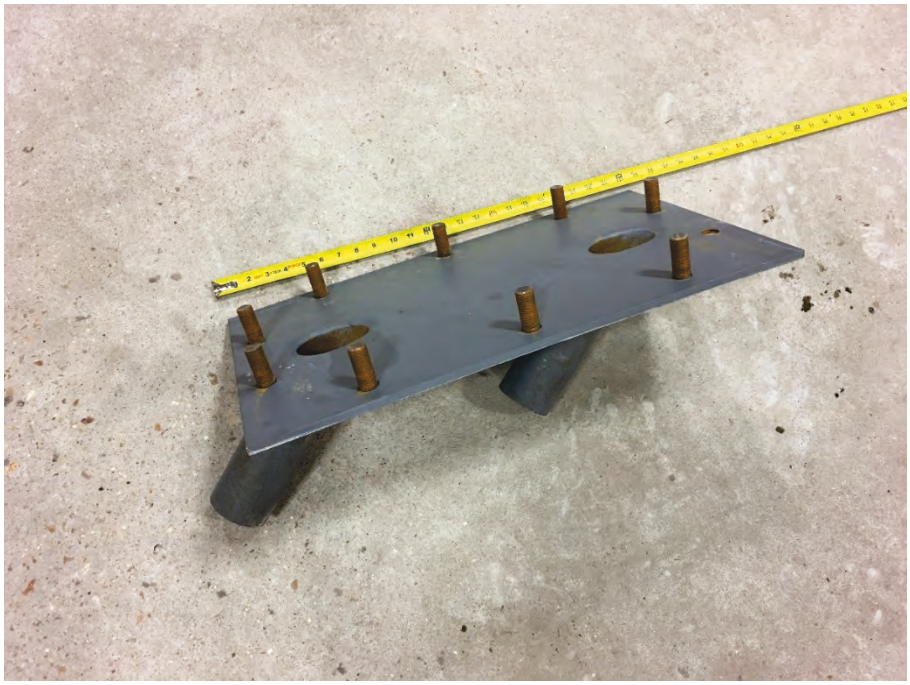

A roller was fabricated to attach to the center jack to allow the sling to move more easily. The roller device is shown in Figure 65 and was constructed of COTS bearing blocks mounted to a plate. The red tab on the right side of the device was used for mounting a string potentiometer to measure displacement during testing.

Figure 65. Roller device for center jack.

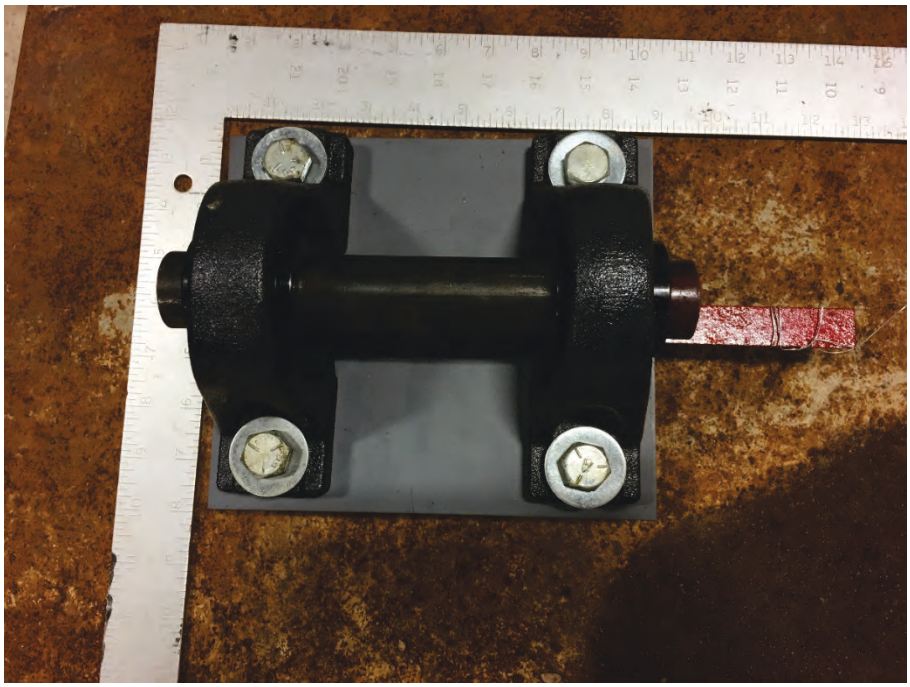

Test 1 used 10-ft and 3-ft Slingmax Twin-Path synthetic slings with a 10,000-lbf working load limit. Test 2 used only the 10-ft synthetic sling.

6.6.3 Test setup

6.6.3.1 Proof-of-concept Test #1

The completed setup for the proof-of-concept Test #1 is shown in Figure 66. As the goal of this test was to evaluate concepts quickly and at low cost, cinder blocks were used to provide enough height to the COTS trolley jack to achieve a 20-deg angle at the anchor. A full-scale design would employ a taller center jack assembly, which would require fabrication. The installation process for these small-scale tests was fairly simple and is summarized in the following paragraphs.

1. Locate existing anchors with sufficient capacity.
2. Place trolley jack to achieve 20-deg angle at anchor to be loaded. In this test, the jack was positioned 14 in. away from true center, testing setup tolerance to slight load imbalances.
3. Attach sling to existing anchors, running over center jack.

Figure 66. Layout for proof-of-concept Test #1.

6.6.3.2 Proof-of-concept Test #2

Test 2 was conducted in three stages:

1. Install Manta Ray in Configuration A (using angled cores)
2. Install Manta Ray in Configuration B (using drop-in anchors)
3. Load test Manta Ray (Configuration A) to determine stability

6.6.3.2.1 Configuration A: Angled cores

First, a template was used to mark locations for the angled cores. Then, the portable coring jig was placed and a core drill was positioned at 45 deg and lined up with the marks (Figure 67). The jig is designed so that no anchor bolts are required. The weight of the jig and two technicians is sufficient to keep the setup from moving during drilling operations. The drilling process is shown in Figure 68. A barrel guide is used to prevent the barrel from chattering when starting the hole.

Figure 67. Positioning core drill on portable jig.

Figure 68. Core drilling.

After the two cored holes were drilled, the cores were broken off using a wedge and hammer, then extracted with a wire loop. A wet/dry vacuum was used to clean the holes. The finished holes are shown in Figure 69.

Figure 69. Cored holes after core removal and cleaning.

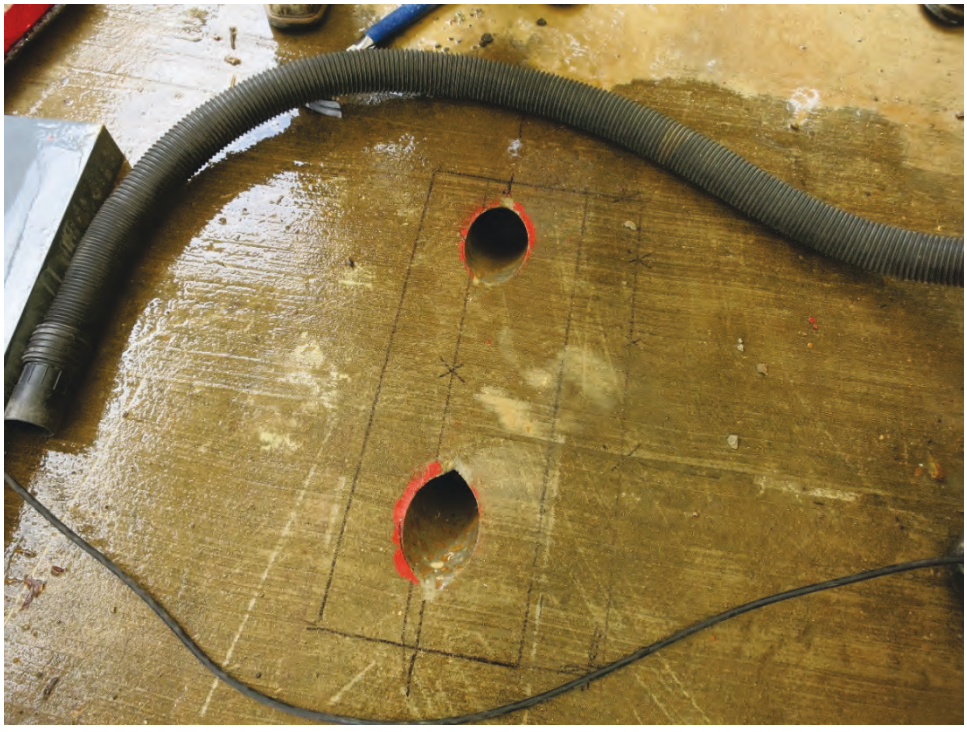

The footing plate was then inserted into the cored holes (Figure 70). Finally, the MR was mounted on the footing plate and secured to the threaded studs (Figure 71).

Figure 70. Footing plate in cored holes.

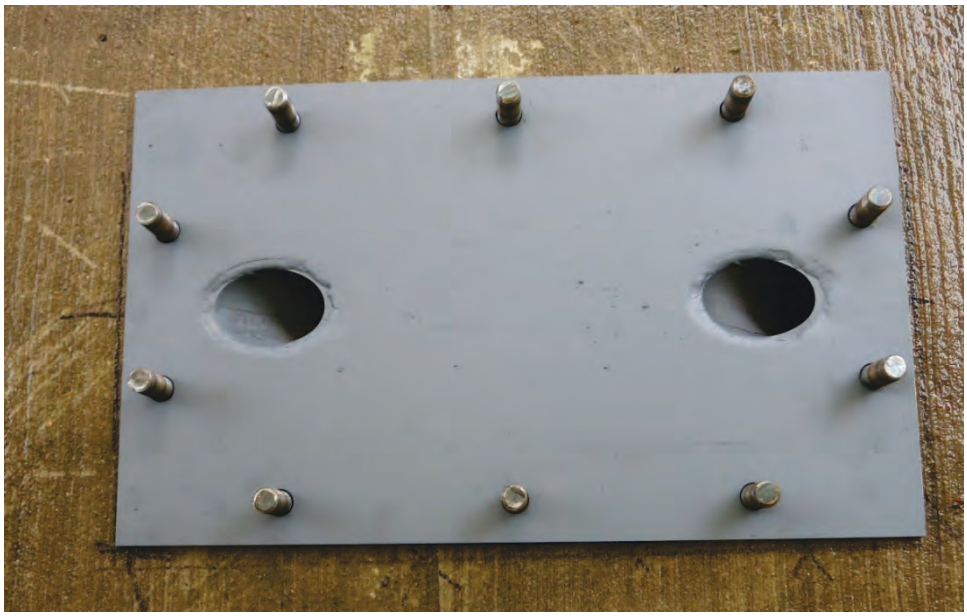

Figure 71. MR mounted to footing plate.

6.6.3.2.2 Configuration B: drop-in anchors

A template was used to mark the locations for ¾-in. ID drop-in threaded anchors. Holes were drilled using a hammer drill (Figure 72). The MR was then secured to the drop-in threaded anchors with bolts and washers.

Figure 72. Drilling holes for drop-in anchors.

6.6.4 Instrumentation

6.6.4.1 Proof-of-concept Test #1

The instrumentation setup for Test #1 is shown in Figure 73. A 10-kip capacity load shackle was used for in-line load measurement. Two string potentiometers were used to monitor the center jack's extension. In their initial positions, string potentiometer #1 measured vertical movement and string potentiometer #2 measured horizontal movement. The two measurements can be used to triangulate the position of the roller assembly if desired. Due to the trolley jack's design, the jack raises in a circular motion.

Figure 73. Instrumentation for proof-of-concept Test #1.

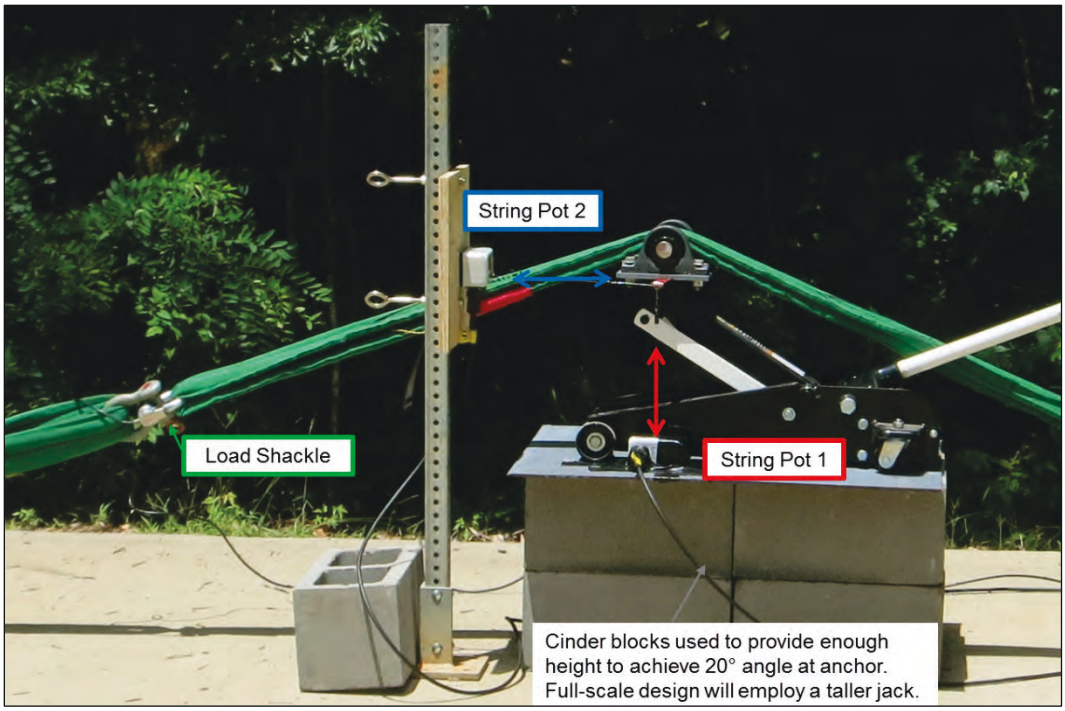

6.6.4.2 Proof-of-concept Test #2

The instrumentation setup for Test #2 is shown in Figure 74. A 10-kip capacity load shackle was used for in-line load measurement. String potentiometer #1 measured uplift at the rear of the MR assembly. String potentiometer #2 ran along the same path that the sling took through the MR frame and measured sling travel. String potentiometer #3 measured vertical movement on the center stand.

Figure 74. Instrumentation for proof-of-concept Test #2.

6.6.5 Loading

Two slightly different loading schedules were used for the two tests. For Test #1, the assembly was loaded to 500, 800, and 1,000 lbf, holding at each step until the sling relaxation leveled off. For Test #2, the assembly was loaded to 800 lbf with the MR jack, then the jack displacement was held while monitoring for uplift at the rear of the footing plate. The assembly was unloaded after 7 min and the process was repeated. After performing these stability checks, the assembly was loaded to 3,500 lbf in 500-lbf increments.

6.6.6 Results

6.6.6.1 Proof-of-concept Test #1

Time-histories of the data recorded during Test #1 are given in Figure 75. A large amount of vertical travel was required to take the slack out of the sling and begin applying tension. The sling was loaded from 500 lbf to 1,000 lbf over a displacement of about 1 in. Because of stress relaxation in the slings, it is difficult to make a theoretical comparison for the sling tension–jack displacement behavior of the system. The synthetic slings relaxed under sustained displacement, reducing the stress. Notice that both string potentiometer readings remained constant during the hold periods, whereas the tension decreased. This indicates that the load decrease is not due to the jack creeping downward.

Figure 75. Proof-of-concept Test #1 (center jack) load and displacement time-histories.

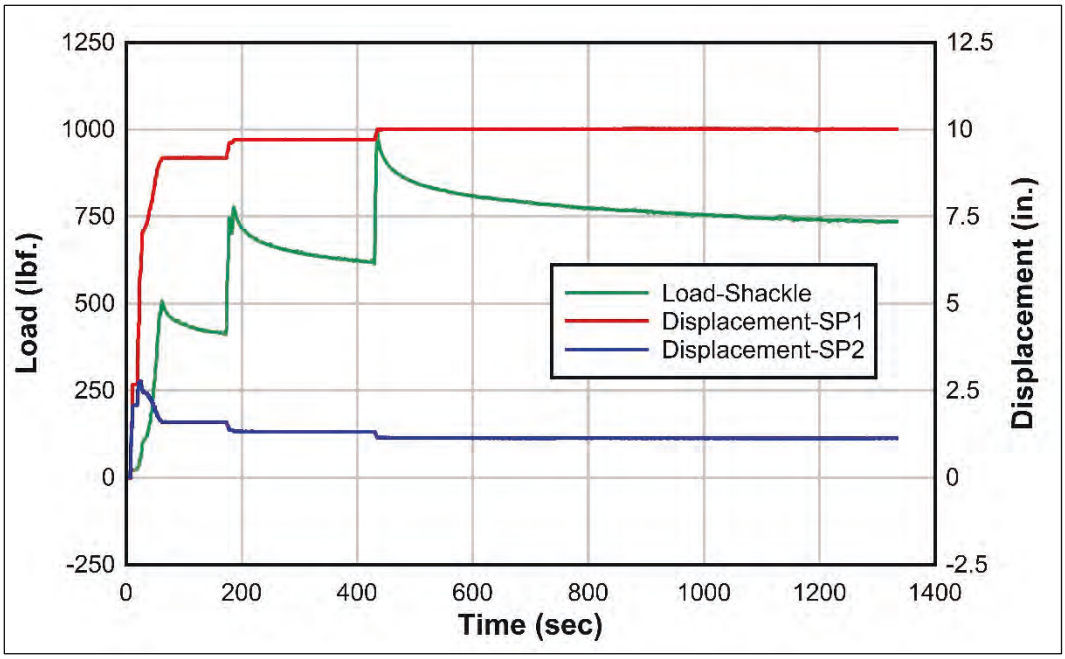

6.6.6.2 Proof-of-concept Test #2

As described in Section 6.6.5, the MR and angled core footing plate were loaded to a relatively low load and unloaded twice to check for seating or stability issues before testing to higher loads. Time-history data for the stability checks are given in Figure 76 and Figure 77. The MR uplift measurement (SP1) shows no significant change from zero. The first test run required about 2 in. of sling displacement (SP2) to achieve 800 lbf; the second test run required about 2.1 in. The center stand height measurement (SP3) decreased during load application, but did not change during the load hold.

Figure 76. Proof-of-concept Test #2 (MR and angled core) load and displacement time-histories for stability check #1.

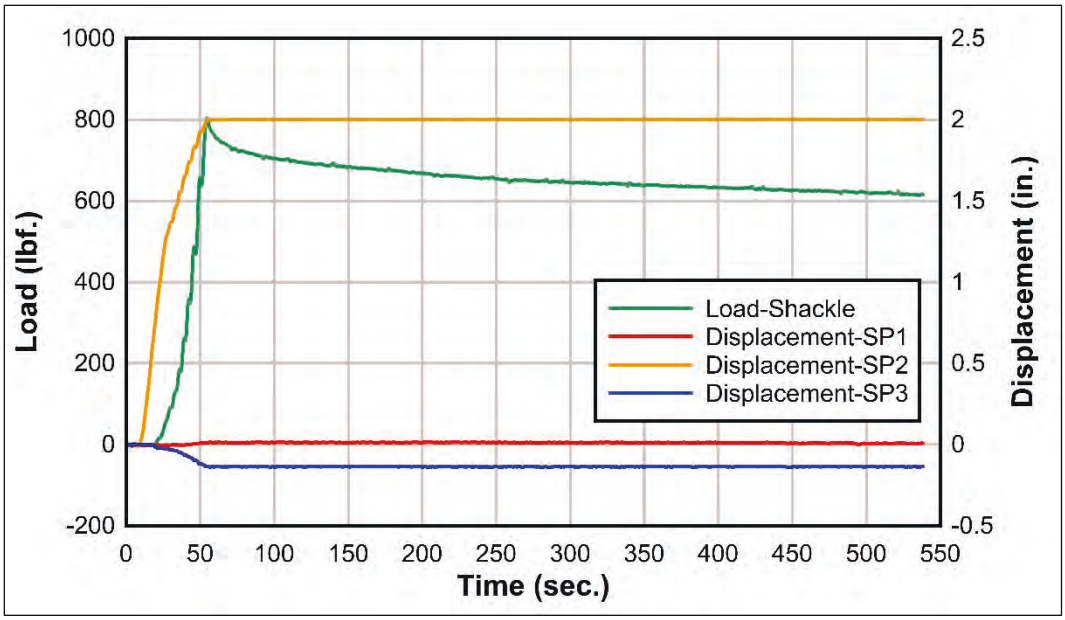

Figure 77. Proof-of-concept Test #2 (MR and angled core) load and displacement time-histories for stability check #2.

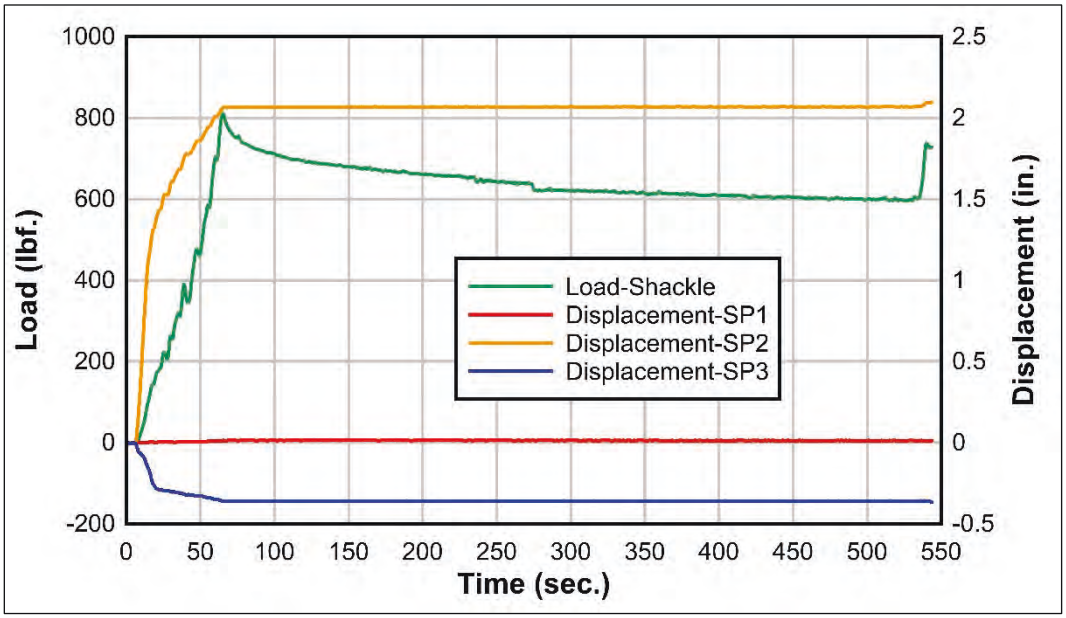

A load-time plot for the primary loading portion of Test #2 is shown in Figure 78. Note that the string potentiometers were removed during this phase to avoid possible damage. As the data show, the sling exhibited considerable stress relaxation in this test as well.

Figure 78. Proof-of-concept Test #2 (MR and angled core) load history for tensioning up to 3,500 lbf.

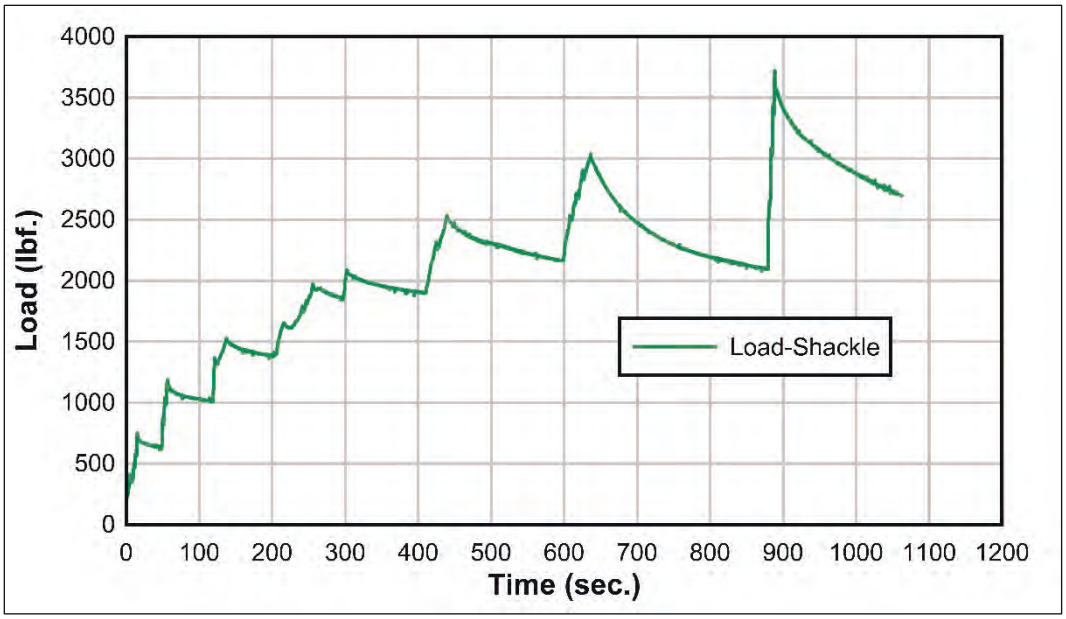

6.6.7 Lessons learned through proof-of-concept testing

Proof-of-concept testing showed that angled cores can be drilled using a portable jig; anchor bolts are not required to secure the coring drill. Core drilling was performed in 60 min for two nominal 3-in. by 12-in.-long cores on an unreinforced slab (design f_c' = 5 ksi) with chert aggregate. Chert aggregate is a worst case and typical airfield concrete should allow faster core extraction.

The installation of drop-in threaded anchors took roughly the same amount of time as core drilling. However, the greater number of holes (10 vs. 2) requires more precise alignment. A full-scale design would require oversized holes in its baseplate to allow the device to function as a template for hole alignment. A separate template could also be used.

TSPWG M 3-260-03.00-2, *Inspection of trim pad anchor systems* (Tri-Service Pavements Working Group 2017), specifies Slingmax Twinpath slings due to their high strength-to-weight ratio and low stretch under load. However, significant stress relaxation was observed with these slings in the PoC test.

These key observations were made and used to inform the final, full-scale design:

- The MR design allowed the angled core concept to be used without stability issues. However, the sling pass-through design placed high stresses on the MR frame. Because of this, an MR-like frame was deemed inefficient at full-scale.
- When placing concrete anchors, hole alignment is critical. The final design must include a robust template.
- Sling stress relaxation effectively increases the amount of sling stretch that needs to be overcome to achieve a desired tension. Despite this, synthetic slings are still the best, low-weight option for carrying high tensile loads.

6.7 Final LAIK design

The lessons learned from the small-scale testing and the exploration of multiple concepts culminated in the final LAIK prototype design. Section 6.7.1 gives an overview of the final LAIK design. The structural design analysis that was performed is described in Section 6.7.2.

6.7.1 LAIK design overview

Three requirements were deemed most critical to the LAIK prototype design:

1. The system must be capable of applying a 100-kip proof load at an angle of 20 deg ± 5 deg w.r.t. the horizontal.
2. The system must be lightweight. Each component must weigh 50 lb. or less and no heavy equipment shall be required for setup or execution of the proof test.
3. The system must be rapidly deployable, i.e. setup and testing should take 8 hr or less.

A variant of the sling and center jack concept, described in Section 6.1.1 was determined to be the most efficient and stable configuration capable of fulfilling these three design requirements. Figure 79 shows an overview of the final LAIK design. The primary structural components of the system are a reaction anchor (deadman), an actuator base, and a load bridge. A sling wraps around the deadman, over the load bridge, and is shackled to the anchor being proof tested. Two hydraulic actuators are seated in a base frame to provide stability and the initial height required to produce the 20-deg load angle. As the actuators extend, tension develops in the sling. An in-line load cell (dynamometer) is used to measure the load. Additional

details, including a full list of components and design drawings can be found in the LAIK User's Manual (Appendix A). CAD models of the custom components are also provided on the enclosed disc.

Figure 79. Schematic overview of final LAIK design.

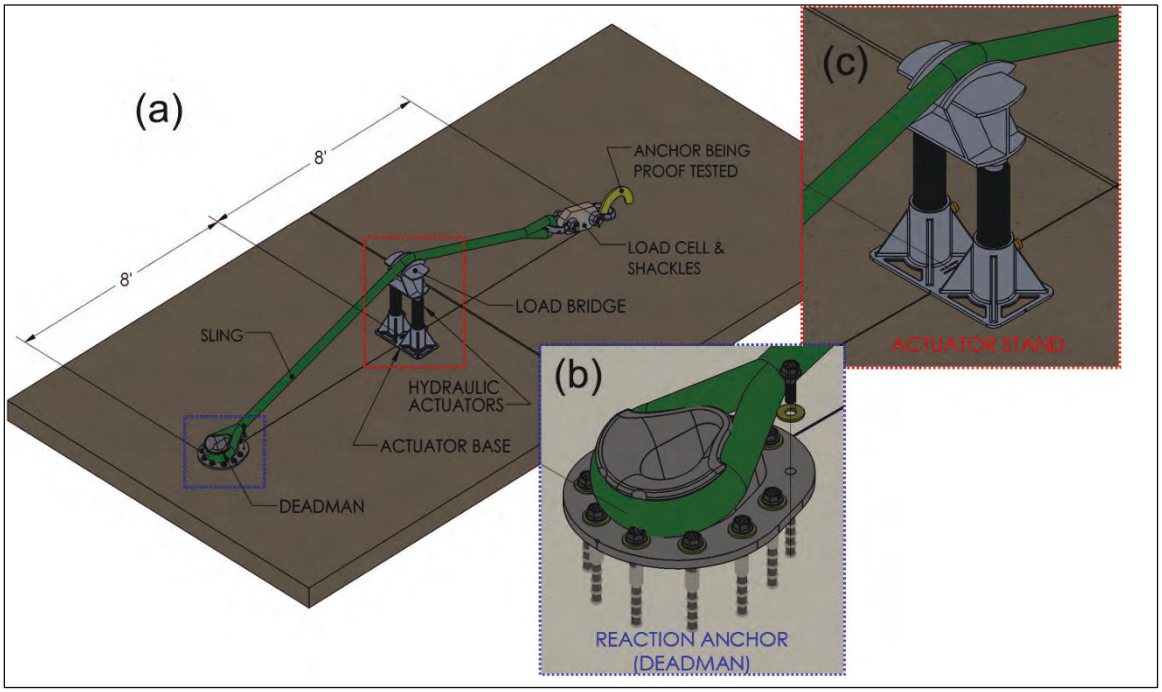

For trim pad anchors, the minimum desirable distance from anchor to actuator was determined to be 8 ft. This determination was based on review of relevant design and construction specifications (e.g., Department of the Air Force 2001; Unified Facilities Criteria 2008), as well as measurements taken during the site visits (described in Section 2). In most cases, the 8-ft standoff should be sufficient to allow the actuator stand to be located on a slab adjacent to one in which the trim pad anchor is embedded. Thus, any confinement effects due to the actuators should be minimal.

Setting the standoff distance as 8 ft was the first step to defining the geometry of the setup, shown in Figure 80. The sling length needed to be determined such that the initial angle was less than 20 deg. The 20 deg angle would be attained after all slack is removed from the system. It was conservatively assumed that the sling would stretch 2 percent under load, i.e. $d^* = 1.02d$. This is the loaded geometric state where the angle should equal 20 deg, i.e. $\beta^* = 20$ deg. With those values defined, the remaining dimensions could be readily calculated. The required actuator stroke was

determined to be $y^* - y = 6.4$ in. With the geometry fully defined, the appropriate length of sling and actuators with sufficient stroke and capacity could be chosen.

Figure 80. Setup geometry. The initial (untensioned) geometry is shown in black. The loaded (tensioned) geometry is shown in red.

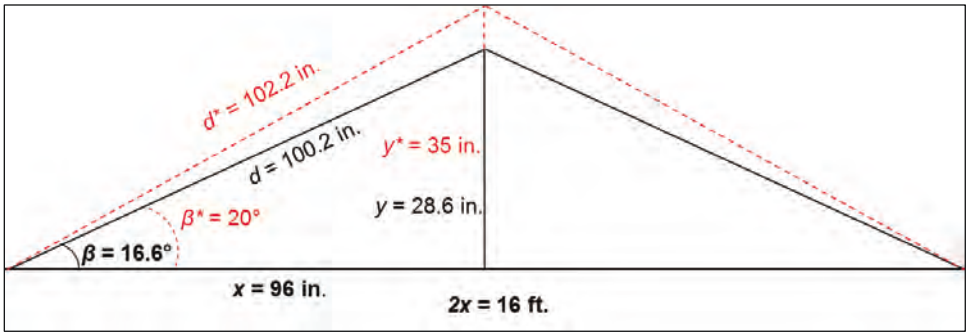

One of the most challenging design aspects involved deciding how to anchor the deadman to the concrete slab. The choice of deadman anchorage is an optimization of number of holes vs. ease of installation. Based on recommendations from those experienced in concrete drilling operations and in consideration of the no heavy equipment requirement, a decision was made to go with 1-in. diameter holes.

Based on a 1-in. diameter hole, among the strongest commercially available concrete anchors was the Wej-It PS2-34 POWER-Sert adhesive insert anchor (Wej-It 2015), shown in Figure 81. The Wej-It insert is internally threaded and when installed lies completely below grade. This was attractive, since the anchor would not need to be removed after testing was complete.

Hilti HIT-HY 200-A epoxy was chosen as the preferred adhesive for use with the Wej-It insert anchors based on its short curing time and high strength. The curing and working times for HIT-HY 200-A epoxy are given in Table 9. For temperatures above 50 °F, the curing time is 1 hr or less.

Figure 81. Wej-It PS2-34 POWER-Sert adhesive insert anchor (adapted from Wej-It 2015).

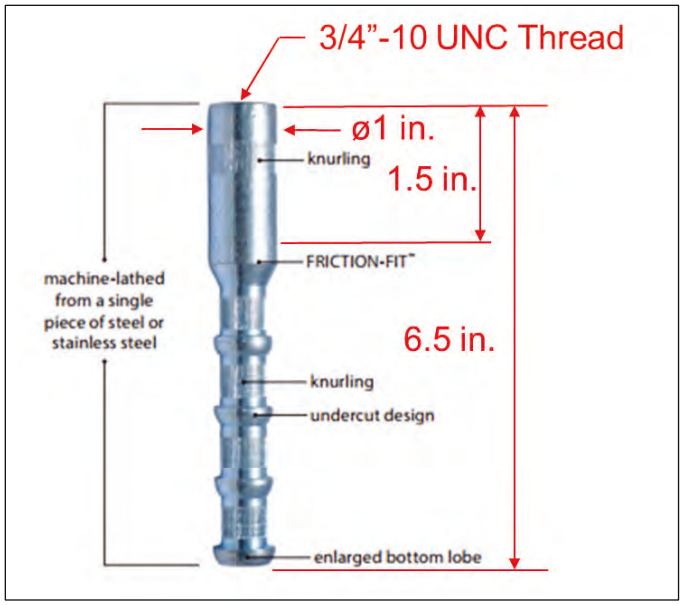

Table 9. Curing and working times for HIT-HY 200-A epoxy (Hilti n.d.).

Base material temperature (°F)	Maximum working time	Minimum curing time
14	90 min	7 hr
23	90 min	7 hr
32	50 min	4 hr
50	15 min	1 hr
68	7 min	30 min
86	4 min	30 min
104	3 min	30 min

The number of Wej-It PS2-34 anchors required to sustain the combined tensile and shear load was calculated using the interaction equation specified in ACI 318-11 Appendix D:

$$\left(\frac{T/n}{T_{allowable}}\right)^{5/3} + \left(\frac{V/n}{V_{allowable}}\right)^{5/3} \leq 1 \quad (5)$$

where:

Tensile load, $T = 100 \text{ kip} \cdot \sin(20°) = 34.2 \text{ kip}$
Allowable tensile load, $T_{allowable} = 18.8 \text{ kip}$

Shear load, $V = 100 \text{ kip} \cdot \cos(20°) = 94.0 \text{ kip}$
Allowable shear load, $V_{allowable} = 9.0 \text{ kip}$
$n =$ number of anchors

Thus, the number of anchors required, $n \geq 11$. The deadman was designed with a bolt pattern comprising 11 equally spaced anchor points.

An installation jig for the deadman was devised to help precisely locate and drill the eleven 1-in. diameter anchor holes. Details about the installation jig and its use can be found in the LAIK User's Manual (Appendix A).

6.7.2 LAIK design analysis

Each of the components in the LAIK was designed to maximize the strength-to-weight ratio based on the magnitude and direction of the forces acting upon them. Figure 82 is a free-body diagram showing the load distribution through the system. Finite element models of the deadman anchor, load bridge, and actuator base were created employing half symmetry using Solidworks Simulation 2016. An iterative design and analysis process was used to optimize the strength-to-weight ratio for each component.

Figure 82. Free-body diagram showing magnitude and direction of the forces acting on LAIK components.

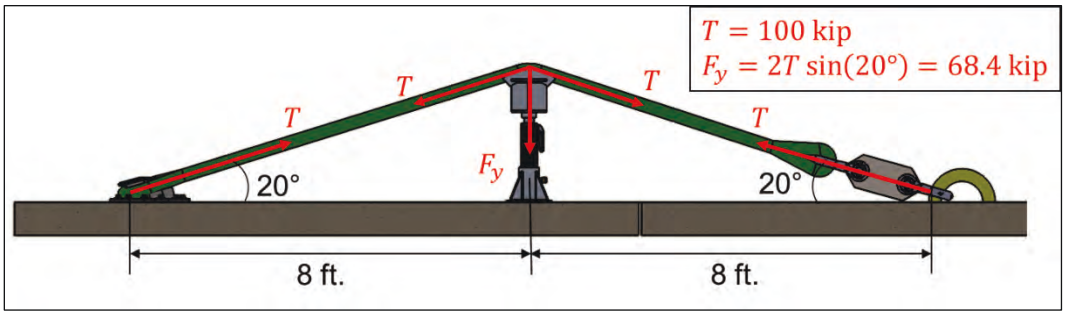

The deadman anchor half-symmetric finite element model is shown in Figure 83. A distributed load with a total magnitude of 50 kips (equivalent to 100 kips without symmetry) was applied to the face where sling contact occurs. The direction of the force vector is 20 deg from the horizontal. A symmetry boundary condition was applied to the face representing the mid-plane of the part. Bolt connector elements were used to model the 3/4"-10 × 2.5" long UNC bolts used to anchor the deadman. A 75 ft-lb preload torque was assigned to each bolt and a friction factor of 0.2 was assumed.

Figure 83. Deadman anchor finite element model (a) overview and (b) bolt connector properties.

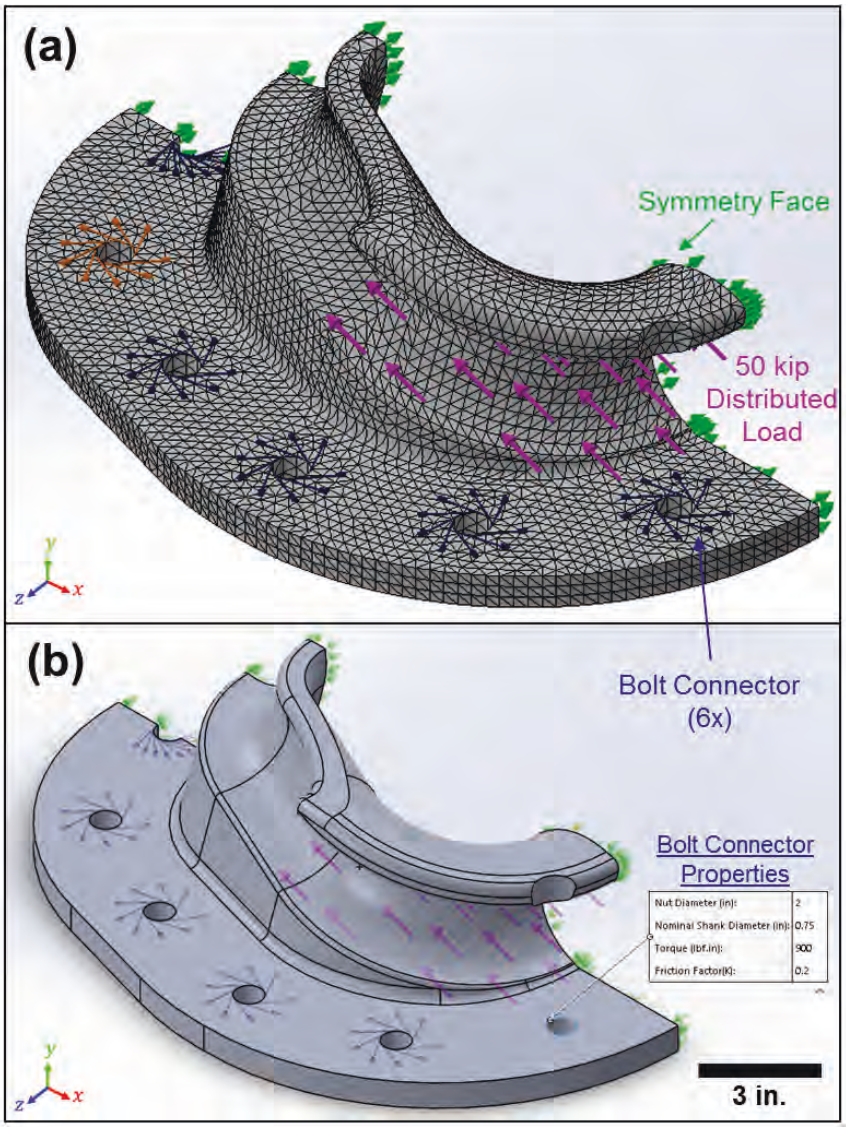

The analysis results are plotted in Figure 84. The material chosen for the deadman anchor is 7075-T6 aluminum, with a yield strength of 73.2 ksi. As seen in the Figure 84 stress contour, the peak stress for the specified loading is 42.1 ksi. It is worth noting that the fatigue strength of 7075-T6 aluminum is 23 ksi. Therefore, the deadman anchor is expected to have a finite fatigue life.

Figure 84. Deadman anchor FEA contours: (a) displacement, (b) equivalent strain, and (c) von Mises stress.

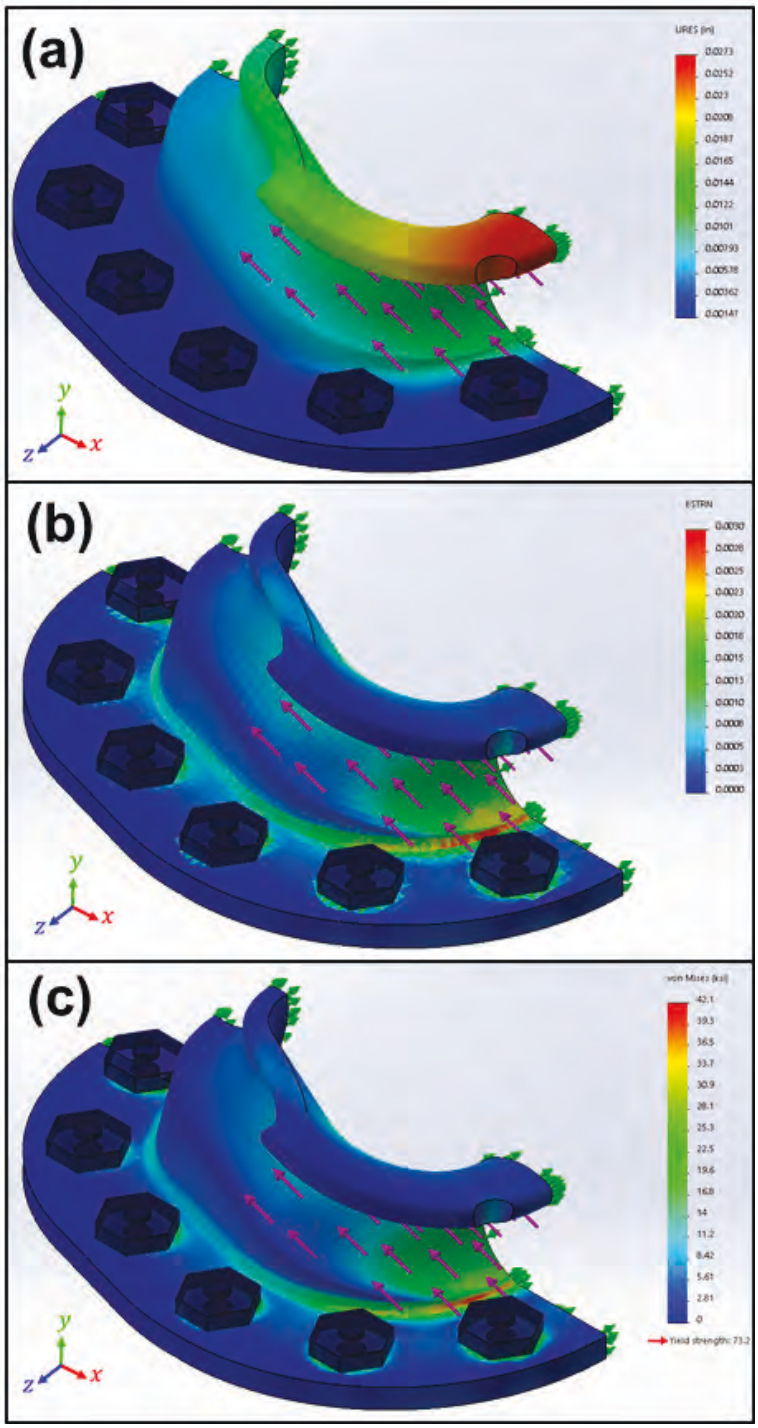

The finite element model used to analyze and optimize the load bridge is shown in Figure 85. A 35-kip distributed load (equivalent to a 70-kip load without symmetry) was applied in the negative *y*-direction on the face where sling contact occurs. A symmetry boundary condition was applied to the face representing the mid-plane of the part. The face where the actuator cylinder rests was fixed in the y-direction.

Figure 85. Load bridge finite element model (a) overview and (b) rotated view showing boundary condition representing actuator.

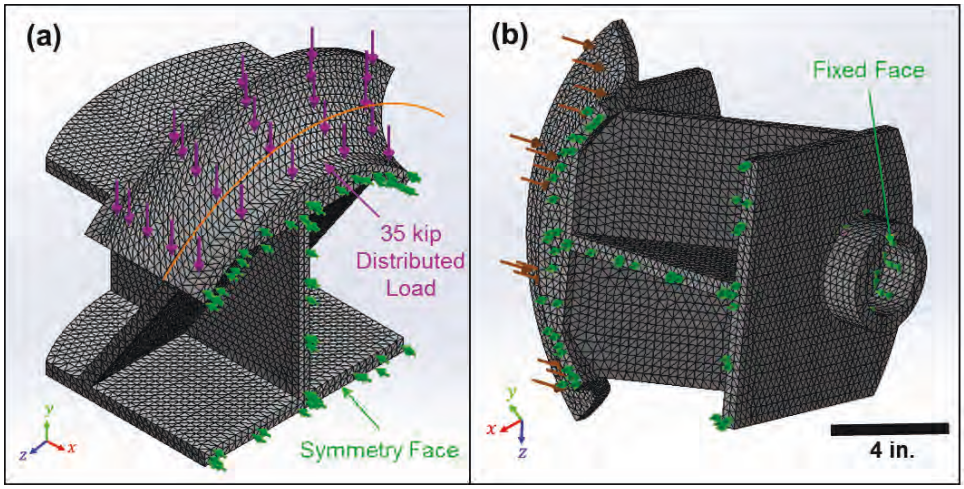

Figure 86 shows the FEA results for the load bridge. The peak stress for the specified loading is 29 ksi and is primarily compressive. 6061-T6 aluminum with a yield strength of 39.9 ksi was chosen for the load bridge. Note the fatigue strength of 6061-T6 aluminum is 14 ksi. Thus, the load bridge is also expected to have a finite fatigue life.

Figure 86. Load bridge FEA contours: (a) displacement, (b) equivalent strain, and (c) von Mises stress.

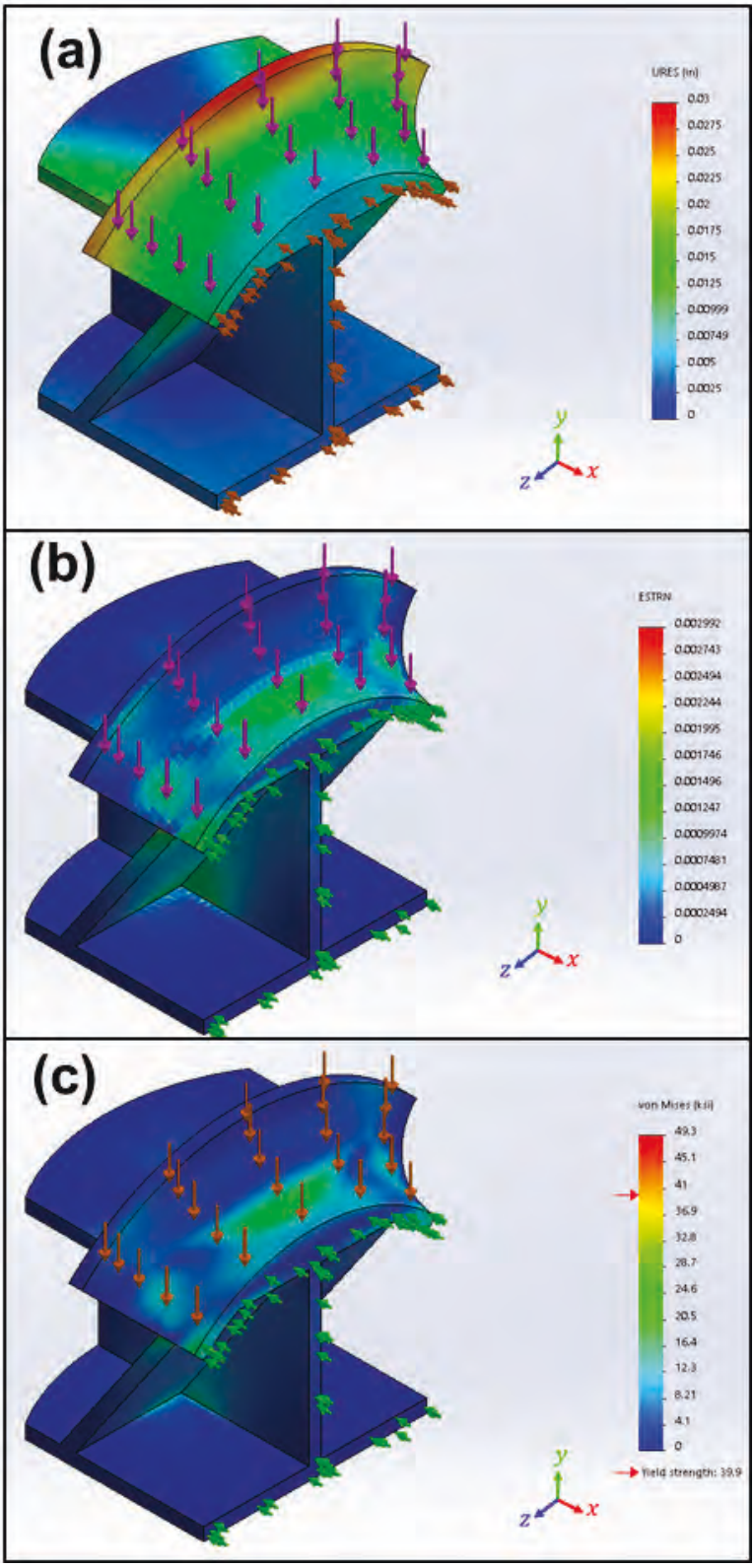

The half-symmetric finite element model of the actuator base is shown in Figure 87. A 60-kip distributed, compressive load was applied to the face where the actuator interfaces with the part. A 60-kip load was used here, since that is the maximum load generated by a 30-ton hydraulic cylinder. The bottom face of the stand was fixed in the y-direction, and a symmetry boundary condition was specified for the face intersecting the symmetry plane.

Figure 87. Actuator base finite element model overview.

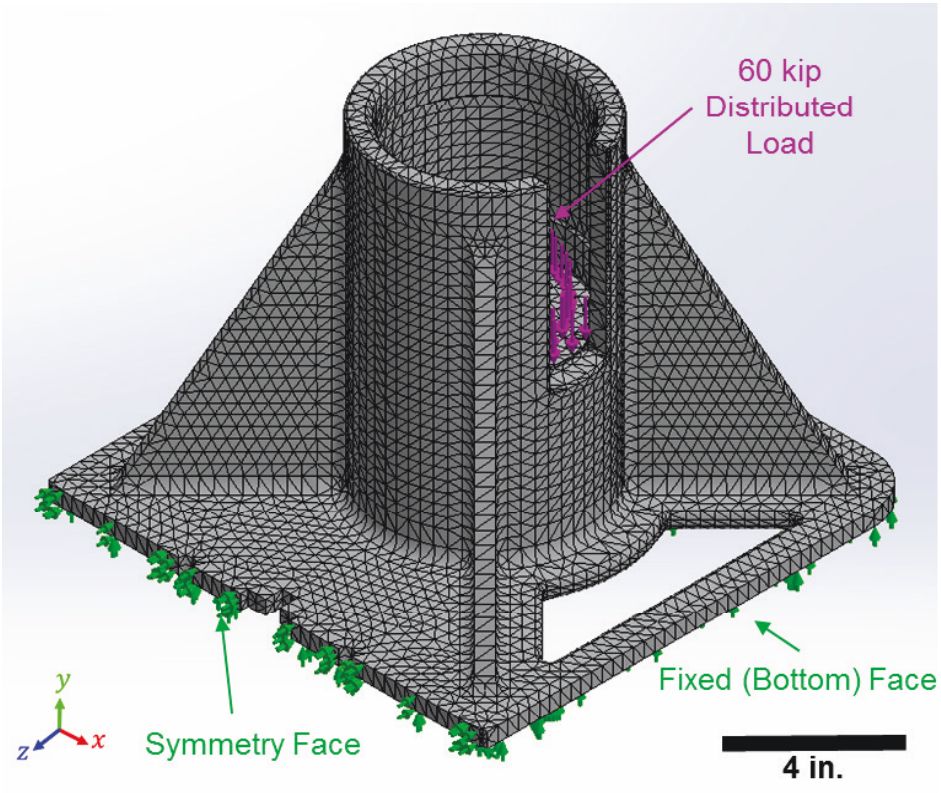

The FEA results for the actuator base analysis are shown in Figure 88. The peak stresses generated from the 60-kip load are only ~5 ksi, and 6061-T6 aluminum has sufficient strength to withstand these stresses. Fatigue is not as much of a concern for the actuator base compared to the load bridge and deadman anchor.

Figure 88. Actuator base FEA contours: (a) displacement, (b) equivalent strain, and (c) von Mises stress.

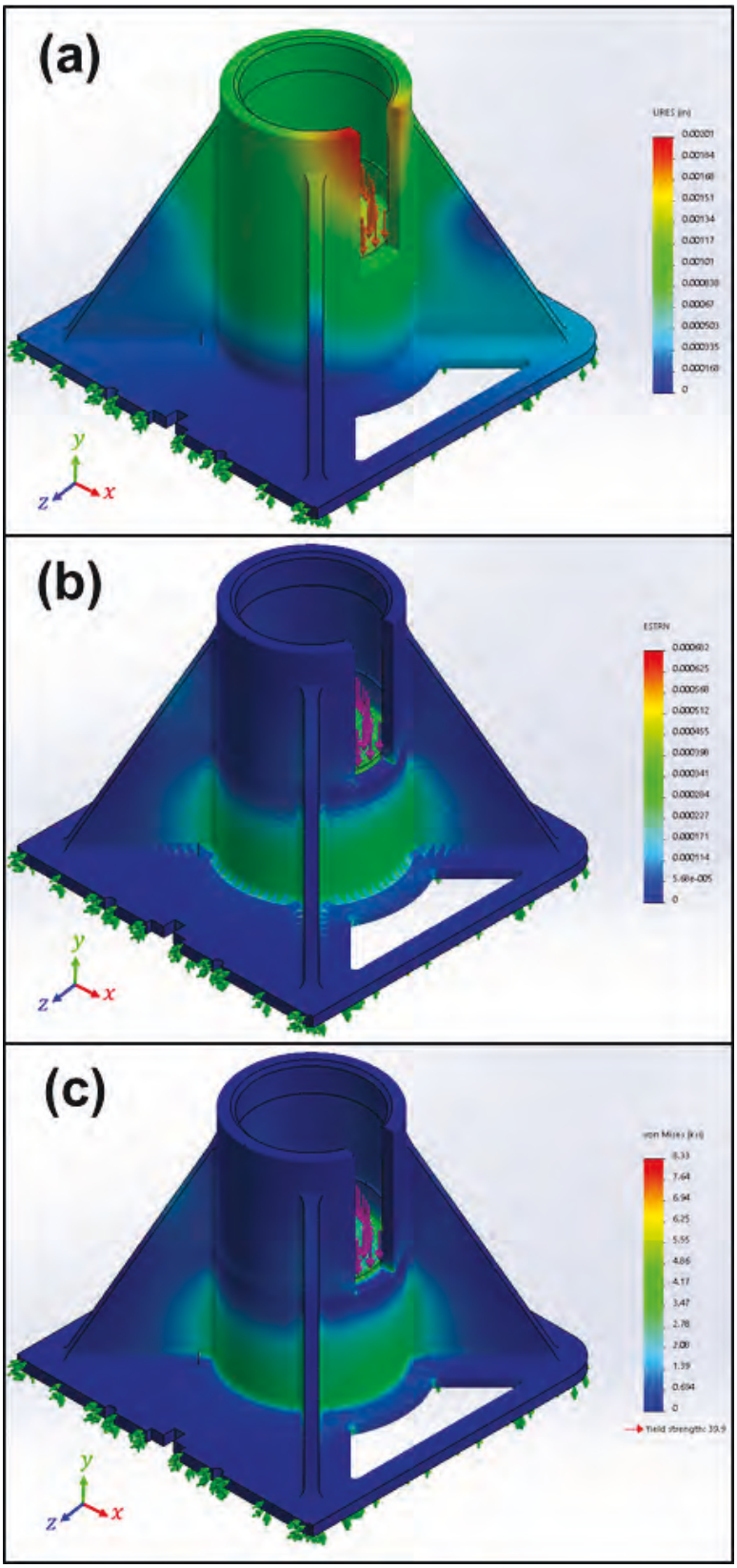

7 Lightweight Anchor Inspection Kit (LAIK) Field Evaluation

7.1 Test site and overview

ERDC personnel conducted three proof load tests using the LAIK prototype at Eglin AFB, FL, on 15 and 16 November 2017. The airfield manager at Eglin AFB gave permission for tests to be conducted on bidirectional F-22 trim pad anchors located on Hardstand 10. The location of the test site within Eglin AFB is shown in Figure 89. Figure 90 is a photograph of Hardstand 10 with the anchors labeled. These anchors were most recently tested by the AFCESA Airfield Pavements Evaluation Team in September 2011 (Rogers et al. 2011). The proof load used in the 2011 test was 70 kips. For reference, Anchors A and B in the current report are referred to as F-22 Anchors 1 and 2, respectively, in the AFCESA report.

Figure 89. Map of Eglin AFB showing the test location.

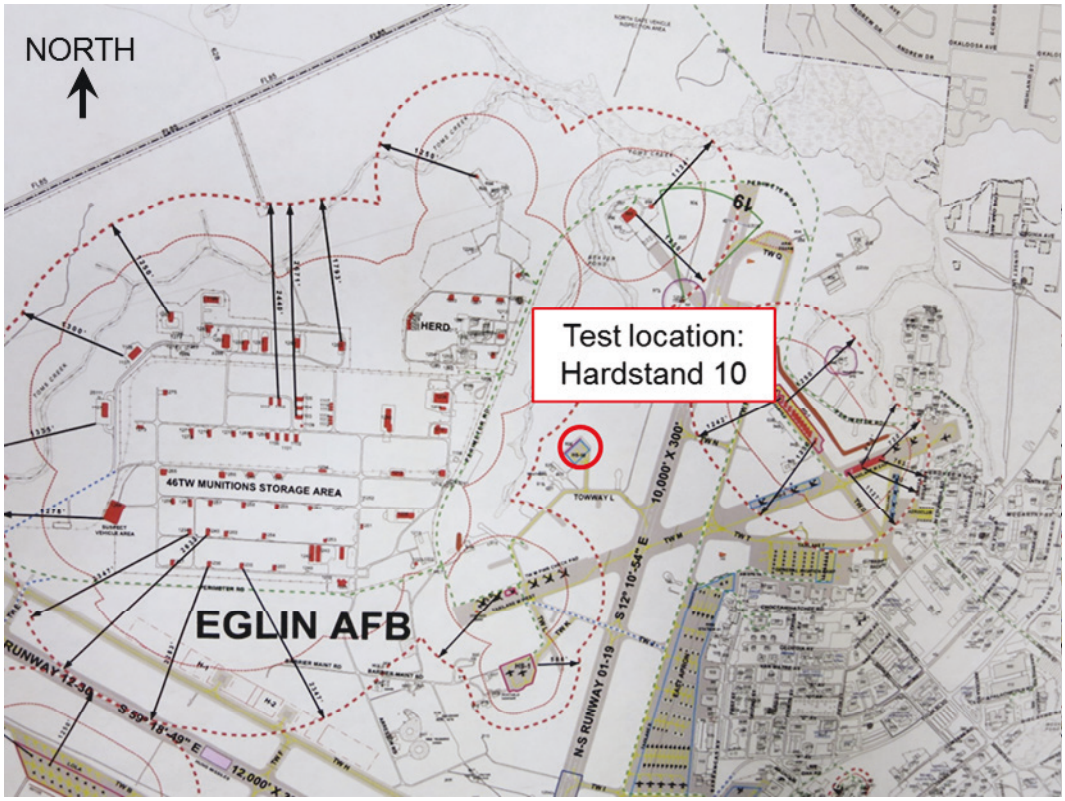

Figure 90. Hardstand 10 looking toward blast deflector.

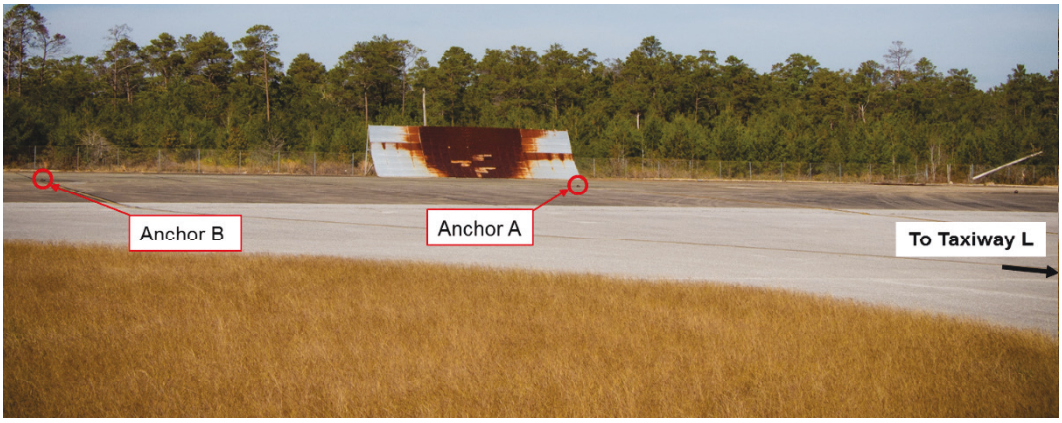

The tests conducted at Eglin AFB are summarized in Table 10.

Table 10. Proof load test matrix for Eglin AFB trim pad anchors.

Test #	Date executed	Anchor tested	Max. load (kip)	Comments
1	15-Nov-2017	A	100	
2	16-Nov-2017	A	100	Replicate of Test #1
3	16-Nov-2017	B	100	

7.2 Test procedure

The test procedure described in the LAIK User's Manual (Appendix A) was followed during installation of the deadman anchor and setup of the system. Refer to the User's Manual for full details. This section provides comments on any changes that were made, primarily for instrumentation, and documents the conditions encountered during the Eglin AFB tests.

The trim pad anchors both had metal links permanently attached, as shown in Figure 91. The link had a 2 in. by 2 in. square cross section and an inside-to-inside length of 9 in.

Figure 91. Permanently attached link on Anchor A.

Rebar was encountered in several holes at both the Anchor A and Anchor B deadman locations. A photograph of rebar at the bottom of one such hole is given in Figure 92, with rebar covering the full width of the 1-in.-diameter hole. A rebar cutting bit was used to cut the rebar, allowing hammer drilling to continue with the hollow concrete bit. The presence of rebar increased the installation time, but also increased the concrete strength around the deadman anchor due to confinement.

Figure 92. Rebar encountered during hammer drilling.

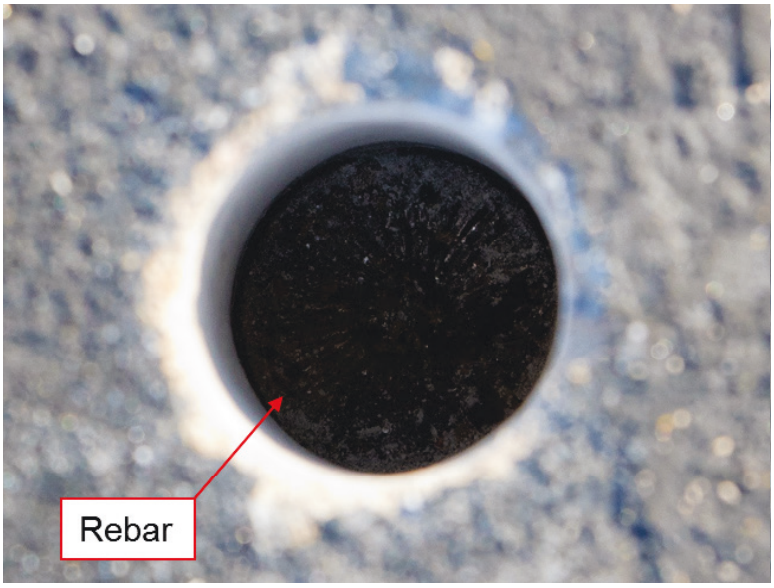

When drilling holes for the deadman anchor at the Anchor B location, several holes broke all the way through the slab. At those holes, the slab thickness was measured to be approximately 7 in. Plastic caps were inserted into all holes that broke through the slab (Figure 93) to keep epoxy in the hole.

Figure 93. Inserting a plastic cap into a hole that broke through the slab.

The deadman anchor was installed, and the bolts were torqued after the epoxy cured. The epoxy age at testing varied somewhat due to instrumentation setup and other factors. Test #1 was performed at an epoxy age of about 1.5 hr, Test #2 was performed using the same epoxy at an age of about 20 hr, and Test #3 was performed at an epoxy age of about 3 hr.

7.2.1 Instrumentation

7.2.1.1 LAIK Test #1

The instrumentation setup used on Anchor A for Test #1 is shown in Figure 94. A 100-kip dynamometer-type load cell was used for in-line load measurement at the trim pad anchor. A digital angle indicator was attached to the load cell with a Velcro strip. String potentiometers were used to measure the actuator stroke (SP2) and displacement at the deadman and trim pad anchors (SP1 and SP3, respectively). Both the string potentiometers and digital dial gauges used for measuring anchor displacement were mounted at approximately a 45-deg angle. The load cell

and the string potentiometers were connected to a data logger, which stored data locally and also transmitted the data wirelessly to a laptop for monitoring during the test.

Figure 94. Instrumentation setup for LAIK Test #1.

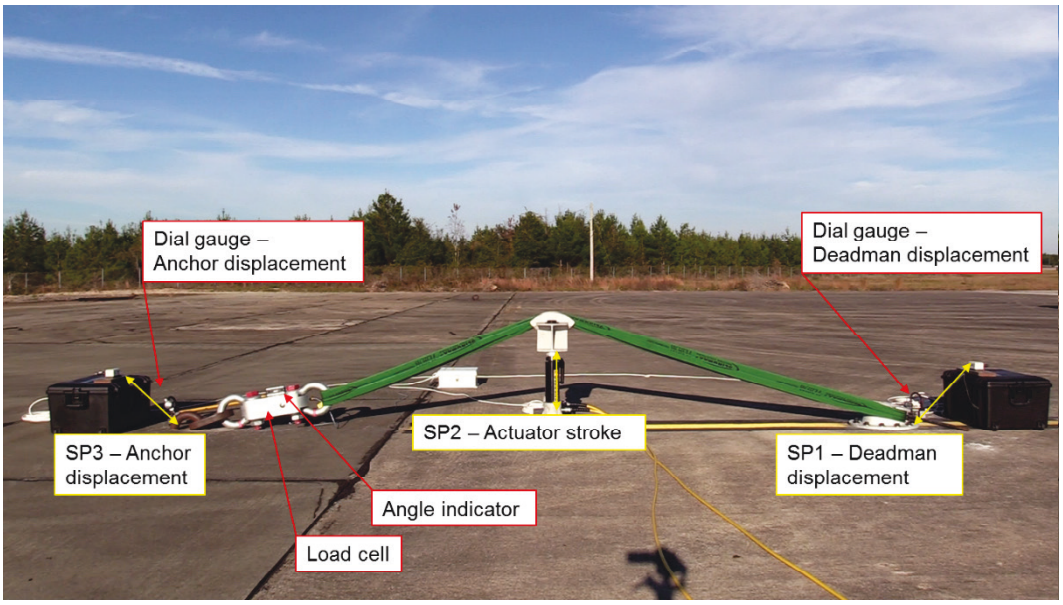

7.2.1.2 LAIK tests #2 and #3

The instrument setup used on Anchor A for Test #2 and Anchor B for Test #3 is shown in Figure 95. A 100-kip dynamometer-type load cell was used for in-line load measurement at the trim pad anchor. A digital angle indicator was attached to the load cell with a Velcro strip. String potentiometers were used to measure the actuator stroke (SP2) and horizontal and vertical displacement at the deadman anchors (SP1 and SP3, respectively). A digital dial gauge mounted at approximately 45 deg was used to measure trim pad anchor displacement. The load cell and the string potentiometers were connected to a data logger, which stored data locally and also transmitted data wirelessly to a laptop for monitoring during the test.

Figure 95. Instrumentation setup for LAIK Tests #2 and #3.

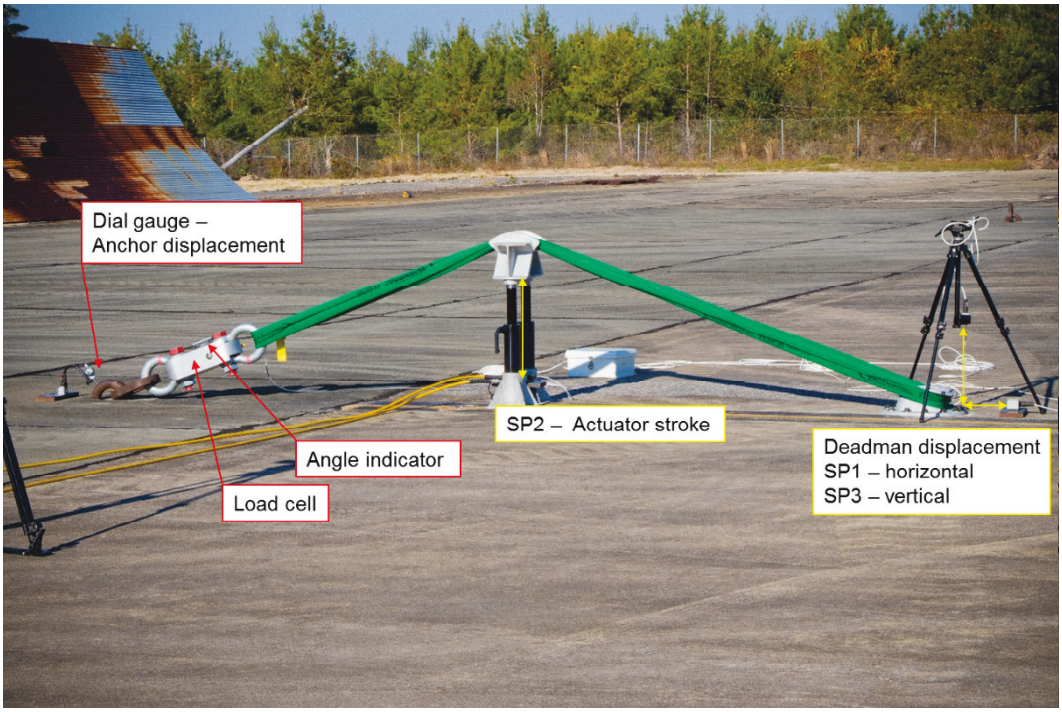

7.2.2 Loading

The nominal loading schedule used for all three tests is given in Table 11. The approximate hydraulic pressure was calculated for two RAC-3010 rams with a combined cylinder area of 13.7 in.^{2}. Pressures were rounded up to the nearest 10 psi. The hold time was increased during Test #1 for additional inspection at each increment.

Table 11. Loading schedule with approximate hydraulic pressures.

Sling tension, load cell reading (lbf)	Calculated actuator force at β = 20° (lbf)	Approximate hydraulic pressure (psi)	Hold time (min)
10,000	6,840	500	2
20,000	13,681	1,000	2
30,000	20,521	1,500	2
40,000	27,362	2,000	2
50,000	34,202	2,500	2
60,000	41,042	3,000	2
70,000	47,883	3,500	2
80,000	54,723	4,000	2
90,000	61,564	4,500	2
100,000	68,404	5,000	2

7.3 Results

Results for the three tests are presented here. Time-histories of the load cell reading are presented in Figure 96. Test #1 had longer holds between load increments for more detailed inspection. Tests #2 and #3 followed the 2-min hold time more closely.

Figure 96. Load vs. time for anchor proof load tests using the LAIK prototype.

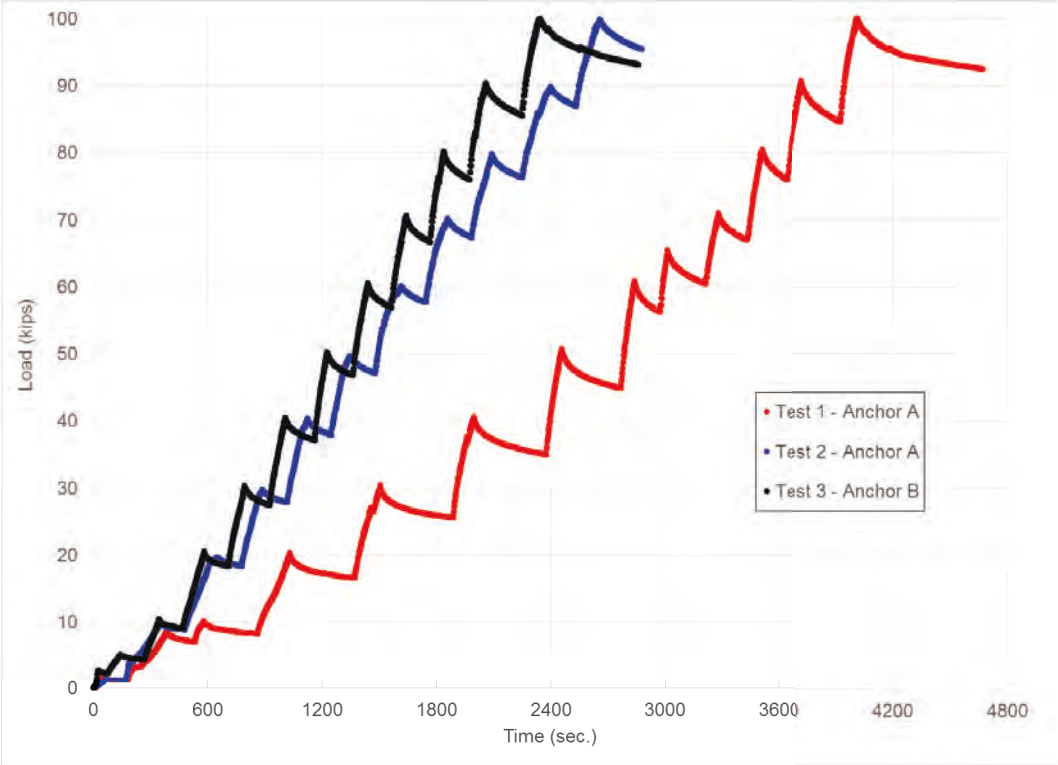

Figure 97 shows sling tension–actuator displacement plots for the three tests to give an indication of the test system's behavior. Test #1 was the first use of the sling for a trim pad test, but not the first time the sling was loaded, since the sling was proof loaded to 130 kips by the manufacturer. All the curves exhibit a toe-in region followed by an approximately linear region. The data for Tests #1 and #2 coincide up to about 5.5 in. (20 kips). The toe-in region for Test #1 continues farther than that for Test #2. Between 6 and 10 in. of actuator displacement was required to achieve 100 kips of tension using the two setups tested in this work. Test 3 required the least stroke because the system had less slack initially. The actuator stroke needed for other setups would vary depending on the total height of the center stand, the amount of slack in the sling, and the total length of the sling assembly (sling and connecting hardware).

Figure 97. Sling tension vs. actuator displacement for proof load tests using the LAIK prototype.

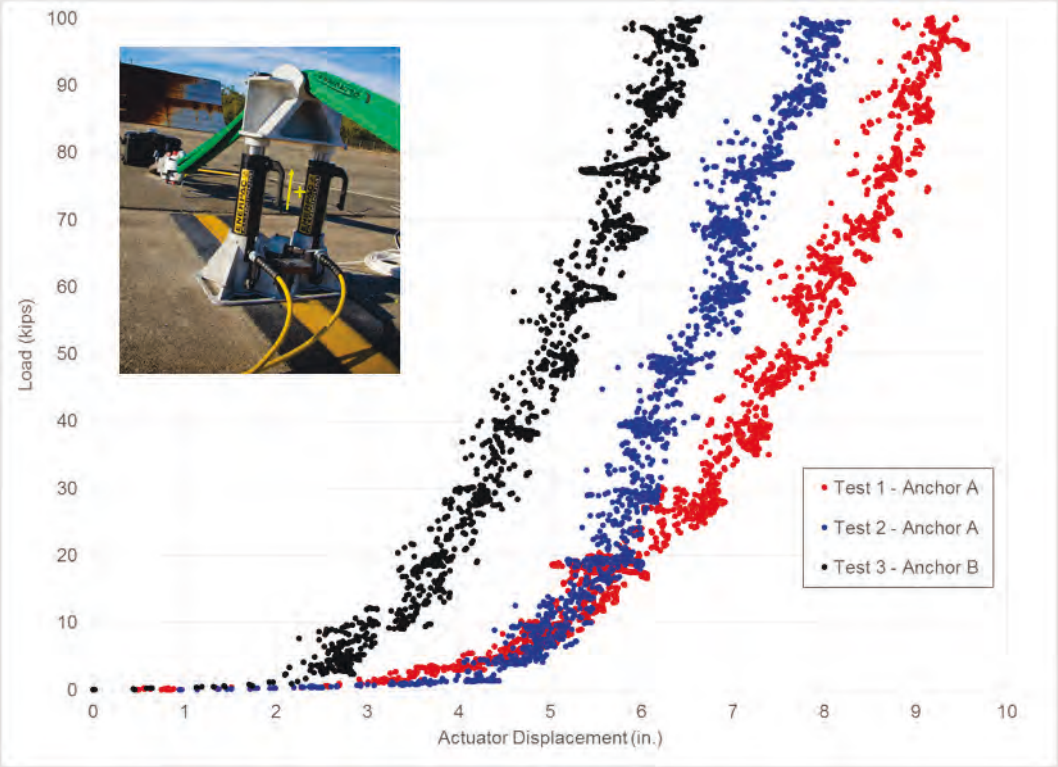

Figure 98 shows the load as a function of the load cell angle. The LAIK system is designed to start at a low angle and reach the desired angle at or near the proof load. In Test #1, the load angle was 20 deg at roughly 50 kips and was 21.1 deg at 100 kips. In Tests #2 and #3, the load angle was 20 deg at roughly 70 kips. Test #2 achieved 100 kips at a load angle of 20.6 deg and Test #3 achieved the same load at a load angle of 20.7 deg. These results show that the angle of application should be within an acceptable range for proof loads between 70 and 100 kips.

Figure 98. Load vs. angle of application. Angle is relative to the horizontal and was measured with a digital angle indicator mounted on the load cell.

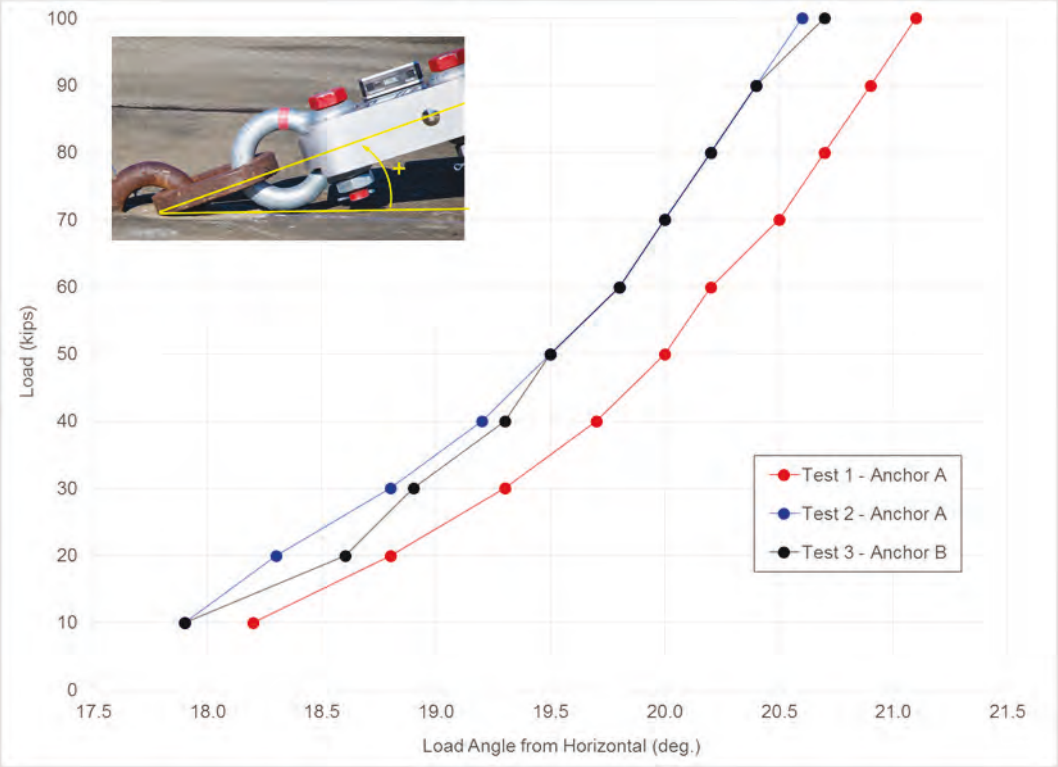

Figure 99 shows load versus anchor displacement curves for the three LAIK tests. The anchor displacement measurement was made using a digital dial gauge mounted at approximately 45 deg. There was some concern as to the stability of the indicator holder that was used during the test. The dial gauge reading was observed to increase due to the indicator holder slowly creeping down under the weight of the gauge. Dial indicator measurements were made to the nearest 0.00005 in. and would be sensitive to even the smallest movement of the positioning arm. Therefore, the dial indicator displacement results presented here should be interpreted with some caution. A sturdier indicator positioner was procured for the final kit to help prevent such issues in future tests.

Figure 99. Load vs. dial indicator displacement reading. The non-zero displacement after unloading is attributed to suspected drift of the positioner holder, not permanent deformation of the anchors.

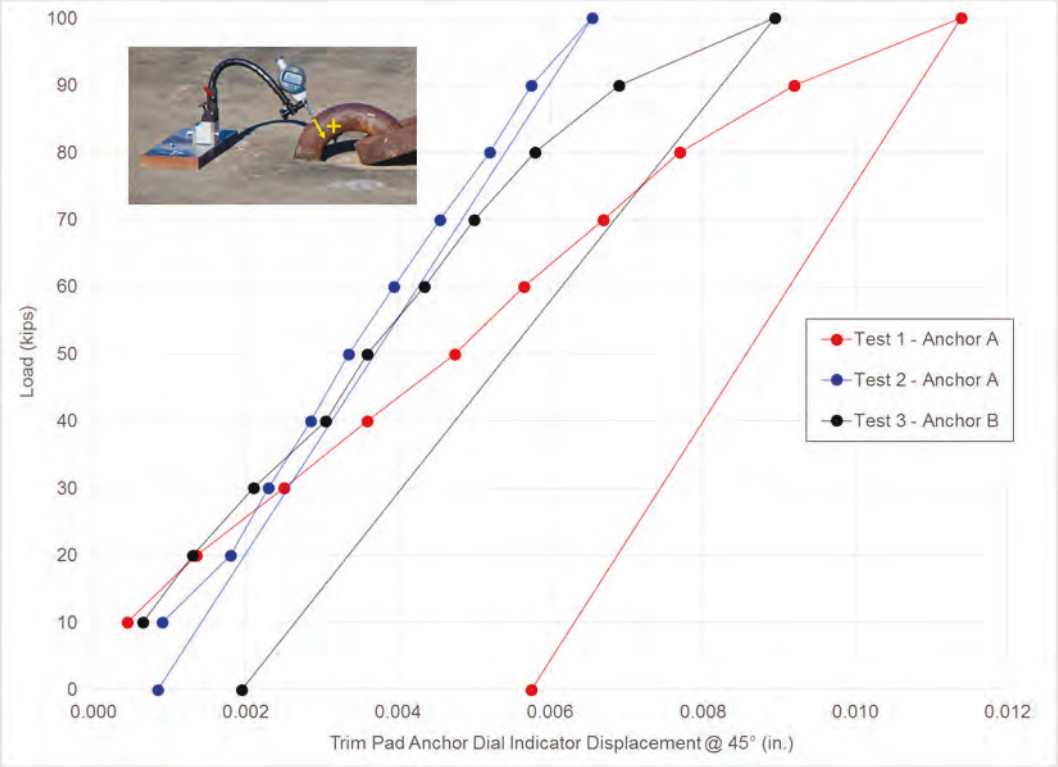

7.4 Summary

The LAIK prototype was used to proof load two bidirectional trim pad anchors to 100 kips. All tests were performed with the deadman installed in a reinforced slab. Due to the close proximity of rebar, the concrete around the deadman anchor can be considered confined. Additional testing is recommended to determine if the deadman can react the full 100-kip load when installed in an unreinforced slab.

8 Conclusions and Future Work

This report documented the results of a project involving the development of a prototype lightweight anchor testing kit for AFCEC. Site visits were conducted at Dannelly Field (Montgomery, AL) and Eglin AFB (Okaloosa County, FL). These visits provided information about the anchors in use on airfields and the environment in which the testing kit would be used. A number of test device concepts were considered before selecting a design. During the design process, the feasibility of concepts was evaluated using engineering computations at varying levels of complexity as well as a small scale proof-of-concept test.

The prototype kit developed in this project comprised three devices: a COTS device (QualiAnchor 2005) for proof loading studs or threaded anchors, a LAIK system for proof loading trim pad anchors, and a load beam system for proof loading tie-downs and mooring points. The LAIK system and the load beam system were both designed and fabricated in-house at ERDC and use the same lightweight, aluminum hydraulic actuators.

This report also documented test results from three test series. Small-scale proof-of-concept testing was conducted at ERDC as part of the design process. Poly panel stud testing was performed at ERDC to demonstrate operability of the QualiAnchor 2005. Lastly, the final LAIK prototype was used to test trim pad anchors at Eglin AFB.

It should be emphasized that the anchor testing kit is a prototype and has not been evaluated under all possible use conditions. Some possible areas for future work are summarized in the following paragraphs.

- The LAIK deadman was anchored in a reinforced concrete slab for all tests at Eglin AFB. Additional tests are needed to determine the deadman anchor's capacity for other concrete conditions.
- Studs and threaded anchors are often installed in groups. Loading such anchors individually may result in a higher capacity for the anchor than could be achieved when the other anchors in the group are stressed as well. If loading the entire anchor group is not feasible, the proof loads for single anchors should be adjusted to account for interaction effects during in-service loading. Adjustment factors could be conservatively derived from current design methods for concrete anchors.

- Analytically determining the ultimate capacity, and hence the factor of safety, for complex anchorages in concrete is difficult. The capacity of the LAIK deadman (or other deadman concepts) could be investigated using high-fidelity nonlinear modeling, testing to failure, or a combination thereof.
- The interaction between shear and tensile loading on embedded anchors is not well understood. A test device that applies only a vertical load would be more efficient than one that applies a load with both vertical and horizontal components. Research is needed to determine what level of vertical loading would be required to ensure the proof load test is still conservative.

References

A-Aerial Service Company. n.d. *Manta LL-2 load locker*. https://www.linemen-tools.com/MANTA_LL_2_LOAD_LOCKER_p/manta-ll-2-load-locker.htm

ACI Committee 318. 2011. *Building code requirements for structural concrete. Appendix D – Anchoring to concrete*. ACI 318-11. Farmington Hills, MI: American Concrete Institute.

Crosby Group LLC. 2017. *Crosby® HR-125 UNC swivel hoist ring*. https://www.thecrosbygroup.com/products/hoist-rings-eye-bolts-lifting-points/standard-hoist-rings/standard-bail/crosby-hr-125-unc-swivel-hoist-ring/

Dassault Systemes Simulia Corp. 2016. *Abaqus documentation*. Version 2016. Providence, RI: Dassault Systemes Simulia Corp.

Department of the Air Force. 2000. *Inspection and testing of trim pad anchoring systems*. Engineering Technical Letter (ETL) 00-2. Tyndall AFB, FL: Headquarters Air Force Civil Engineer Support Agency.

———. 2001. *Design and construction of high-capacity trim pad anchoring systems*. ETL 01-10. Tyndall AFB, FL: Headquarters Air Force Civil Engineer Support Agency.

Department of Defense. 2008. *Airfield and heliport planning and design*. Unified Facilities Criteria (UFC) 3-260-01. Air Force Civil Engineer Support Agency.

Eaton, J. W., D. Bateman, S. Hauberg, and R. Wehbring. 2017. *GNU Octave version 4.2.1 manual: a high-level interactive language for numerical computations*. http://www.gnu.org/software/octave/doc/interpreter/

Ferreira, A. J. M. 2009. *MATLAB codes for finite element analysis*. Dordrecht, The Netherlands: Springer Science+Business Media B.V.

Grau, R. H., and D. L. Cooksey. 1992. *Evaluation of grounding and mooring points for Army aircraft*. Miscellaneous Paper GL-92-10. Vicksburg, MS: U.S. Army Engineer Waterways Experiment Station.

Hilti. n.d. *HIT-HY 200-A*. https://www.hilti.com/content/hilti/W1/US/en/products/catalog-page-editorials/anchors/hit-hy-200-a.html

Lotze, D., R. E. Klingner, and H. L. Graves. 2001. Static behavior of anchors under combinations of tension and shear loading. *ACI Structural Journal* 98(4):525-536.

Oluokun, F. A., and E. G. Burdette. 1993. Behavior of channel anchors in thin slabs under combined shear and tension (pullout) loads. *ACI Structural Journal* 90(4):407-413.

QualiTest. n.d. *Quali Anchor 2005 heavy duty tester kit*. http://www.worldoftest.com/pdf/Qualitest_Quali%20Anchor2005.pdf

Rogers, R. C., H. Muniz, T. Wyatt, and J. Almanzar. 2011. *Aircraft anchor tests: Eglin AFB, Florida*. AFCESA-ANCHOR TEST-12. Tyndall AFB, FL: Air Force Civil Engineer Support Agency.

Smith, J. E., and J. E. Schroeder. 1958. *Strength tests of aircraft mooring eyes in concrete pavement*. Technical Report R-014. Port Hueneme, CA: U.S. Naval Civil Engineering Laboratory.

Transducer Techniques. 2015. *THD series through hole donut load cells (3.00 O.D.)*. https://www.transducertechniques.com/thd-load-cell.aspx

Tri-Service Pavements Working Group (TSPWG). 2017. *Inspection of trim pad anchor systems*. TSPWG M 3-260-03.00-2. Air Force Civil Engineer Center. https://www.wbdg.org/FFC/DOD/STC/tspwg_m_3-260-03_00-2.pdf

Wej-It. 2015. *POWER-Sert adhesive insert anchors*. http://www.toggler.com/wejit/powersert.pdf

Appendix A: Lightweight Anchor Inspection Kit (LAIK) User Manual

USER MANUAL

Engineer Research and Development Center

US Army Corps of Engineers®
Engineer Research and Development Center

ERDC
INNOVATIVE SOLUTIONS for a safer, better world

USER MANUAL

U.S. AIR FORCE

PROTOTYPE

LAIK

LIGHTWEIGHT ANCHOR INSPECTION KIT

Approved for public release; distribution is unlimited.

The U.S. Army Engineer Research and Development Center (ERDC) solves the nation's toughest engineering and environmental challenges. ERDC develops innovative solutions in civil and military engineering, geospatial sciences, water resources, and environmental sciences for the Army, the Department of Defense, civilian agencies, and our nation's public good. Find out more at www.erdc.usace.army.mil.

Contents

Introduction 2
- Purpose and scope 2
- Safety 2
- Requirements for use of kit 2
- Unpacking the kit 3
- Inspection 4
- Overview of LAIK layout 4

Procedure 5
- Step 1: Dimensions and layout 5
- Step 2: Anchor installation 7
  - *Step 2A: Secure deadman drilling template 7*
  - *Step 2B: Drill anchor holes 9*
  - *Step 2C: Install threaded adhesive concrete anchors 11*
- Step 3: Deadman installation 14
- Step 4: Hydraulic actuator installation 14
- Step 5: Dynamometer and sling assembly 17
- Step 6: Instrumentation setup 20
- Step 7: Proof Load Testing 20
- Step 8: Disassembly 22

References/Additional sources of information 23

Data Sheets 25

Components List 29

LAIK DWG. 1: DEADMAN ANCHOR INSTALLATION JIG COMPONENTS REQUIRING FABRICATION 31

LAIK DWG. 2: LAIK TEST COMPONENTS REQURING FABRICATION 37

Introduction

Purpose and scope

This draft manual describes the use of the Lightweight Anchor Inspection Kit (LAIK) for proof load testing of trim pad tie down anchors. As of this writing, the LAIK is still in prototype status. While it has been successfully used for several tests, it has not been evaluated for use under all conditions that might be encountered. Also, several of the LAIK components have a finite fatigue life, which has not been fully quantified. Therefore, the aluminum LAIK components should be replaced periodically. As this is a prototype, a recommended replacement interval has not yet been determined.

Safety

This draft manual attempts to identify major safety-related points, but does not purport to address all possible health or safety issues that might arise from use of the LAIK.

Required PPE:

- Hearing protection
- Safety glasses
- Steel-toed boots
- Work gloves

Recommended PPE:

- Knee pads

Requirements for use of kit

The LAIK is intended to be used by base civil engineers or others with similar training. The following items are assumed to be available:

- Torque wrench (capable of at least 75 ft-lb)
- Stop watch (or stop watch function)
- Heavy magnetic object for indicator holder base (e.g., toolbox, ammo box, steel plate, etc.)

If drilling through rebar or other embedded steel, the following items are also recommended:

- Electric drill, SDS Plus chuck (must have rotary-only mode)
- Generator for the drill

These items increase efficiency when cutting through rebar with the rebar cutter bit (included in kit). The included cordless SDS-Max drill and SDS-Max to SDS-Plus adapter may also be used for drilling through rebar, but battery usage may be excessive.

Unpacking the kit

Check that all cases listed in Table 1 have been received. Verify that none of the parts in the components list are missing.

Table 1. Pelican cases containing the LAIK.

Case no.	Contents
1	User Manual, Deadman Anchor Template, Concrete Anchors, Tools
2	Cordless SDS-Max Drill, SDS-Max to SDS-Plus Adapter, Drill Bits
3	Aluminum Deadman Reaction Anchor and Hardware
4	Aluminum Actuator Base
5	Aluminum Load Bridge
6	Cordless Vacuum and Accessories
7	Battery Packs, Hilti Epoxy and Dispenser
8	Aluminum 30-ton Hydraulic Actuators
9	Hydraulic Pump and Accessories
10	Slingmax Twin-Path Sling (175" Long), Hydraulic Hose (50')
11	Shackle for 100-kip Dynamometer (1 of 2)
12	Shackle for 100-kip Dynamometer (2 of 2)
13	100-kip Dynamometer
14	Instrumentation and Accessories
15*	Tie-Down Tester Components
16*	Qualianchor Threaded Stud Tester

*Cases 15 and 16 contain components for testing additional anchor types not covered in this manual and are not required to execute the testing described here.

Inspection

Begin by completing the inspection record sheet provided with this manual (pg. 27). Inspect all steel components of the anchor system for rust, deformation, cracks, or any other defect that reduces the cross-sectional area of the component. Also inspect the concrete anchor block. Look for spalling or cracking, particularly at the interface of the steel anchor eye and the concrete anchor block. Record findings on the inspection record sheet and write any additional observations or notes in the space provided.

Overview of LAIK layout

Figure 1 illustrates a typical LAIK layout. The hydraulic actuators extend, producing tension in the sling and thereby loading the anchor at a ~20° angle from the horizontal. The magnitude of the load is measured via an in-line load cell (dynamometer), and the direction is measured with an angle indicator.

Figure 1. Schematic overview of typical LAIK layout.

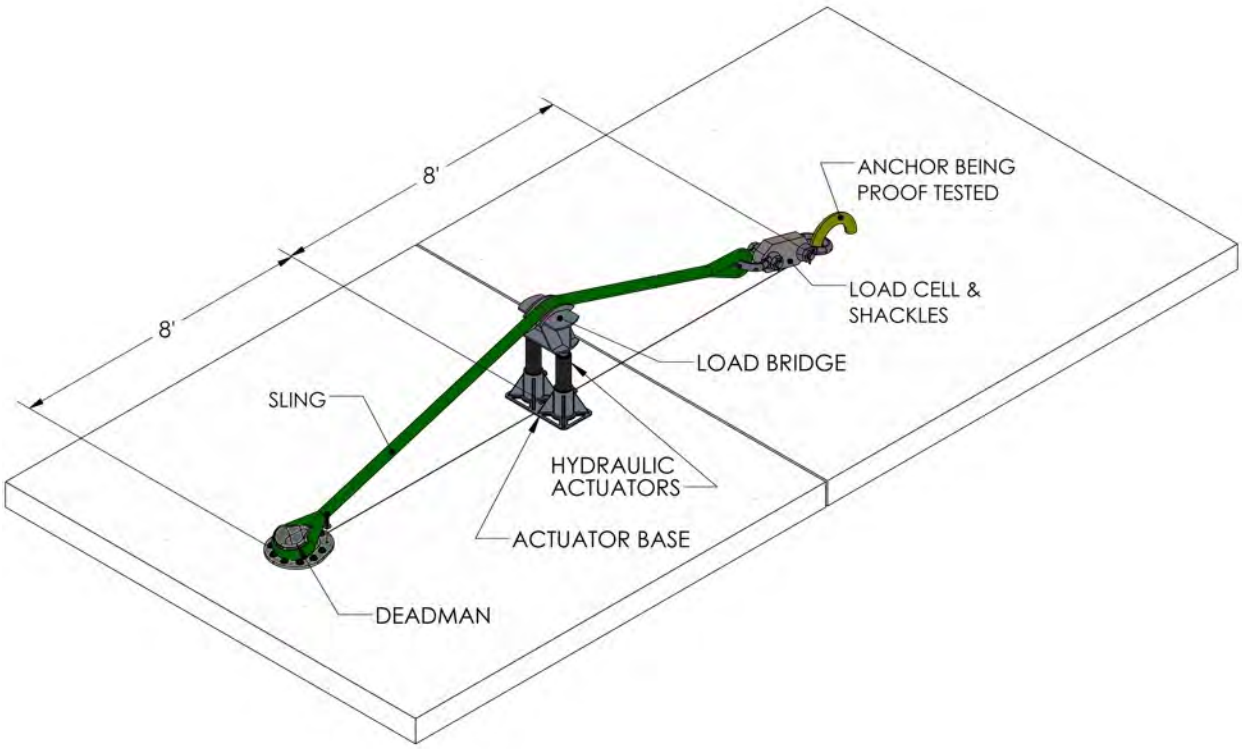

Procedure

Step 1: Dimensions and layout

1.1. Use a chalk line to mark a straight line directed away from the trim pad anchor to be tested. Position the line so that it is in the same direction that the anchor is pulled on in normal use.

1.2. If the trim pad anchor has a link permanently attached to it (see example in Figure 2), measure the length of the link from inside edge to inside edge.

NOTE: The presence of any link or other connecting hardware will increase the actuator stroke needed to reach a given load. The addition of 1 ft of length or less to the system should pose minimal problems.

Figure 2. Trim pad anchor with link permanently attached.

1.3. Consult Figure 3 to determine the distances at which the actuators and deadman should be located from the anchor. All measurements should be made from the front edge of the anchor.

Figure 3. Distances from front of anchor to actuators (distance 1) and deadman (distance 2).

If no link is present…

Distance 1 (to Actuators)	Distance 2 (to Deadman)
8'-0"	16'-0"

If a permanently attached link is present…

Link inside length	Distance 1 (to Actuators)	Distance 2 (to Deadman)
6"	8'-2 ½"	16'-5"
9"	8'-4"	16'-8"
12"	8'-5 ½"	16'-11"

If another size of link or another type of connecting hardware is present, proceed as follows:

L = inside length of link, or length from bearing point to bearing point for other hardware

$X = 0.5 \cdot L - ½"$

Distance 1 = 8' + X

Distance 2 = 16' + 2·X

NOTE: The actuators must always be located exactly midway between the anchor and deadman, i.e., the angle of the sling with respect to vertical must be equal on both sides of the load bridge. Otherwise, the horizontal loads will be unbalanced, resulting in damage to the actuators.

1.4. Use the permanent marker to place marks on the ground perpendicular to the chalk line at the two distances from the front edge of the trim pad anchor. These lines will be used to locate the actuator base and deadman. See Figure 4 for an illustration.

Figure 4. Plan view of layout. Not to scale.

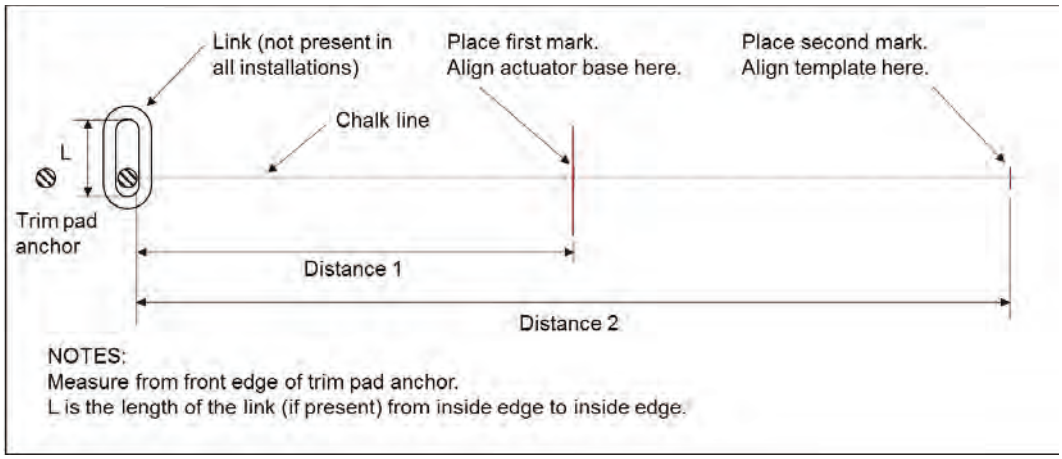

Step 2: Deadman anchor installation

If performing a test at a location where a deadman anchor for the LAIK was previously installed and is in good condition, skip this section and proceed to "Step 3: Deadman installation" (pg. 14).

Step 2A: Secure deadman drilling template

The drilling template is secured by four 5/16-in. by 2-1/4-in. Tapcon screws to prevent movement while drilling the eleven anchor holes. Installing the Tapcons in the sequence shown in Figure 5 helps prevent misalignment.

2A.1. Align the crosshairs on the drilling template with the 2nd distance mark. See Figure 5 for correct orientation.

2A.2. Use the ¼-in. by 7-in. carbide bit to drill a pilot hole for Tapcon #1 (in the middle of the crosshairs) through the small center hole in the template. Take care to keep the drill bit as close to vertical as possible. Then, use the vacuum and straw attachment to evacuate all debris from the hole. Finally, loosely install Tapcon #1 (Figure 6 and Figure 7).

> **WARNING:** The Tapcon screw will break if over-torqued or forced and will need to be extracted.

2A.3. Make sure the template is still correctly aligned with the chalk line using the alignment marks on the template. Drill, evacuate the hole, and loosely install Tapcon #2.

NOTE: Installing each Tapcon prior to drilling the next hole ensures correct alignment.

2A.4. Repeat the process of drilling a hole, evacuating the hole, and then inserting a screw for Tapcon screws #3 and #4.

2A.5. Tighten all four Tapcon screws to secure the template. Take care to not over-torque and break a screw.

Figure 5. Deadman Drilling template alignment.

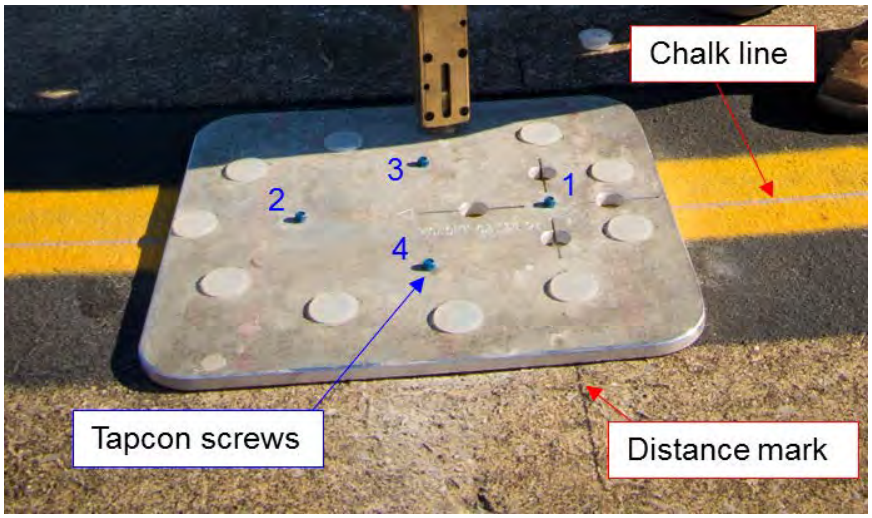

Figure 6. Drilling a hole for the Tapcon screw.

Figure 7. Installing the Tapcon screw #1. Do not force the screw.

Step 2B: Drill deadman anchor holes

Once the template has been secured with four Tapcon screws, the 1-in. holes for the concrete anchors can be hammer drilled with the Hilti TE-YD hollow drill bit. The template has eleven threaded holes for the drill guide. Keep the plastic cover on all holes except for the hole currently occupied by the drill guide. Dust and debris created during hammer drilling may clog the threads on the template. A small brush is provided in the kit for cleaning dust and debris from the threads. An example of the template in use is shown in Figure 8.

WARNING: Avoid drilling into soil. If the hollow drill bit does break through the bottom of a slab, stop drilling immediately and thoroughly clean the drill bit cavity. Attempting to operate the drill when the hollow bit is clogged will prevent the vacuum from removing debris, and the bit will become very hot. The heat will cause soil, especially clayey soil, to harden, making the obstruction difficult or impossible to remove.

2B.1. Remove the plug at the 3 o'clock position from the template (where the arrow on the template points to 12 o'clock) and screw the drill guide into the threaded hole, hand-tight.

2B.2. Attach the drill and connect the vacuum to the hollow drill bit.

NOTE: It is good practice to lubricate the SDS-Max connection periodically with the oil provided with the drill.

2B.3. Drill to a depth of 7.5 in. Be sure to always run the vacuum while drilling.

NOTE: It is good practice to mark or place tape around the drill bit to indicate proper depth.

NOTE: Routinely check that the vacuum has adequate suction. Empty the vacuum and clean the filter as needed.

2B.4. Disconnect the drill from the bit and unscrew the drill guide from the template. Then insert a template alignment pin into the hole using a hammer. The alignment pin provides additional security against template movement.

2B.5. Remove the plug at the 9 o'clock position from the template, screw the drill guide into the threaded hole, and repeat steps 2B.2 thru 2B.4.

2B.6. Remove the plug at the 12 o'clock position from the template and screw the drill guide into the threaded hole and repeat steps 2B.2 thru 2B.4. Once the three alignment pins are installed, the remaining eight holes can be drilled in any order.

2B.7. Drill the remaining eight holes using the template and drill guide. Be sure to replace each hole plug immediately after each hole has been drilled to prevent dust from entering the hole and/or clogging the threads on the template.

Figure 8. Template in use for hammer drilling. Two template alignment pins (shown at the 3 and 9 o'clock positions) have been placed to secure the template. Hole plugs protect the other holes from dust or debris which might damage the threads.

Step 2C: Install threaded adhesive concrete anchors

2C.1. Carefully back out the four Tapcon screws and discard—do not reuse the Tapcon screws.

2C.2. Remove the drilling template and vacuum any residual dust. It is good practice to use a wire brush to clean the holes thoroughly.

> **WARNING:** Concrete dust severely reduces the adhesive strength of the epoxy. Ensure holes are free of dust before applying epoxy.
>
> **WARNING:** Avoid epoxy contact with skin and eyes. The epoxy generates heat as it cures and can cause burns.
>
> **WEAR SAFETY GLASSES AND GLOVES**

2C.3. Install the Hilti HIT-HY 200-A epoxy cartridge in the dispensing gun.

NOTE: When working with Hilti HIT-HY 200-A epoxy, be aware of the working time listed in Table 2. The epoxy in this kit is supplied in packages. A disposable mixing nozzle is included with each epoxy cartridge.

Table 2. Gel and cure times for HIT-HY 200-A epoxy.

Base Material Temperature (°F)	Maximum working time	Minimum curing time
14	90 min	7 hrs
23	90 min	7 hrs
32	50 min	4 hrs
50	15 min	1 hr
68	7 min	30 min
86	4 min	30 min
104	3 min	30 min

2C.4. Before injecting any epoxy into an anchor hole, squeeze a small amount of epoxy out of the dispenser onto a disposable surface to verify the mixing nozzle is working properly.

2C.5. Inject the epoxy into the hole at the 12 o'clock position (the hole closest to the trim pad anchor), moving from the bottom of hole up, slowly, so as to avoid air pockets.

NOTE: The holes should be filled so that a small amount of epoxy squirts out when the anchor is installed. You may need to experiment to find the correct amount to fill the holes. Generally, 10 to 12 pumps work well. It is always better to overfill the hole than under-fill it.

The threaded adhesive concrete anchors closest to the trim pad anchor being tested experience lower tensile loads compared to those farther from the trim pad anchor. So, it is good practice to begin with the holes nearest 12 o'clock and work your way toward 6 o'clock. This allows you to perfect the injection process as you work toward the more critical concrete anchor locations.

2C.6. Immediately after injecting the epoxy in first hole, insert a Wej-It Power-Sert concrete anchor. Use the threaded set tool and mallet to set the anchor. The top of the anchor should be ⅛ in. below the pavement surface. See Figure 9.

NOTE: The Wej-It Power-Sert anchors have a flat on one side. The epoxy tends to jet out on that side. Use rags to immediately wipe up any epoxy that could prevent the deadman anchor from sitting flush on the concrete.

Figure 9. Inject epoxy in and use threaded set tool to set the anchor ⅛ in. below the pavement surface.

2C.7. After setting the anchor, install a ¾"-10 plastic set screw to prevent epoxy from getting into the threads (see Figure 10). Clean the set tool after each use to make sure the threads stay clean.

Figure 10. Plastic set screws are used to keep epoxy out of the anchor threads.

2C.8. Repeat this process until all eleven anchors are installed. Typically two cartridges of epoxy are needed to set all eleven anchors.

ATTENTION: The Hilti HIT-HY 200-A epoxy must cure for at least the time indicated in Table 2 before the deadman anchor can be installed. Do not disturb the anchors while the epoxy is curing. You may proceed with steps 4, 5.1-3, and 6 while waiting for the epoxy to cure.

Step 3: Deadman installation

3.1. Line up the deadman anchor over the threaded inserts and eleven ¾"-10 × 2.5-in. flanged hex head screws and washers to anchor the deadman. Torque bolts in a star pattern to 75 ft-lb.

Figure 11. Recommended torque sequence.

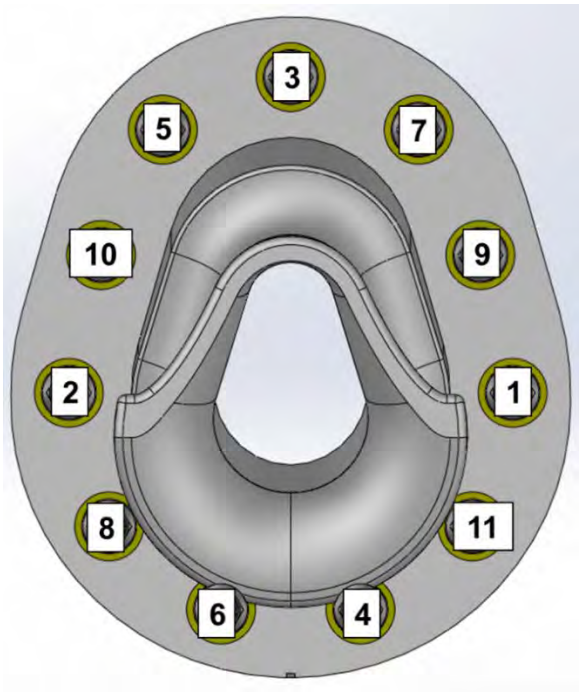

Step 4: Hydraulic actuator installation

The actuator base is secured with two 5/16-in. by 2-1/4-in. Tapcon screws.

4.1. Position the actuator base so that the 1st mark from Step 1.4 lines up with the crosshairs on the actuator base. See illustration in Figure 12.

Figure 12. Actuator base in correct position.

4.2. Use the ¼-in. by 7-in. carbide bit to drill a pilot hole for one of the Tapcon screws through one of the two holes in the template. Take care to keep the drill bit as close to vertical as possible. Then, use the vacuum and straw attachment to evacuate all debris from the hole. Finally, loosely install the first Tapcon screw.

4.3. Make sure the template is still correctly aligned with the chalk line using the alignment marks on the template. Drill, evacuate the hole, and install the second Tapcon screw. Tighten both Tapcons.

WARNING: The Tapcon screw will break if over-torqued or forced.

4.4. Check that the extensions are threaded securely into the top of the hydraulic actuators (see Figure 13) and the actuators are fully retracted. Then, place the two aluminum hydraulic cylinders into the actuator stand. Make sure that the cylinders sit level in the stand.

Figure 13. Hydraulic cylinders with extensions installed.

4.5. Place the Enerpac hand pump approximately 50 ft from the anchor to be tested and connect one end of the 50-ft hydraulic hose to the hand pump and the other end to the AM-21 manifold. Then, using the two 6-ft hydraulic hoses, connect the manifold to the two cylinders. See Figure 14.

NOTE: All hydraulic hoses and components in the kit are provided with quick-connect couplers. Remove the plastic dust caps before connecting.

Figure 14. Hydraulic system layout.

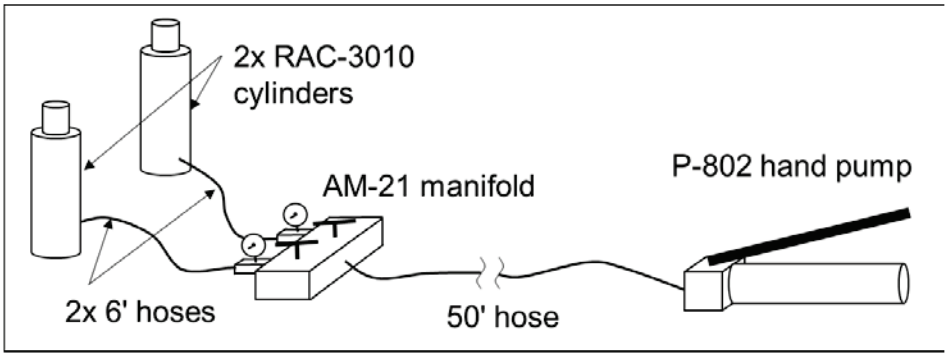

4.6. Before loading, adjust the needle valves on the manifold to fully open so that the two actuators raise evenly and equally. Use the level to verify.

4.7. Place the load bridge on top of the cylinders. The circular lip on the bottom of the bridge should fit securely over the extenders on top of the cylinders. Check that the entire setup is level using the incorporated bubble level on the load bridge. The completed actuator stand is shown in Figure 15.

Figure 15. Assembled actuator stand.

Step 5: Dynamometer and sling assembly

5.1. Place one shackle around the trim pad anchor (or permanently attached link, if present), then attach the load cell (dynamometer) by inserting the shackle pin.

5.2. Use the other shackle to attach the load cell to the sling. See Figure 16 for the complete setup. Note that this picture shows a trim pad anchor with a link permanently attached. If there is not a permanently attached link, the shackle would attach directly to the anchor (step 5.1).

Figure 16. Load cell attached between trim pad anchor and sling.

5.3. The sling supplied with the kit has an external warning indicator (EWI), shown in Figure 17. If the EWI is not visible, do not use the sling. Measure the length of the EWI that is visible outside the cover.

Figure 17. The external warning indicator on the sling is a visual check that the sling is in good condition.

5.4. Check that the friction-reducing tape on the load bridge and deadman anchor is in good condition. Reapply the Syn-Glide tape as needed.

5.5. Place the sling around the deadman anchor as shown in Figure 18.

Figure 18. Sling placement around deadman anchor.

5.6. Lift the sling into the half-pipe guide of the load bridge. It is easier to lift one path of the sling at a time. The paths should rest one on top of the other. The sling should not have twists in it, except for the 90° rotation the sling makes to wrap around the deadman. See Figure 19 for an example.

Figure 19. Lifting the sling into position on top of the load bridge.

Step 6: Instrumentation setup

6.1. Turn on the load cell and the load cell remote display. The devices should be pre-configured to communicate with each other. If problems are encountered or different functionality is desired, refer to the user's guides for the load cell (Measurement Systems International 2016a) and/or the remote display (Measurement Systems International 2016b).

6.2. Connect the Mitutoyo digital dial indicator to the indicator holder. Attach the magnetic base of the indicator holder to a suitable heavy, magnetic object and position the digital indicator on the edge of the anchor, at approximately a 45° angle, as shown in Figure 20.

Figure 20. Instrumentation setup.

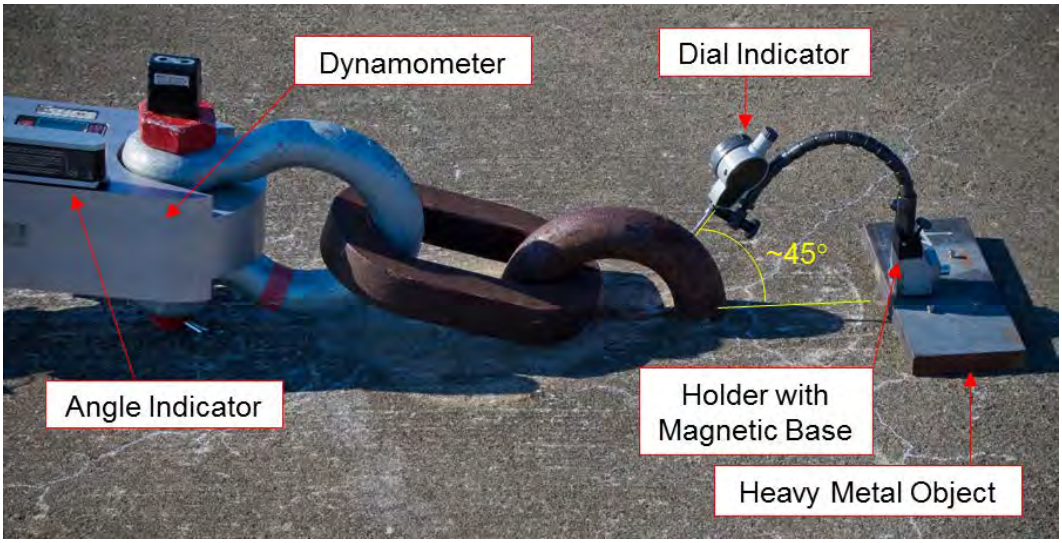

6.3. Check that the indicator holder is stable, then zero the indicator with the rod depressed halfway. Ensure the digital indicator is reading in inches.

6.4. Finally, mount an angle indicator on the upward face of the dynamometer using a Velcro strip.

Step 7: Proof Load Testing

The maximum load should not exceed 100,000 lbf or the anchor proof load, whichever is lower. The test protocol calls for the load to be applied in 10,000-lbf increments, with a 2-min hold after each increment. Monitor the load using the wireless load cell readout. Binoculars can be used to view the dial indicator from a safe distance.

Safety precautions

Observe the following safety precautions during the test:

- Only test personnel should be in the trim pad anchor area during loading.
- Use cones, flags, etc., to mark off the area.
- Do not approach within 50 ft of components under tension.
- It is recommended that test personnel monitor the instrumentation from behind a shield vehicle or other shield.

7.1. Load the system to 1,500 lbf using the hand pump to initially tension the sling. At this level of tension, the load cell should lift off of the ground and more or less be in line with the sling. Some sag is unavoidable, however.

7.2. Verify that the load bridge remains level.
a. If level, continue with the test.
b. If not level, release tension and correct the center stand alignment, then repeat the initial tensioning process (step 7.1).

7.3. Apply load via the hand pump in increments of 10,000 lbf. After each increment, hold for two (2) minutes.

NOTE: The P-802 hand pump is a two-speed pump. At low pressures, pumping requires more effort but moves a larger volume of oil with each stroke. When pressure reaches approximately 400 psi and the handle is completely raised, the pump will automatically switch to the high pressure stage. You may then continue pumping. A pressure of 400 psi roughly corresponds to a tension of 10,000 lbf; this will vary somewhat based on the sling angle when this pressure is reached. If needed, additional information can be found in the pump instruction sheet (ENERPAC 2009).

NOTE: During each hold, it is expected that the load will decrease somewhat as the system relaxes under load.

7.4. The following data should be recorded for each increment. Use a copy of the data sheet provided with this manual (pg. 28).
a. Start stopwatch.
b. Record the load cell reading at the following times (m:ss):
0:30
1:00

1:30
2:00

c. Record deflection from digital indicator reading.

7.5. Continue to increase the load in increments until reaching 100 kips or desired load. **Do not exceed 100 kips.**

7.6. Maintain the desired load for ten (10) minutes. Then, record the following measurements:

- Vertical distance from pavement surface to top of load bridge.
- Angle on angle indicator.
- Distance 1 from Step 1.4.
- Distance 2 from Step 1.4.

Unloading

7.7. Reduce the pressure in the hydraulic system by slowly opening the release valve (turn counter-clockwise). The center stand will lower slowly.

7.8. Disconnect the sling from around the deadman anchor immediately after the system is completely unloaded.

Step 8: Disassembly

8.1. Disassemble the components of the system and return them to the appropriate cases. Note all items marked consumable on the Components List (pg. 29) are not reusable and should be discarded.

NOTE: The LAIK is designed so that the threaded concrete anchors can be reused for future testing. To preserve the integrity of the concrete anchors follow step 8.2.

8.2. Apply anti-seize to eleven 3/4"-10 × 1.5" long corrosion resistant set screws and screw them completely into each concrete anchor. A silicone sealant is recommended to cover the top of the set screw.

References/Additional sources of information

ENERPAC. 2009. Instruction sheet: hydraulic hand pumps. https://www.enerpac.com/sites/default/files/products/downloads/l1763_i_4_0.pdf

Hilti. n.d. *HIT-HY 200-A*. https://www.hilti.com/content/hilti/W1/US/en/products/catalog-page-editorials/anchors/hit-hy-200-a.html

Measurement Systems International. 2016a. *MSI-7300 Dyna-Link 2 tension dynamometer technical manual*. https://www.ricelake.com/Portals/0/Resources/32d04ed09cde473ea07239d4f0649204-orig.pdf

———. 2016b. *MSI-8000 RF remote display technical manual*. https://www.ricelake.com/Portals/0/Resources/b3368f91aed546dc92a1bb6623d8f85f-orig.pdf

Tri-Service Pavements Working Group (TSPWG). 2017. *Inspection of trim pad anchor systems*. TSPWG M 3-260-03.00-2. Air Force Civil Engineer Center. https://www.wbdg.org/FFC/DOD/STC/tspwg_m_3-260-03_00-2.pdf

Data Sheets

Blank checklists and data sheets are included on the following pages. These sheets are based on those included with TSPWG M 3-260-03.00-2, *Inspection of trim pad anchor systems*.

TRIM PAD ANCHOR TESTING CHECKLIST	
Date: _____ Location: _____	
Start Time: _____ End Time: _____	
Working Load: _____ Proof Load: _____	
	ANCHOR TESTING SEQUENCE
	Perform visual inspection and complete inspection record sheet.
	Check sling external warning indicator (EWI). If the EWI is not visible, replace sling.
	Document sling EWI length (pre-test).
	Snap chalk line and mark distances on ground.
	Anchor template.
	Mark 7.5" length on 1” hollow drill bit and oil SDS-Max connector.
	Hammer drill 1” holes.
	Remove template and clean holes.
	Place epoxy and install anchors. Protect anchor threads using plastic caps.
	Allow full epoxy cure time before using anchors.
	Align and anchor actuator base.
	Place actuators in base fixture.
	Connect hydraulic system. Check that valves are set so that both actuators raise evenly.
	Place load bridge on actuators. Check that center stand assembly is stable and plumb.
	Attach shackles to anchor, load cell, and sling.
	Turn on load cell and wireless display and check communication.
	Mount digital indicator and zero.
————————————Do not continue past this point until epoxy has fully cured.————————————	
	Fasten deadman plate with flanged hex head screws and washers.
	Place sling around deadman and over load bridge.
	Clear the testing area. Relocate personnel behind a shield vehicle.
	Load to 1.5 kips to pretension system. Check that center stand remains level.
	Load in increments of 10 kips until desired load is reached. Hold for 2 minutes after each increment. Record load and digital indicator reading on data sheet as specified in manual.
————————————Do not exceed 100 kips or the anchor proof load, whichever is less.————————————	
	Hold the desired load for 10 minutes. Make and record the following measurements:
	• Vertical distance from pavement surface to top of load bridge.
	• Angle reading from angle indicator on load cell.
	• Distance 1 from Step 1.4.
	• Distance 2 from Step 1.4.
	Release hydraulic pressure.
	Disconnect the sling.
	Check sling EWI.
	Document sling EWI length (post-test).
	Disassemble and pack components.
	Prepare anchors for future use with anti-seize and set screws.

NOTE: Shaded boxes are provided for the entry of data.

TRIM PAD ANCHOR TESTING INSPECTION RECORD SHEET		
Date: _____ Location: _____		
Start Time: _____ End Time: _____		
Working Load: _____ Proof Load: _____		
YES	**NO**	**QUESTION**
		1. Do any of the steel components of the anchor system exhibit rust, deformation, cracks, or any other defect that reduces the cross-sectional area?
		2. Does the anchor block or surrounding concrete slab exhibit any spalling or cracking?
		3. Does the anchor block or surrounding concrete slab exhibit any evidence of upheaval?
		4. Does spalling and/or cracking exist at the interface of the steel anchor eye and the concrete anchor block?
		5. Has the anchor been evaluated and/or inspected recently? Enter date if known: _____
		6. Has any maintenance been done to the anchor since its last evaluation/inspection?
		7. Have any of the connections been replaced since the last evaluation/inspection?
		8. If these connections are commercially available shackles, are the manufacturer's data and rating certification for the shackles available?
		9. What is the main aircraft that uses the trim pad anchor? _____
		10. What is the typical trim operation used (e.g., single engine only)? _____
		11. How many trim operations does the anchor support annually? _____
		12. Have there been any significant environmental events since the last evaluation/inspection that could have compromised the anchor's integrity (e.g., flooding, earthquakes)?
OBSERVATIONS/COMMENTS		
Signature: _____		
Printed Name/Rank: _____		

TRIM PAD ANCHOR TESTING DATA SHEET		
Date: _____ Location: _____		
Start Time: _____	End Time: _____	
Working Load: _____	Proof Load: _____	
LOAD CELL (lbf)	**TIME (mm:ss)**	**DIGITAL INDICATOR READING (× 10^{-5} in.)**

Components List

Item #	Storage Case #	Item/Description	Qty.	Recommended Vendor
CUSTOM LAIK DEADMAN ANCHOR INSTALLATION JIG COMPONENTS:				
1A	1	1A – Drilling Template	1	Items require fabrication See LAIK DWG. 1
1B	2	1B – Drill Guide	1	
1C	1	1C – Template Alignment Pins	3	
CUSTOM LAIK TEST COMPONENTS:				
2A	3	2A – Deadman Anchor	1	Items require fabrication See LAIK DWG. 2
2B	4	2B – Actuator Base	1	
2C	5	2C – Load Bridge	1	
COTS Items:				
3[c]	1	Tapcon 5/16 in. x 2-1/4 in. Hex-Washer-Head Large Diameter Concrete Anchors (Model # 24292)	6	---
4[c]	1	Wej-It Power-Sert™ 1" x 6-1/2" Anchors - Carbon Steel (Toggler Part # PS2-34)	11	www.toggler.com
5	1	Hilti Round brush HIT-RB 1" (Hilti Item # 273212)	1	---
6	1	Hilti Brush T-handle HIT-RBH (Hilti Item # 229138)	1	---
7[c]	1	Nylon Flat-Tip Set Screws, 3/4"-10 Thread, 1/4" Long (McMaster Part # 94564A705)	11	www.mcmaster.com
8[c]	1	18-8 Stainless Steel Set Screw, 3/4"-10 Thread, 1.5" Long (McMaster Part # 92311A839)	11	www.mcmaster.com
9	1	Socket Set with 1/2" Drive Ratchet, Extension, 3/8" and 1-1/8" Sockets	1	---
10	1	Slingmax Synglide Friction Reducing Film	1	www.marineandindustrial.com
11	1	Chalk line	1	---
12	1	Tape measure, 25 ft	1	---
13	1	Hammer	1	---
14	1	Small wire brush	1	---
15	1	Framing square	1	---
16	1	Allen wrench set	1	---
17	2	Milwaukee M18 FUEL 18-Volt Lithium-Ion Brushless Cordless 1-9/16 in. SDS-Max Rotary Hammer Kit with 2 9.0Ah Batteries (Model # 2717-22HD)	1	---
18	2	Bosch SDS-max to SDS-plus Rotary Hammer Adapter (Part # HA1030)	1	---
19	2	Tapcon SDS+ 1/4" x 7" carbide drill bit (Model # 11493)	1	---
20	2	Hilti Hollow Drill Bit TE-YD 1" X 24" (Hilti Item # 2018963)	1	---
21	2	Bosch SDS-plus Rebar Cutter (Bosch Part # RC2164)	1	---

22[c]	3	High-Strength Grade 8 Steel Hex Head Screw, Flanged, 3/4"-10 Thread Size, 2.5" Long (McMaster Part # 92316A843)	11	www.mcmas-ter.com
23[c]	3	Grade 8 Steel Washer, Zinc Yellow-Chromate Plated, for 3/4" Screw Size, 2" OD (McMaster Part # 98026A036)	11	www.mcmas-ter.com
24[c]	3	Loctite Antiseize Lubricant, Corrosion-Resistant (Loctite Part # 76732)	1	---
25	6	Milwaukee M18 18-Volt Lithium-Ion Cordless Wet/Dry Vacuum (Model # 0880-20)	1	---
26	6	Vacuum straw attachment ("VaccUFlex" or similar)	1	---
27	7	Milwaukee M18 18-Volt Lithium-Ion High Demand Bat-tery Pack 9.0Ah (Model # 48-11-1890)	2	---
28[c]	7	Hilti HIT-HY 200-A Epoxy (Hilti Item # 2022791)	3	---
29	7	Hilti HDM 500 Adhesive Dispenser + Red Cartridge (Hilti Item #: 3498314)	1	---
30	8	Enerpac Aluminum Hydraulic Cylinder, 30 ton, 10" stroke (Enerpac Part # RAC-3010)	2	---
31	9	Enerpac Hydraulic Hand Pump (Enerpac Part # P-802)	1	---
32	9	Enerpac Hydraulic Manifold Valve, Two Way (Enerpac Part # AM-21)	1	---
33	9	Enerpac Hydraulic Pressure Gauge (Enerpac Part # DGR-2)	2	---
34	9	Enerpac Hydraulic Hose, 6' (Enerpac Part # HC-7206C)	2	---
35	10	Enerpac Hydraulic Hose, 50' (Enerpac Part # HC-7250C)	1	---
36	10	Slingmax Twin-Path TPXCF6500 Sling, 175" Long	1	www.marineandin-dustrial.com
37	11	Shackle for 100kip Dynamometer (MSI Part # 23650-0050)	1	---
38	12	Shackle for 100kip Dynamometer (MSI Part # 23650-0050)	1	---
39	13	MSI-7300 Dyna-Link 2 Dynamometer with wireless con-nectivity 100,000 x 50 lb (MSI Part # 503381-0007)	1	---
40	14	MSI-8000 RF Remote Display for MSI-7300 (MSI Part # 139381)	1	---
41	14	Electronic Dial Indicator, Mitutoyo - 0 to 1" Range, 0.00005" Graduation (MSC Part # 70049093)	1	www.mscdi-rect.com
42	14	Noga MA61003 Articulated Arm Indicator Positioner and Holder (MSC Part # 09560392)	1	www.mscdi-rect.com
43	14	Angle Indicator	1	---

[c]: Consumable items – must be replaced for each test.

LAIK DWG. 1:
DEADMAN ANCHOR INSTALLATION JIG
COMPONENTS REQUIRING FABRICATION

LAIK DEADMAN ANCHOR INSTALLATION JIG
COMPONENTS REQUIRING FABRICATION

ITEM NO.	ITEM / DESCRIPTION	SEE SHEET
1A	Drilling Template	2
1B	Drill Guide	3
1C	Alignment Pin	4

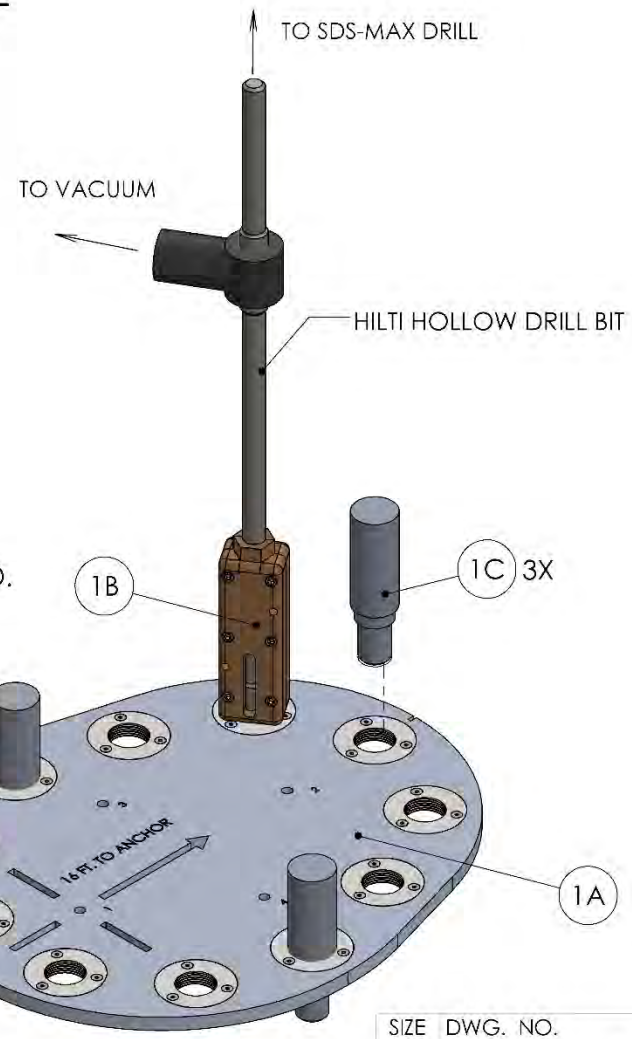

GENERAL NOTES:

1. THE PURPOSE OF THIS DRAWING IS TO PROVIDE MANUFACTURING INFORMATION FOR THE COMPONENTS OF THE DEADMAN ANCHOR INSTALLATION JIG THAT REQUIRE FABRI CATION.
2. CAD MODELS OF EACH COMPONENT ARE PROVIDED.

ALL DIMENSIONS ARE IN INCHES UNLESS NOTED OTHERWISE.

SIZE	DWG. NO.	REV
A	LAIK DWG. 1	-
SCALE: NTS		SHEET 1 OF 4

ITEM 1A
DRILLING TEMPLATE

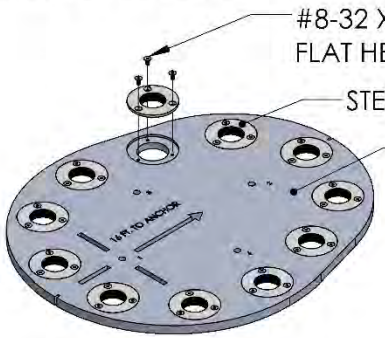

ITEM 1A NOTES:
1. RECOMMENDED MATERIAL IS 6061-T6 ALUMINUM FOR TEMPLATE AND 4140 STEEL FOR THREADED INSERTS.
2. MIN. PLATE SIZE FOR TEMPLATE: 18.7" X 15.75" X 0.5".
3. MIN. ROUND SIZE FOR THREADED INSERTS: ∅2.55" X 0.5" (QTY: 11)
4. EST. WT: 15 LBS.

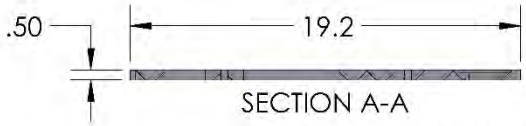

SECTION A-A

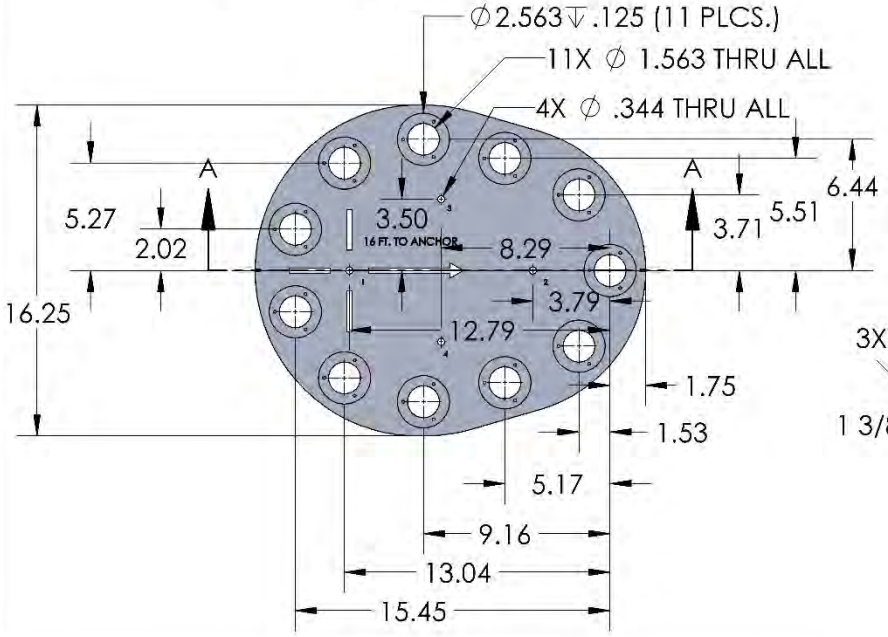

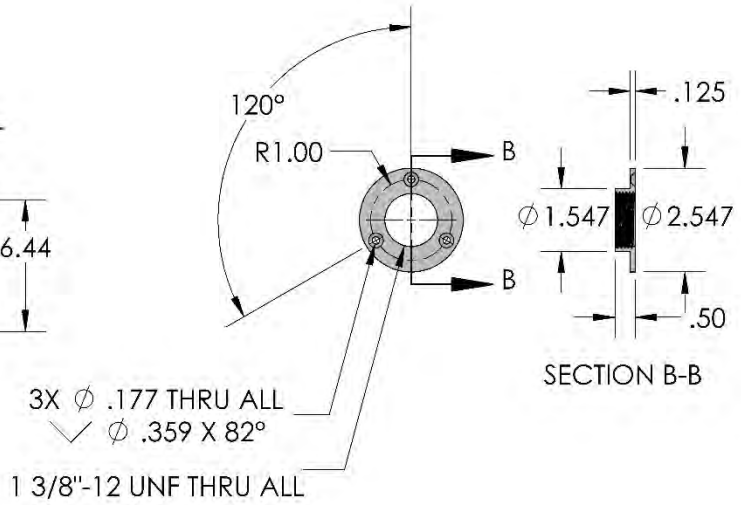

SECTION B-B

SIZE	DWG. NO.	REV
A	LAIK DWG. 1	-
SCALE: NTS		SHEET 2 OF 4

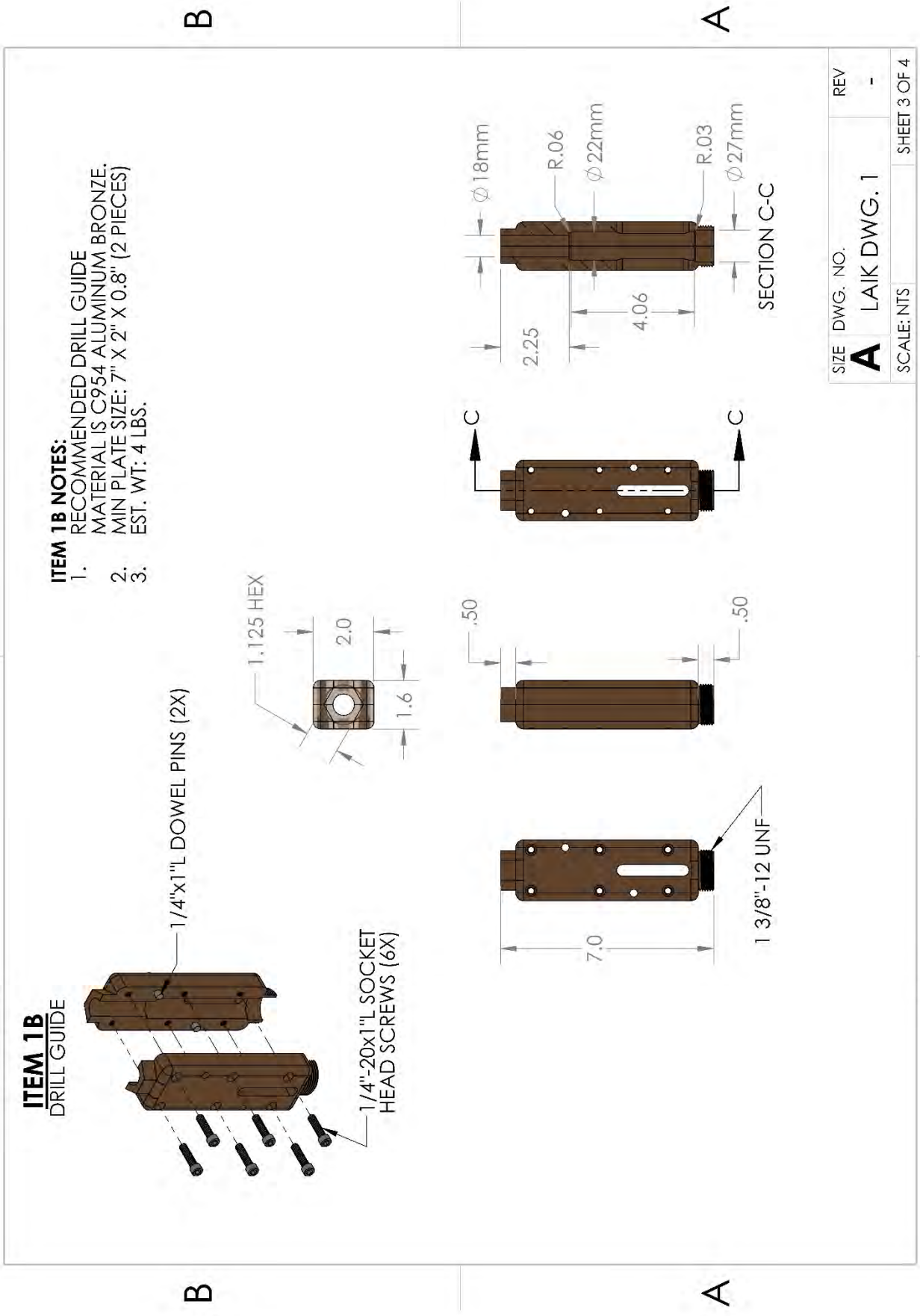
ITEM 1B NOTES:
1. RECOMMENDED DRILL GUIDE MATERIAL IS C954 ALUMINUM BRONZE.
2. MIN PLATE SIZE: 7" X 2" X 0.8" (2 PIECES)
3. EST. WT: 4 LBS.
ITEM 1B
DRILL GUIDE
1/4"x1"L DOWEL PINS (2X)
1/4"-20x1"L SOCKET HEAD SCREWS (6X)
1.125 HEX
2.0
1.6
.50
.50
7.0
1 3/8"-12 UNF
C
C
SECTION C-C
Ø18mm
R.06
Ø22mm
R.03
Ø27mm
2.25
4.06
SIZE A
DWG. NO. LAIK DWG. 1
REV -
SCALE: NTS
SHEET 3 OF 4

2 1

B B

A A

ITEM 1C
ALIGNMENT PIN

ITEM 1C NOTES:
1. RECOMMENDED ALIGNMENT PIN MATERIAL IS 6061-T6 ALUMINUM
2. MIN ROUND SIZE: ∅1.5" X 5.5" L (QTY: 3)
3. EST. WT: 4 LBS.

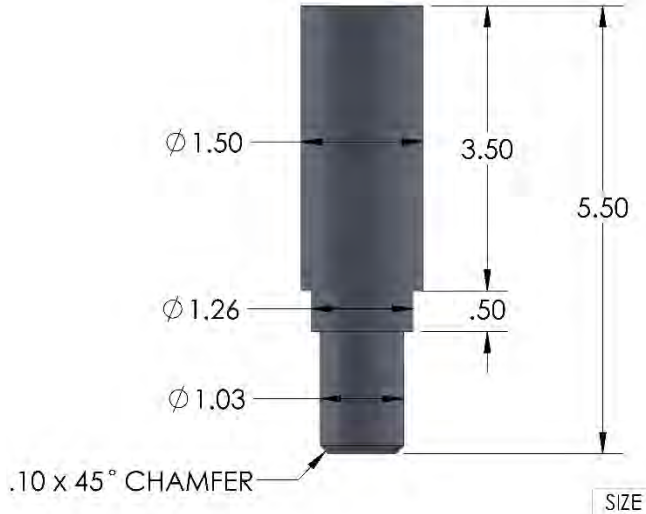

SIZE	DWG. NO.	REV
A	LAIK DWG. 1	-
SCALE: NTS		SHEET 4 OF 4

2 1

LAIK DWG. 2:
LAIK TEST COMPONENTS REQURING FABRICATION

LAIK TEST COMPONENTS REQUIRING FABRICATION

ITEM NO.	ITEM/DESCRIPTION	SEE SHEET
2A	Deadman Anchor	2
2B	Actuator Base	3
2C	Load Bridge	4

GENERAL NOTES:

1. THE PURPOSE OF THIS DRAWING IS TO PROVIDE MANUFACTURING INFORMATION FOR THE LIGHTWEIGHT ANCHOR INSPECTION KIT (LAIK) TEST COMPONENTS THAT REQUIRE FABRICATION.
2. CAD MODELS OF EACH COMPONENT ARE PROVIDED.

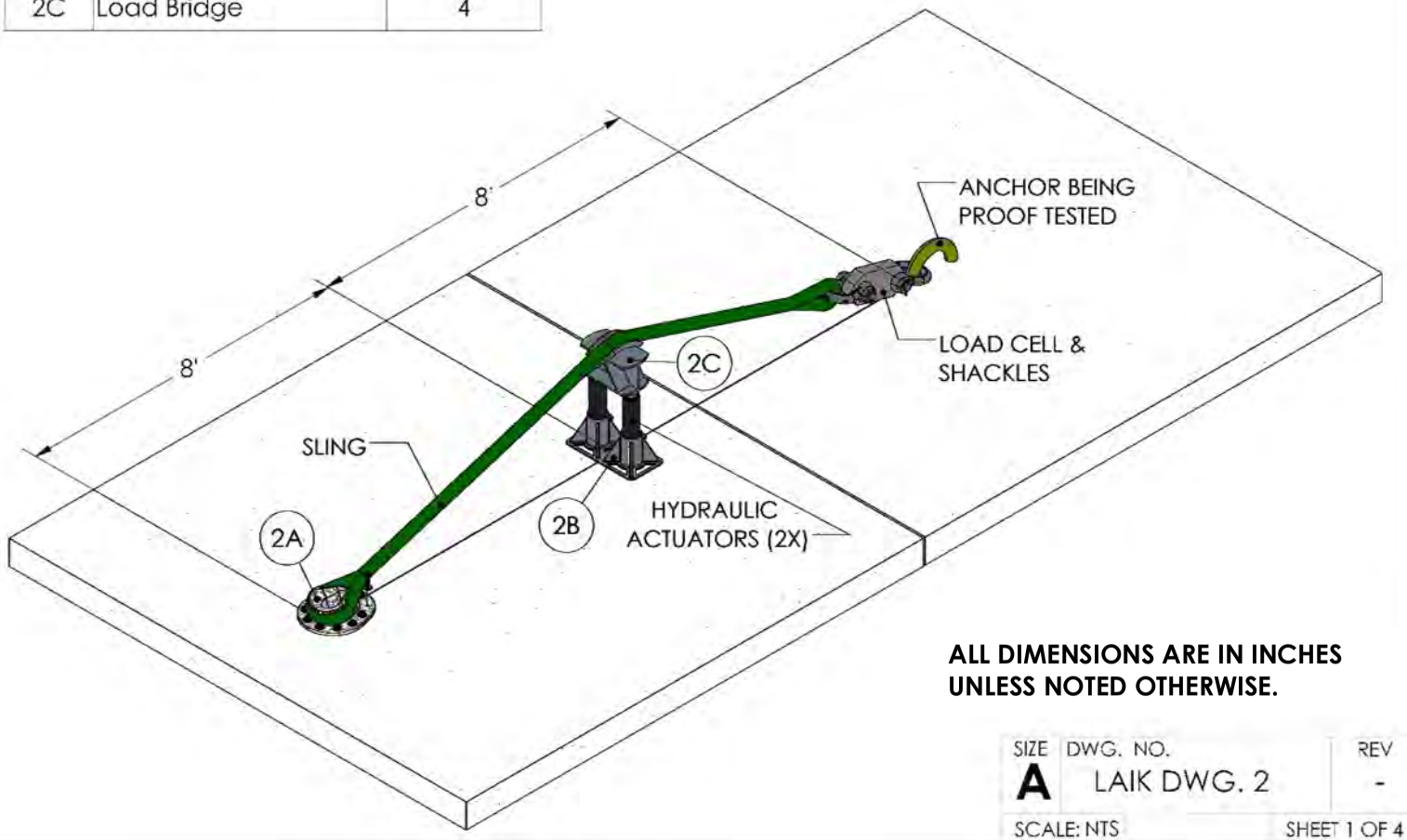

ALL DIMENSIONS ARE IN INCHES UNLESS NOTED OTHERWISE.

SIZE	DWG. NO.	REV
A	LAIK DWG. 2	-
SCALE: NTS		SHEET 1 OF 4

ITEM 2A
DEADMAN ANCHOR

ITEM 2A NOTES:
1. RECOMMENDED MATERIAL IS 7075-T6 ALUMINUM.
2. MIN. PLATE SIZE: 19 1/4" X 16 1/4" X 6".
3. EST. WT: 35 LBS.

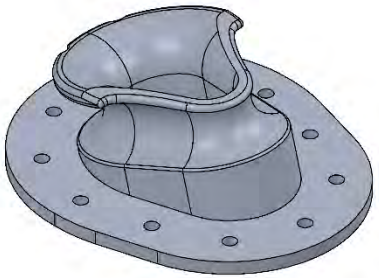

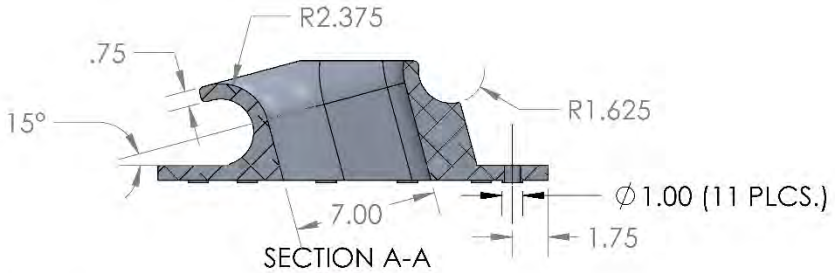

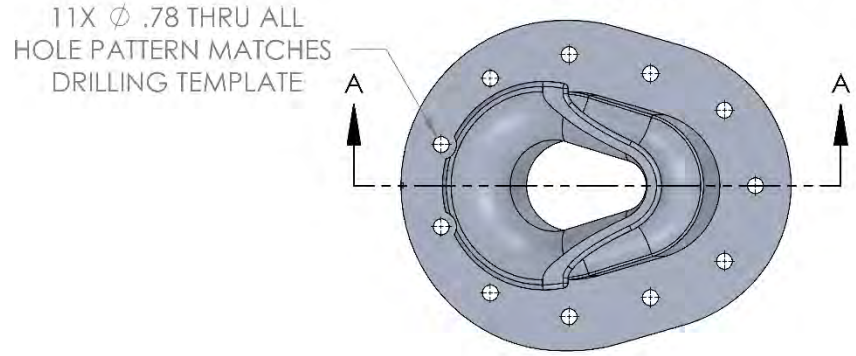

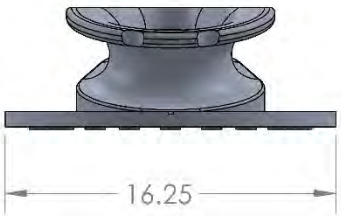

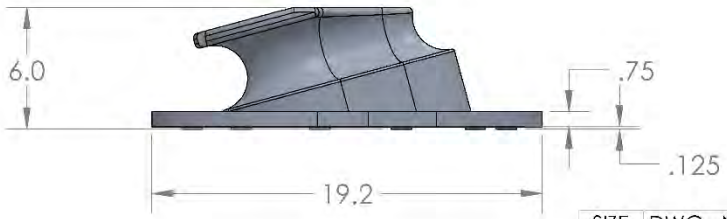

SIZE	DWG. NO.	REV
A	LAIK DWG. 2	-
SCALE: NTS		SHEET 2 OF 4

ITEM 2B
ACTUATOR BASE

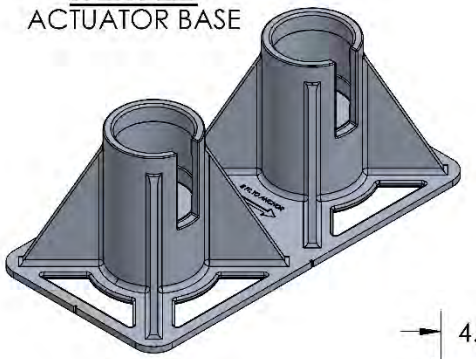

ITEM 2B NOTES:
1. RECOMMENDED MATERIAL IS 6061-T6 ALUMINUM.
2. PART CAN BE EITHER MACHINED FROM SOLID STOCK OR ASSEMBLED WITH FASTENERS.
3. EST. WT: 30 LBS.

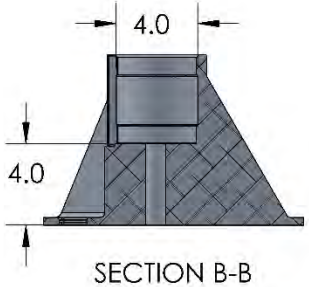

SECTION B-B

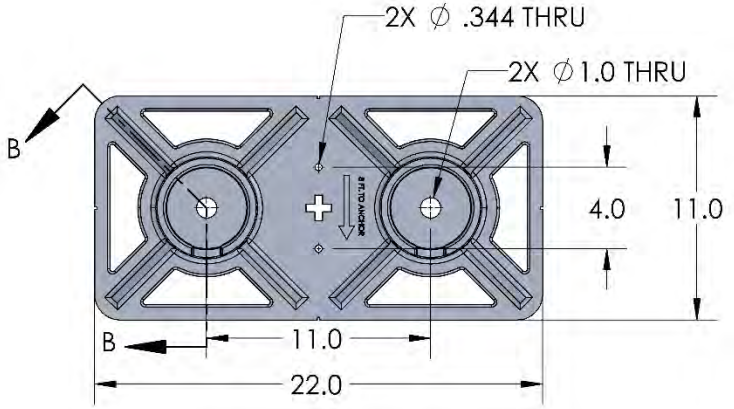

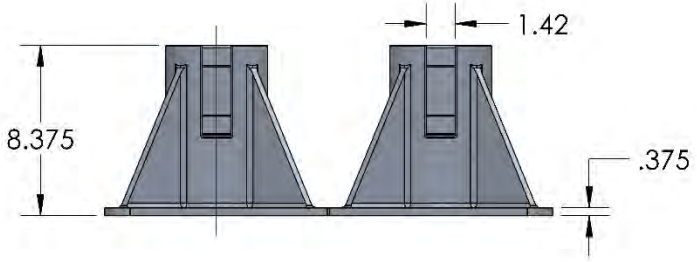

SIZE	DWG. NO.	REV
A	LAIK DWG. 2	-
SCALE: NTS		SHEET 3 OF 4

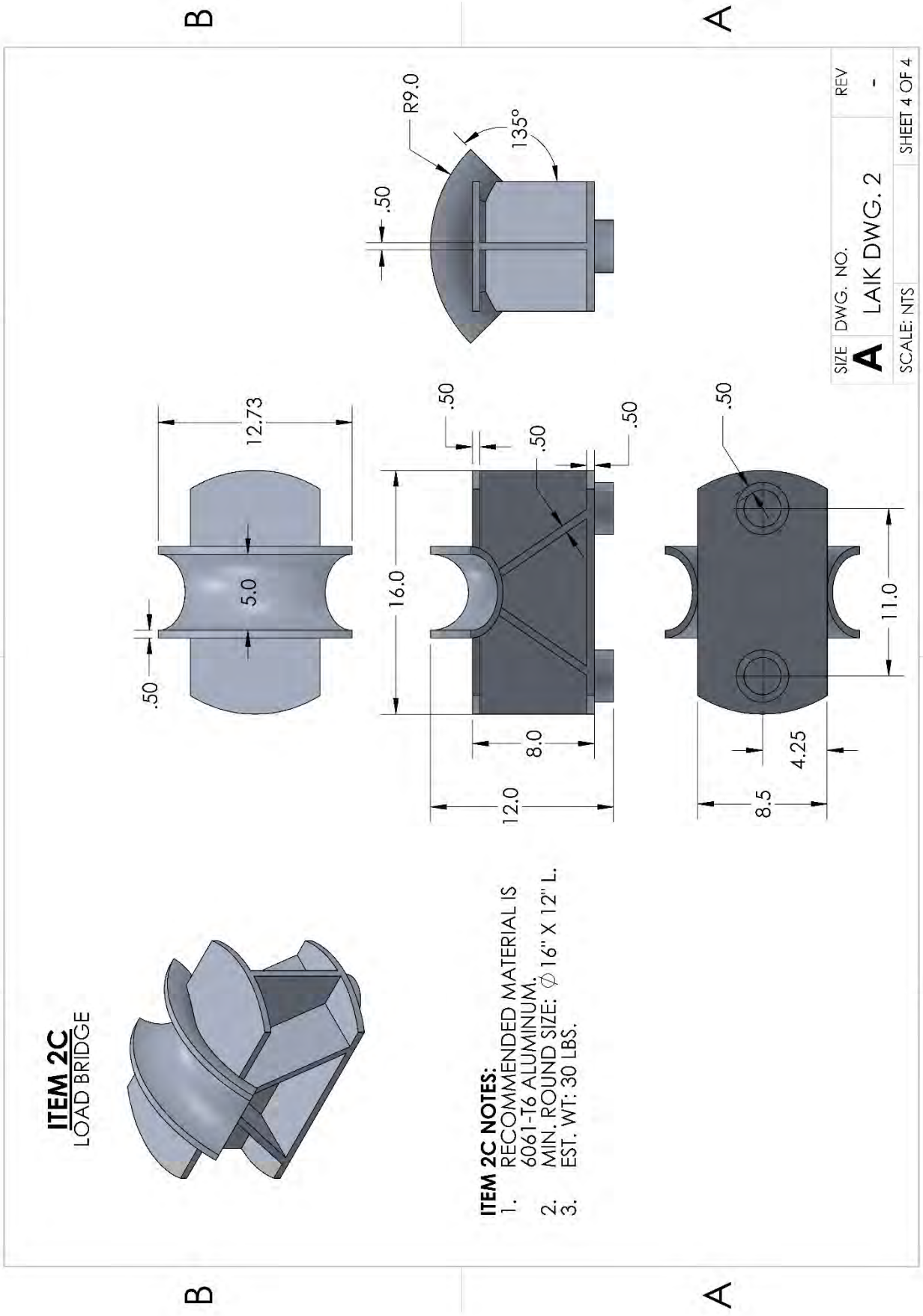
ITEM 2C
LOAD BRIDGE
ITEM 2C NOTES:
1. RECOMMENDED MATERIAL IS 6061-T6 ALUMINUM.
2. MIN. ROUND SIZE: ⌀16" X 12" L.
3. EST. WT: 30 LBS.
R9.0
135°
.50
12.73
5.0
16.0
8.0
12.0
11.0
4.25
8.5
SIZE A
DWG. NO. LAIK DWG. 2
REV -
SCALE: NTS
SHEET 4 OF 4

REPORT DOCUMENTATION PAGE

Form Approved
OMB No. 0704-0188

Public reporting burden for this collection of information is estimated to average 1 hour per response, including the time for reviewing instructions, searching existing data sources, gathering and maintaining the data needed, and completing and reviewing this collection of information. Send comments regarding this burden estimate or any other aspect of this collection of information, including suggestions for reducing this burden to Department of Defense, Washington Headquarters Services, Directorate for Information Operations and Reports (0704-0188), 1215 Jefferson Davis Highway, Suite 1204, Arlington, VA 22202-4302. Respondents should be aware that notwithstanding any other provision of law, no person shall be subject to any penalty for failing to comply with a collection of information if it does not display a currently valid OMB control number. **PLEASE DO NOT RETURN YOUR FORM TO THE ABOVE ADDRESS.**

1. REPORT DATE *(DD-MM-YYYY)*
March 2019

2. REPORT TYPE
Final report

3. DATES COVERED *(From - To)*

4. TITLE AND SUBTITLE
Development of a Lightweight Airfield Anchor Test Kit

5a. CONTRACT NUMBER

5b. GRANT NUMBER

5c. PROGRAM ELEMENT NUMBER

6. AUTHOR(S)
Andrew B. Groeneveld, M. Wesley Trim,
Mariely Mejías-Santiago, and Craig A. Rutland

5d. PROJECT NUMBER
462312

5e. TASK NUMBER

5f. WORK UNIT NUMBER
J3051D

7. PERFORMING ORGANIZATION NAME(S) AND ADDRESS(ES)

U.S. Army Engineer Research and Development Center
Geotechnical and Structures Laboratory
3909 Halls Ferry Road
Vicksburg, MS 39180-6199

8. PERFORMING ORGANIZATION REPORT NUMBER

ERDC/GSL TR-19-10

9. SPONSORING / MONITORING AGENCY NAME(S) AND ADDRESS(ES)
Headquarters, Air Force Civil Engineer Center
Tyndall Air Force Base, FL 32403-5319

10. SPONSOR/MONITOR'S ACRONYM(S)
AFCEC

11. SPONSOR/MONITOR'S REPORT NUMBER(S)

12. DISTRIBUTION / AVAILABILITY STATEMENT

Approved for public release; distribution is unlimited.

13. SUPPLEMENTARY NOTES

14. ABSTRACT
The Air Force Civil Engineer Center (AFCEC) tasked the Army Engineer Research and Development Center (ERDC) with developing a lightweight kit for proof load testing anchors used in airfield operations. The design was required to be rapidly deployable, lightweight (i.e., no heavy equipment), and leave no permanent damage to the airfield. For the purposes of the project, airfield anchors were divided into three main types: studs/threaded anchors, aircraft trim pad anchors, and aircraft tie-downs/mooring points. Stud or threaded anchor testing can be performed expediently using a commercial testing device. Operability of the commercial device was tested at ERDC by pulling poly panel threaded rods to failure. A prototype anchor loading apparatus for trim pad anchors, the Lightweight Anchor Inspection Kit (LAIK), was designed, built, and successfully tested to demonstrate operability. Trim pad anchors at Eglin AFB were proof loaded to 100 kips using the LAIK. The LAIK user's manual, list of components, and design drawings are included as an appendix to the report. A tie-down anchor testing device was also designed and built. This testing device is intended to proof load aircraft tie-downs/mooring points up to 70 kips. The tie-down tester makes use of the same hydraulic equipment included in the LAIK.

15. SUBJECT TERMS
Proof load testing
Airfield anchor
Threaded anchor
Trim pad anchor
Aircraft tie down
Runways (Aeronautics)
Anchorage (Structural engineering)- Testing
• Air bases

16. SECURITY CLASSIFICATION OF:			**17. LIMITATION OF ABSTRACT**	**18. NUMBER OF PAGES**	**19a. NAME OF RESPONSIBLE PERSON**
a. REPORT	**b. ABSTRACT**	**c. THIS PAGE**			**19b. TELEPHONE NUMBER** *(include area code)*
UNCLASSIFIED	UNCLASSIFIED	UNCLASSIFIED		152	